TRANSIENTS IN COOLING WATER SYSTEMS OF THERMAL POWER PLANTS

PART I

405997

-nraningies

TRANSIENTS IN COOLING WATER SYSTEMS OF THERMAL POWER PLANTS

WT P3 B3 SAFW.1

PROEFSCHRIFT

TER VERKRIJGING VAN DE GRAAD VAN DOCTOR IN DE TECHNISCHE WETENSCHAPPEN AAN DE TECHNISCHE HOGESCHOOL DELFT, OP GEZAG VAN DE RECTOR MAGNIFICUS IR. H. R. VAN NAUTA LEMKE, HOOGLERAAR IN DE AFDELING DER ELEKTROTECHNIEK, VOOR EEN COMMISSIE

UIT DE SENAAT TE VERDEDIGEN OP DINSDAG 27 JUNI 1972 TE 14.00 UUR

DOOR

HEMMAT H. SAFWAT

doctor in de technische wetenschappen

geboren te Cairo-Egypte

Bibliotheek TU Delft

3092772

0653 154

WT Po3 Bo3

Dit proefschrift is goedgekeurd door de promotoren Prof. Ir. J.J.C. van Lier en Prof. Ir. J.O. Hinze

SAMENVATTING

Een beschouwing wordt gegeven over de problemen, die ontstaan na het uitvallen van een pomp in het koelwatercircuit van een elektrische centrale. Bij deze beschouwing wordt vooral aandacht besteed aan de gebeurtenissen bij waterslag en het scheiden van de waterkolommen. De noodzaak wordt aangetoond om te komen tot een meer betrouwbare berekeningsmethode voor het voorspellen van de drukveranderingen, die in een koelwatercircuit bij waterslag kunnen optreden. Een stapsgewijze benadering van de gecompliceerde verschijnselen bij waterslag in het koelwatercircuit met behulp van een experimentele opstelling wordt besproken. De voorkeur wordt gegeven aan het uitvoeren van een studie in drie fasen en wel ten eerste waterslag in een horizontale leiding, vervolgens waterslag in een leiding met een hevel om dan te komen tot het uiteindelijke onderzoek en wel waterslag in een leiding met een hevel met in het hoogste punt van de hevel het model van een condensor. Vermeld worden de uitgangspunten voor het onderwerp van de proefopstelling. Stilgestaan wordt o.a. bij de speciaal ontworpen afsluiter met stuureenheid aan het begin van de leiding, die tot taak heeft de drukveranderingen ten gevolge van het uitvallen van een pomp te simuleren. De metingen ter bepaling van de wrijvingscoëfficienten van de leiding en de afsluiter in stationaire toestand worden vermeld. Ter bepaling van de snelheidsveranderingen, die optreden tijdens waterslag, werden twee meetmethoden ontwikkeld; de eerste methode behelst een fotografische meting, die digitaal wordt uitgewerkt en de tweede methode een inductieve meting met directe registratie. Aan de tweede methode wordt met het oog op een snelle uitwerking van de metingen de voorkeur gegeven. De met behulp van de laatste meetmethode verkregen snelheidspatronen zijn uniek en uitermate waardevol gebleken voor het verkrijgen van een goed beeld van het verschijnsel waterslag. Om de verschijnselen bij waterslag ook visueel te kunnen waarnemen is de leiding van de experimentele opstelling vervaardigd van plexiglas. Het gedrag van dit materiaal bij de optredende drukveranderingen werd bestudeerd en aangetoond kon worden dat het plexiglas zich bij de metingen gedroeg als een elastisch materiaal. Uit deze studie blijkt het mogelijk te zijn niet-stationaire drukveranderingen bij waterslag indirect te meten en wel met behulp van rekstrookjes op de buitenzijde van de betreffende leiding. Dit kan zeer nuttig zijn in die gevallen waar doorboring van de leiding met het oog op het transport van gevaarlijke vloeistoffen niet is toegestaan. Om een inzicht te verkrijgen in de gebeurtenissen bij het scheiden van de waterkolommen zijn opnamen gemaakt van het leidinggedeelte achter de afsluiter met behulp van een high-speed filmcamera. Deze opnamen geven een zeer goed beeld van de volgorde van de gebeurtenissen en hebben bijgedragen tot een beter begrip van het verschijnsel van het scheiden van de waterkolommen bij waterslag. Bij de metingen in de drie reeds vermelde fasen zijn verschillende grootheden gevarieerd zoals de initiële snelheid in stationaire toestand, de sluitingstijd van de afsluiter en de geometrie van de leiding. Met de karakteristieke berekeningsmethode zijn de drukveranderingen berekend en vergeleken met de gemeten waarden. Een aantal discrepanties is hierbij vastgesteld. Deze vaststelling tesamen met het door de high-speed filmcamera verkregen beeld leidde tot een nieuw wiskundig model ter beschrijving van de stromingstoestand in geval van een één-dimensionale stroming, waarin de resulterende drukken de dampdruk benaderen of bereiken. Bij het opstellen van dit model is grote aandacht besteed aan de invloed van de bij de drukdaling gevormde cavitatiebelletjes op het impulsverlies en aan het verloop van de voortplantingssnelheid van de drukgolven. In het nieuwe wiskundig model wordt een impulsverlies-faktor geïntroduceerd. Deze faktor vertegen-woordigt de invloed van de wandwrijving en de invloed van de weerstand door het expanderen en comprimeren van de cavitatiebelletjes. De differentiaalvergelijkingen worden omgewerkt tot eindige differentievergelijkingen, die bijzonder geschikt zijn voor het gebruik op een digitale rekenmachine. Methoden ter bepaling van de impulsverlies-faktor en de afname van de voortplantingssnelheid van de drukgolven worden besproken. De met behulp van de nieuwe berekeningsmethode verkregen resultaten worden vergeleken met de in de verschillende studiefasen gemeten waarden en blijken zeer goed met elkaar overeen te stemmen.

THESES

- 1. In transient flows involving pressures near the vapour pressure, the momentum loss associated with cavitation plays an important role.
- 2. Engineers lack dependable data of friction factors for unsteady flow.
- 3. A better evaluation of performance of hydraulic devices such as pumps, valves, etc. under unsteady flow conditions is needed for description of boundary conditions representing these devices in water hammer calculations.
- 4. For some applications the estimation of the largest pressure surge occurring during transient conditions may fall short of complete satisfaction for the designer and a complete history of the pressure changes may be needed.
- 5. The introduction of air as a means for suppressing pressure surges during hydraulic transients associated with water column separation is an effective method, but air must be introduced at the right location and right time.
- 6. Experimental observations show that as regards travel of pressure waves during hydraulic transients in pipelines, extra consideration of strength aspects of the design of bents and change of cross sections is needed.
- 7. The efficiency of computer use has been developing at slower pace than advancements in hard-ware computer technology.
- 8. Exploring space has brought mankind a lot of advancements in technology that are of use on earth.
- 9. A lot of ideas and techniques that have been developed in the last decade in the area of surface radiation heat transfer can be used in other engineering applications.
- 10. Ecologists must remember that there is a continuous need for the growth in power production and power producers should keep in mind the environmental changes associated with their expansion programmes.
- 11. Developing nations should try to shape up their development with great attention to environmental problems as they have a good chance to avoid dangerous effects of industrialization.
- 12. The question of amateur and professional status of athletes would continue to be unresolved.

ACKNOWLEDGEMENTS

This dissertation is based on an investigation under the same title and is sponsored by Delft University of Technology, Delft Hydraulics Laboratory and Joint Nuclear Power Plant Dodewaard. Special thanks are due to Mr. J.E. Prins, President of Delft Hydraulics Laboratory, and Mr. R. van Erpers Royaards, director of Joint Nuclear Plant Dodewaard for their encouragement and support.

It is only the co-operation and assistance of a large number of people that made this work possible. The author wishes to express his thanks to all the staff of the thermal power laboratory of the Delft University of Technology and of the Delft Hydraulics Laboratory.

Acknowledgements are due to his assistant J. van den Polder for his efforts during all stages of the project. The author wishes to thank his students R.L. Krabbendam, J.P. de Kluyver, K.A.F. Prinse who made an excellent team and who shared in an effective manner in bringing the project to its goals.

Thanks are also due to Mr. J. v.d. Wel and Mr. H. de Vries and Dr.A.C.E. Wessels and the instrumentation group of Delft Hydraulics Laboratory for their efforts. A word of appreciation is due to Dr. Wessels for the design and the development of the induction flow-meter. The author wishes to thank Mr. J. Timmers and the workshop staff of the Delft Hydraulics Laboratory for their work in building up the experimental model. The author is grateful to Misses I.H.A. Kneip and M. Burgers for many helpful improvements in the manuscript and its typing. Thanks to Miss Heuvelman for typing the final manuscript.

TABLE OF CONTENTS

PART I

	Chapt	er_		Page
	SYMBO	OLS		9
	LIST	OF TAB	LES	11
	LIST	OF FIG	URES .	12
	LIST	OF COM	PUTER PROGRAMMES	18
1.	INTRO	ODUCTIO:	N .	20
	1.1.	Genera	l Aspects of the Problem and Motivation	20
	1.2.	Method	of Approach to the Investigation	21
	1.3.	Outlin	e of Dissertation .	22
2.	WATE	R-намие:	R AND WATER-COLUMN SEPARATION ANALYSIS	25
	2.1.	Litera	ture Survey	25
	2.2.	Basic	Laws of Fluid Mechanics for Water-Hammer Applications	28
	2.3.	Charac	teristics Method	31
	2.4.	Finite	Difference Solution	33
	2.5.	Illust	rative Description of the Phenomena of Water-Hammer	
		and Wa	ter-Colomn Separation	35
3.	EXPE	RIMENTA	L STUDY	40
	3.1.	Water-	Hammer Water-Colomn Separation Experimental Circuit	40
		3.1.1.	General description	41
		3.1.2.	Details and data of main parts of circuit	41
	3.2.	Instru	mentation	46
	3.3.	Experi	ments	48
		3.3.1.	Steady conditions measurements	49
		3.3.2.	Measurement of transient flow velocities	51
		3.3.3.	High speed camera photographic study of water-colomn	
			separation	56
		3.3.4.	Experimental evaluation of the elastic behaviour of	
			the pipe wall material	57
		3.3.5.	Transient conditions	62

BIBLIOGRAPHY

	Chapter	Page
4.	COMPARISON OF EXPERIMENTAL MEASUREMENTS AND CALCULATED RESULTS	
	USING CLASSICAL WATER-HAMMER CALCULATIONS	63
	4.1. Schematization of the Pipe System	63
	4.2. Choice of Input Data for the Programme HOZ	64
	4.3. Investigated Conditions	65
	4.4. Comparison of Experimental Measurements and Calculated Results	65
	4.5. Photographic Study of Water-Column Separation during Tran-	
	sients in the Horizontal Pipe	67
	4.6. Significant Findings	74
5.	NEW MATHEMATICAL MODEL	76
	5.1. Finite Difference Solution	77
6.	TRANSIENTS RESULTING FROM CLOSURE OF THE VALVE AT THE UPSTREAM	
	END OF THE HORIZONTAL PIPE	80
	6.1. Typical Experimental Test	80
	6.2. Schematization of the Line	80
	6.3. Choice of Input Data for the Programme HZD	80
	6.4. Comparison of Experimental Measurements and Calculated Re-	
	sults	85
7.	TRANSIENTS RESULTING FROM CLOSURE OF THE VALVE AT THE UPSTREAM	
	END OF THE SIPHON	89
	7.1. Typical Experimental Tests	89
	7.2. Schematization of the Line	92
	7.3. Choice of Input Data for the Programme WHN	92
	7.4. Comparison of Experimental Measurements and Calculated Re-	
	sults	94
8.	TRANSIENTS RESULTING FROM CLOSURE OF THE VALVE AT THE UPSTREAM	
	END OF THE CONDENSER SYSTEM	97
	8.1. Typical Experimental Tests	97
	8.2. Schematization of the Condenser Configuration	98
	8.3. Choice of Input Data for the Programme WCN	98
	8.4. Comparison of Experimental Measurements and Calculated Re-	
	sults	101
9.	CONCLUSIONS	108

112

<u>Chapter</u>	Page
APPENDIX	
A Digital Calculations of Velocities from Photo-Analyzer Data	119
B On the Pipe Wall Deformation	122
C Numerical Calculations for Transients in a Horizontal Line	
Based on Method of Characteristics	125
D Numerical Calculations for Transients in a Horizontal Line	
Based on the New Mathematical Model	129
E Numerical Calculations for Transients in the Siphon System	
Based on the New Mathematical Model	133
F Numerical Calculations for Transients in the Condenser System	
Based on the New Mathematical Model	135
G List of Experimental Measurements Data	138
VITA	139
ABSTRACT	140

PART II

LIST OF FIGUR	ES	8
IIST OF COMPI	TER PROGRAMMES	1),

TRANSIENTS IN COOLING WATER SYSTEMS OF THERMAL POWER PLANTS

PART I

SYMBOLS

Carmbola	Units	Descriptive identification
Symbols		Descriptive identification
A	m^2	Cross sectional area of pipe
a .	m/s	Celerity of transient pressure pulse
Ъ	m	Outside pipe radius
C+, C-		Characteristics curves
С		Momentum loss coefficient
с (µ)		Parameter depending on type of support of pipe and Poisson's ratio of its material
D, d	m	Inside pipe diameter
E	N/m^2	Modulus of elasticity of pipe wall
e, exp		Napierian base
f		Darcy-Weisbach frictional coefficient
f		Mathematical function
g	m/s ²	Acceleration of gravity
Н	m(water)	Piezometric head (P/pg + z)
н н _А	m(water)	Piezometric head (P/pg + z) Head in high level reservoir
	m(water)	
НА		Head in high level reservoir
H _A H _B , H _O H _{fr} , h ₁₋₄ , h ₂		Head in high level reservoir Head in low level reservoir Head loss due to resistance to flow under
H _A		Head in high level reservoir Head in low level reservoir Head loss due to resistance to flow under steady conditions
H _A H _B , H _O H _{fr} , h ₁₋₄ , h ₂ h _v	-3	Head in high level reservoir Head in low level reservoir Head loss due to resistance to flow under steady conditions V notch weir indicator reading
H _A H _B , H _O H _{fr} , h ₁₋₄ , h ₂ h _v K	-3 N/m ²	Head in high level reservoir Head in low level reservoir Head loss due to resistance to flow under steady conditions V notch weir indicator reading Bulk modulus of elasticity of liquid
H _A H _B , H _O H _{fr} , h ₁₋₄ , h ₂ h _v K	-3 N/m ²	Head in high level reservoir Head in low level reservoir Head loss due to resistance to flow under steady conditions V notch weir indicator reading Bulk modulus of elasticity of liquid Length of pipe
H _A H _B , H _O H _{fr} , h ₁₋₄ , h ₂ h _V K 1	-3 N/m ²	Head in high level reservoir Head in low level reservoir Head loss due to resistance to flow under steady conditions V notch weir indicator reading Bulk modulus of elasticity of liquid Length of pipe Pressure Grid point and intersection point of characteristics curves on x, t plane; frequently

10.			
	Symbols	Units	Descriptive identification
	S		Left grid point on x, t plane; frequently
			used as a subscript
	t	S	Time
	u		Mathematical function
	V	m^3	Volume
	V	m/s	Flow velocity in pipe
	X		Coordinate axis
	x	m	Distance measured in longitudinal space direction
	Y		Coordinate axis
	Z		Coordinate axis
	Z		Elevation above a certain reference level
	α		Angle of valve closure
	г ₁		Equation of motion
	Γ ₂		Equation of continuity
	ε.		Axial strain
	ε		Circumferential strain
	ε C		Poisson's ratio
	ξ		Valve resistance
	ρ	kg/m ³	Liquid density
	σa	N/m ²	Axial stress
	a c	N/m^2	Circumferential stress
	c σ _V	N/m^2	Radial stress
	τ _o	N/m^2	Boundary shear stress at pipe wall
	λ		Parameter (equation (22))
			1//

LIST OF TABLES

Table		Page (I)
1	Instrumentation list	47
2	Observations during steady flow test	49
3	Calculated results for steady flow tests	49
4	List of experimental measurements (for chapter 4)	65
5	Valve resistances for linear closure of the valve	126
6	Computer Tchebichef polynomials coefficients representing valve resistance-angular position of the valve	130
7	List of experimental test conditions for chapter 6 (horizontal line)	85
8	Input data for programme HZD	86
9	List of experimental test conditions for chapter 7 (siphon system)	94
10	Input data for programme WHN	95
11	List of experimental test conditions for chapter 8 (condenser system)	101
12	Input data for programme WCN	102
13	Input data for the modified version of programme WHN	106

LIST OF FIGURES

<u>Figure</u>		Page (I	<u>I)</u>
1	Schematic diagram of a typical cooling water system		
	of a thermal power plant	16	
2	Control volume used for the continuity equation	17	
3	Control volume used for the momentum equation	18	
4	Characteristic curves on the x-t plane	19	
5	Characteristic lines on x-t grid	20	
6	Characteristic lines at boundary conditions on x-t gri	d 21	
7	Sequence of events for two periods after sudden closur of a valve at upstream end of pipe (water-hammer only)		
8	Sequence of events for one period after sudden closure of a valve at upstream end of a pipe (water hammer -	24	
	water column separation)		
9	Three phases of the investigation	26	
10	View of the experimental model	27	
11	Schematic diagram of the experimental model flow circu	it 28	
12	Experimental model arrangements for different phases of the investigation	f 29	
13	View of the means of support of the plexiglass pipe	30	
14	Constructional details of some parts of the model	31	
15	High level water reservoir	32	
16	Low level water reservoir	33	
17	View of valve and its servo-motor	34	
18	View of the specially built electrical function gene- rator	35	
19	Valve closing characteristics (angular position-time)	36	
20	Principle of electric circuit of the function generato	r 38	
21	Choice of voltage and time steps for the function gene rator to obtain a required valve closing characteristi		
22	View of vacuum pump in operation	40	

Figure		Page (II)
23	View of water filter	41
24	Condenser model	42
25	View of the condenser model support in a vertical position	. 43
26	View of the condenser model support in a horizontal position	1414
27	View of the intrumentation	45
28	Schematic diagram of instrumentation set	46
29 .	View of the mounting of a pressure transducer	47
30	View of induction flow-meter	48
31	Schematic diagram showing principle of pressure measurements and their recording on the recorders and the sc	
32	Steady conditions points of measurement	50
33	Steady friction factor in the pipe	51
34	Measured valve resistance for different opening positions at steady flow conditions	52
35	Photographic system arrangement	53
36	Typical frames of the film	54
37	Co-ordinates systems used for calculations of ball diplacement and time for transient flow velocity measurement using the photographic method	
38	Schematic diagram of induction flowmeter	56
39	Experimental measurements during test used for comparison of the photographic and induction system for	
	velocity measurements	57
40	Transient flow velocity changes using the photograph: and induction systems	ic 58
41	Photographic arrangement	59
42	Transient pressure changes resulting from linear clo- sure of the valve in 1 second for a steady flow	
	velocity of 1 m/s	60

Figure		Page (II)
43	View of the tangential and axial strain gauges cemente	ed
	on the outside surface of the pipe at location $\ensuremath{\text{PT}}_2$	
	(Fig. 42)	61
44	Strains at the outside surface of the pipe at lo-	
	cation PT ₂ during transients resulting from linear	
	closure of the valve in 1 second for a steady flow	
	velocity of 1 m/s	62
45	An oscilloscope record (redrawn) showing the pres-	
	sure P_2 and the circumferential strain ϵ_{c2} at loca-	
	tion PT ₂ (Fig. 42), during the transient test whose	
	results are shown in Fig. 44. Triggering time of the	
	scope = 1.4 second. See T-T in Fig. 44	63
46	Strains at the outside surface of the pipe at loca-	
	tion PT ₂ during transients resulting from linear	
	closure of the valve in 2 seconds for a steady flow	
	velocity of 1 m/s	64
47	Transient pressure changes at PT_S (Fig. 42) resul-	
	ting from sudden closure of the auxiliary valve (at	
	downstream end of the pipe) for steady flow velo-	
	cities in the pipe of 0.5 and 0.75 m/s	65
48	Data sheet	66
49	Schematisation of the horizontal line system	67
50	Definition sketch showing space-time grid used for	
	computer programmes	68
51	Principle of linear interpolation used to obtain	
	valve resistance during its closure	69
52	Definition sketch showing space-time grid for the	
	valve boundary condition used for computer programmes	70
53	Definition sketch showing space-time grid for the low	
	level water reservoir boundary condition used for com-	-
	puter programmes	71
54	Comparison of calculated and measured results for test	
	number 6104	72

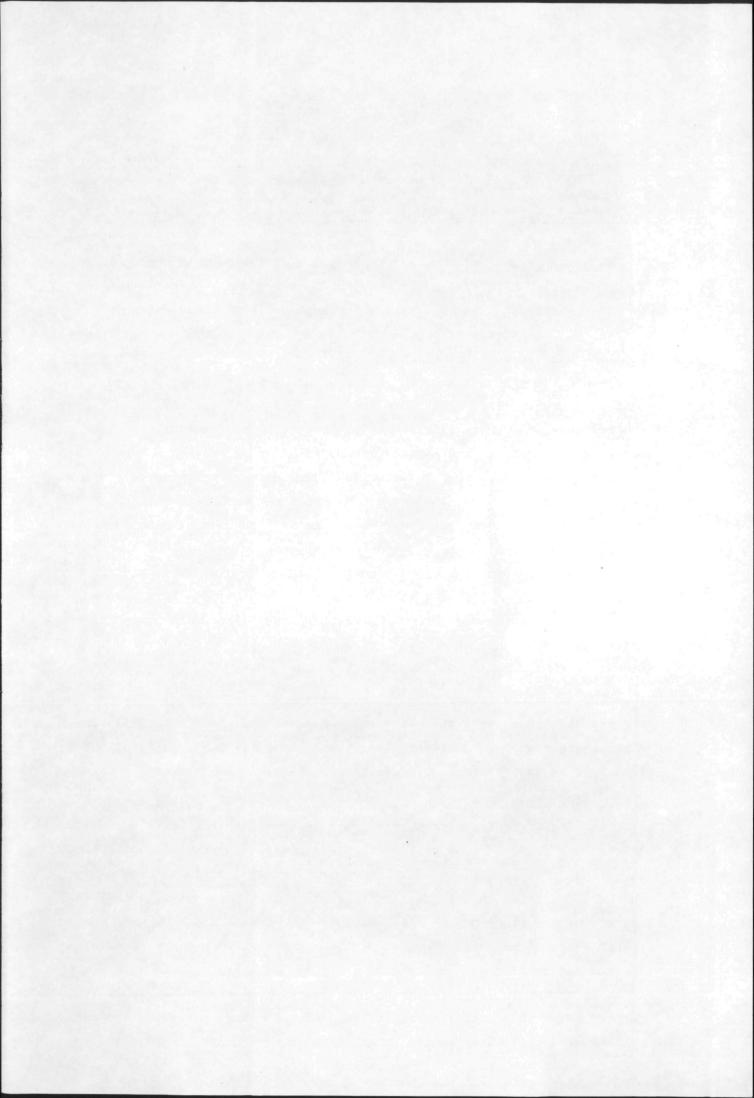
Figure		Page (II)
55	Comparison of calculated and measured results for test	t 73
56	Transient pressure changes resulting from closure of the valve in about 1.7 second for a steady flow velo- city of 1 m/s	74
57	Different frames of the high speed film showing water column separation at the valve	75
58	Finite difference approximation principle	77
59	Space-time grid for finite difference solution using the new mathematical model	78
60	Example of a measurement used for determination of dynamic valve resistances	79
61	Dynamic resistance of valve during closure	80
62	View of arrangement used to visualise small bubbles in the pipe	81
63 ,	Analytical prediction of celerity in bubble and stratified flow regimes (line I), in annular and dispersed flow regimes (line II) 21	82
64	Principle of determination of momentum loss coefficient "c" using logarithmic decrement procedures	83
65	Comparison of experimental measurements and calculated results for test number 6154	84
66	Comparison of experimental measurements and calculated results for test number 6155	85
67	Comparison of experimental measurements and calculated results for test number 6156	86
68	Comparison of experimental measurements and calculated results for test number 6104	87
69	Comparison of experimental measurements and calculated results for test number 6105	88
70	Comparison of experimental measurements and calculated results for test number 6106	89

Figure		Page (II)
71	Experimental transient pressures and velocity changes during test number 8001	90
72	Experimental transient pressure and velocity changes during test number 8005	91
73	View of water column separation at top of the siphon	92
74	Comparison of experimental and calculated results for test number 8008	93
75	Comparison of experimental and calculated results for test number 8011	94
76	Comparison of experimental and calculated results for test number 8016	95
77	Comparison of experimental and calculated results for test number 8018	96
78	Comparison of experimental and calculated results for test number 2034	97
79	Comparison of experimental and calculated results for test number 2043	98
80	Experimental transient pressure and velocity changes during test number 180	99
81	Experimental transient pressure and velocity changes during test number 181	100
82	View of water column separation at top of the condense	er 101
83	Schematic diagram of the condenser system for numerical calculations	102
84	Condenser resistance versus flow velocity in the main pipe (measured under steady flow conditions)	103
85	Comparison of experimental and calculated results for test number C3063	104
86	Comparison of experimental and calculated results for test number C3064	105

<u>Figure</u>	Pag	ge (II)
87	Comparison of experimental and calculated results for test number C3065	106
88	Comparison of experimental and calculated results for test number C2019	107
89	Comparison of experimental and calculated results for test number C1003	108
90	Comparison of experimental and calculated results for test number C5094	109
91	Comparison of experimental and calculated results for test number C6109	110
92	Comparison of measurements of test number C5094 (a condenser system) with measurements of test number 8018 (siphon system)	111
93	Comparison of experimental and calculated results for test number C5094 (based of a siphon schematization)	112
94	Experimental transient pressure and velocity changes during test number C6109 (based on a siphon schemati-	
	zation)	113
95	Experimental transient pressure and velocity changes during test number C6107 (based on a siphon schemati-	
	zation)	114

LIST OF COMPUTER PROGRAMMES

		Page (II)
PDV	Digital Calculations of Velocities from Photo-Analyzer	
	Data	115
HOZ	Numerical Computations for Transients in a Horizontal	
	Line Based on Method of Characteristics	117
HZD	Numerical Computations for Transients in a Horizontal	
	Line Based on the New Mathematical Model	123
WHN	Numerical Computations for Transients in the Siphon	
	System Based on the New Mathematical Model	131
WCN	Numerical Computations for Transients in the Condenser	
	System Based on the New Mathematical Model	143
	Listing of Modifications in Computer Programme WHN	157



CHAPTER 1

1. INTRODUCTION

1.1. General Aspects of the Problem and Motivation

A power failure results in the stoppage of the pump in the cooling water system of a thermal power station. This would cause the initiation of rarefaction waves in the system. The magnitudes of these waves depend on the initial (steady) flow velocity in the system as well as the interruption rate. If these rarefaction waves are large enough, vapour pressure is reached and the phenomenon of water column separation is observed. Vapour pressure is easily reached as most cooling water systems use a siphon system. Thus, they have already low pressures at the condenser top during normal running conditions. As the vapour pressure is reached a vapour void is formed and it continues to grow. In the meantime, the water column between the vapour void at the top of the condenser and the downstream end of the exit pipe stops and then reverses its motion under the influence of the pressure difference between the downstream end pressure and the vapour pressure at the void. Thus, the void grows and then diminishes and finally it collapses. The collapse of the vapour void results in a large pressure surge. The resulting pressure waves travel in the system and the phenomena repeat and damp away. Such transient conditions have been observed. In some instances they caused some damage.

The continuous tendency in growth of power plant sizes involving larger installations and higher flow velocities as well as the security precautions necessary for nuclear power plants motivate the investigation of transient conditions in cooling water systems of thermal power plants.

The number of the recent publications |25, 28, 36, 46| presenting efforts of different researchers to gain insight into the problem demonstrates the inportance as well as the current need for this investigation. The above references (some of which report work done during the same time the work presented in this dissertation was underway) dealt with some aspects of the problem. In reference |36|, Mc Donald and Pilkington, presented a numerical method for calculating surges occurring in cooling water systems due to emergency closure of the pump discharge valves. This method is based on the inelastic water column theory. Some numerical results calculated using this method are found in |36|. However, these results were not compared with experimental data. Actual measurements of transient

pressures during start up and shut down for 120 MW power station are found in reference |46| by Scarborough and Webb. These measurements show large pressure surges during the resulting transients. Jansa's paper |25| covered the disign considerations for cooling water systems for thermal power plants in order to avoid water column separation. He outlined the numerical procedures which he proposed to be adapted for design estimations. These procedures are based on rigid column analysis. In this paper, the emphasis was on taking measures to avoid the occurrence of water column separation during the transients. Kovats |28| discussed the possible unfavourable conditions that may occur in different types of cooling water systems. He covered the design aspects and outlined some of the situations that could result in critical conditions during the transients. He also discussed preventive steps to be taken to avoid water hammer surges.

All the above-mentioned investigations, and many other which will be considered later at a more appropriate place, turn out to yield results that are still not satisfactory when compared with experimental evidence. So it has been considered necessary to take up the matter once again, in particular in view of transient pressure phenomena that may occur in cooling water systems of thermal power plants. Such an investigation requires a better understanding of water hammer - water column separation phenomena still.

A dependable method for predicting pressure changes during transient conditions in these systems is wanted. It is to be hoped that the work presented here contributes to these objectives.

1.2. Method of Approach to the Investigation

It was felt that experimental measurements are needed to obtain good and sound information about water hammer - water column separation phenomena. Thus, we decided to build an experimental model. Two considerations were taken into account at that point. First we felt that the model should be built to simulate a typical cooling water system (Fig. 1) rather than one particular system of a certain power plant. An obvious advantage of such an idea was that it would permit greater flexibility. **)

^{*)}

An example of the other alternative is the experimental model simulating the "Casella" power station cooling water system. Fanelli | 16 | gives very good information about simulation of this prototype by the model.

The other consideration that was decided upon was to carry out the investigation in three testing phases:

- 1. horizontal line
- 2. siphon
- 3. siphon with the condenser on its top

This approach gave a gradual insight in the problem. In addition, the following two major considerations were made in the design of the experimental model:

- a. the simulation of the pressure drops due to the deceleration of the pump in the prototype system was to be achieved by closing a valve according to prescribed conditions.
- b. it was felt necessary to see through the pipe wall of the model; thus a "plexiglass" pipe was used.

The experimental model was built bearing in mind the objectives of the investigation and the considerations discussed above. Experimental tests were started. In the meantime computer programmes were prepared for numerical computations to predict the resulting pressures.

Through the course of the investigation efforts in both the experimental testing and the numerical computations were running in parallel. Qualitative examination of the experimental results lead to better understanding. Quantitative experimental measurements were planned and performed in view of the ideas that were developing as well as the numerically computed results.

The comparison of the experimental and calculated results resulted in attempts to modify the method of characteristics to obtain a more dependable numerical method. A new mathematical model was developed. Numerical computations were done using this new model. Experimental tests were performed to allow more accurate evaluation of input data for the digital programmes based on the new model. Special care had to be given to boundary conditions presentation in the numerical calculations. Efforts were continued in comparing calculated and measured results for the three testing phases.

In the following section, an outline of the investigation development as presented in the following chapters is found.

1.3. Outline of Dissertation

CHAPTER 2 presents a short literature survey of water hammer and water column separation. Also, it gives a derivation of the basic laws of

fluid mechanics for water-hammer applications. The characteristics method commonly used for solving these equations is explained. The finite difference solution procedures which form the basis of the numerical solution of water-hammer problems is found at the end of this chapter. Two illustrative simple examples of water-hammer and water hammer - watercolumn separation sequence of events resulting from sudden closure of a valve at the upstream end of a pipe are presented at the end of this chapter.

CHAPTER 3 consists of a number of sections dealing with the experimental side of the study. The first section describes different aspects of the experimental testing circuit used for simulating hydraulic transients similar to the ones occurring in a typical cooling water system of a thermal power plant. The instrumentation used for carrying out the experimental measurements is presented. A description of the experimental measurements is then found. These experimental measurements include: measurement of transient flow velocities, photographic studies of water column separation, experimental evaluation of elastic behaviour of the pipe wall material under loading conditions resulting from typical hydraulic transients and finally the transients tests. The latter constitute the main results of the experimental study and were carried out for three phases of the investigation, namely transients in: a horizontal line, siphon system and a condenser system.

CHAPTER 4 deals with comparison of experimental measurements to calculated results using classical water-hammer calculations. These comparisons are made for transients resulting from the closure of the valve on the upstream end of the horizontal pipe line. First, the schematization of the pipe line is discussed. Then the principle of the choice of the input data for a digital computer programme HOZ is presented. The programme predicts the pressure and velocity changes using calculations based on the finite difference solution of the equations describing one-dimensional unsteady flow, using the method of characteristics. A section of chapter 4 is devoted to the description of the investigated conditions. A comparison of the measured and calculated results is then introduced. This is followed by a photographic study of water column separation occurring behind the valve during a typical transient test. The latter two sections lead to some significant findings that are the subject of the last section in this chapter. These significant findings form the basis of an attempt to modify the analysis of the equations describing the flow.

CHAPTER 5 gives a new mathematical model to describe the flow conditions of unsteady one-dimensional flow for hydraulic transients involving sub-atmospheric pressures. A finite difference solution of the proposed model is found also in this chapter.

CHAPTER 6 presents transients resulting from closure of the valve at the upstream end of the horizontal pipe. The study gives both experimental results and calculated results based on the new mathematical model discussed in chapter 5. A comparison of the experimental measurement and calculated results is found.

CHAPTER 7 discusses transients resulting from the closure of the valve at the upstream of the siphon. Experimental neasurements and calculated results of such conditions are found.

CHAPTER 8 covers transient conditions resulting from the closure of the valve at the upstream end of the siphon with the condenser model in it. Experimental measurements as well as numerically predicted data are found.

CHAPTER 9 gives a number of conclusions of this study. Also a few suggestions and recommendations for futher studies are listed.

CHAPTER 2

2. WATER HAMMER AND WATER COLUMN SEPARATION ANALYSIS

In this chapter, first, a brief review of literature on water hammer and water column separation is presented. Some other work in related subjects that is of value to some aspects of the phenomena is cited.

In the second part of this chapter, the basic equations of fluid mechanics for one-dimensional transient flow are formulated. Solutions of these equations subject to boundary conditions representing hydraulic devices are discussed. The principle of computer simulations of these solutions is found in the last section of this chapter.

2.1. Literature Survey

The phenomenon of water hammer has been known to hydraulicians since the 19th century. By the end of the 19th century Joukowksy published his treaties |26| on the phenomenon of water hammer in closed circuits. Allievi | 1 | presented a more extended mathematical work together with a graphical treatment of water hammer in 1913. Allievi's work became the basis of the water hammer analysis for transient flow in closed conduits. Since the early years of the 20th century efforts in development of analytic formulation as well as graphical approximate solutions continued, as the practical realization of the phenomenon in different hydraulic systems continuously grew. It is Riemann's explicit solution of the second order differential equation that became the principle of the method of characteristics | 42, 52 | . It is worth mentioning here some of these works: Bergeron 3 offered an extensive study of the graphical solutions of water hammer in hydraulics. Rich |43| used the Laplace-Mellin transformation in water hammer analysis. Parmakian 40 published a comprehensive book on water hammer analysis in 1955.

However, solutions of water hammer problems using such techniques as the ones mentioned above were very tedious and time consuming. It was the introduction of the high speed digital computer that enabled investigators in this area to solve a great variety of problems of transient flow applications. Recent publications e.g. |29, 54, 55, 56, 57| contain solutions of a large number of different problems of transient flow using numerical methods with the aid of digital computers. Streeter and Wylie's book |58| offered workers in this area an excellent text book that deals in a rather

extensive way with different aspects of water-hammer ranging from rigid column and elastic column formulation to numerical methods of solutions of water-hammer problems. Also, recently Analog Computers (Wood |67|) and Hybrid Computers (De Hes |11|) were used for solution of water hammer problems.

Experimental measurements in water hammer received considerable attention from hydraulicians. The literature is rich with experimental measurements in different hydraulic systems. However, we note that the literature contains only transient pressure measurements without any significant data of transient velocity measurements. It is believed that measurements would be very useful and would complement the pressure measurements.

It was the treatment of some of water hammer practical problems that began to focus the attention on the phenomenon of water column separation | 13, 14, 15, 18, 30, 44, 48|. Escande | 15| used a technique based on the graphical solution of water hammer for the evaluation of the pressures peaks resulting from water column separation. Li's theoretical work on column separation downstream of a valve |31| considered steady friction and used rigid column theory. Li and Walsh |32| developed a method for predicting maximum pressure in the collapse of the initial cavity downstream of a valve. This study neglected friction but took into account compressibility and had some experimental verification. Baltzer |2| studied the mechanics of the flow under the cavity resulting from column separation. He assumed an open flow for water flowing underneath the vapour cavity. He compared predicted calculated results with experimentally measured results. Coincident with Baltzer's work, Siemons |50| developed a mathematical technique similar to Baltzer's.

However, |50| does not include experimental results, Baltzer's experiments showed that the system (transient flow in the horizontal pipe with water column separation) lost momentum much faster than predicted. That made Weyler |66| to start his investigation of the effect of cavitation bubbles on momentum loss in transient pipe flow.

Other recent works in this area include |5| by Brown who assumed localized air bubbles at particular points along the pipe whose compression and expansion account for the momentum decrease associated with the phenomena. Dijkman and Vreugdenhil |12| approached the problem in a similar way in a theoretical analysis. Both Baltzer's and Weyler's works offer excellent approaches and treatments of the phenomena and will be referred to in many instances in the course of presentation of the current study.

It is worth noting at this moment two recent papers by Tanahashi and Kasahara |60, 61|. In the first paper, they presented an analysis of water hammer - water column separation. Particular effort was devoted to the adaption of the method of characteristics for digital computations. Interestingly enough they applied their technique to two cooling water systems of two different power plants. However, |60| does not include measurements. The same authors |61|, compared experimental and theoretical results of the water hammer with water column separation. Their study was done for a siphon model and their calculated results were based on a combined rigid column-elastic column analysis. The study is interesting but lacks the introduction of the influence of the momentum loss associated with the phenomena.

Although the above-mentioned works cover a number of aspects of water hammer - water column separation, the results they yield are still not satisfactory when compared with the experimental evidence.

Other works in related subjects that would be of value to note here that throw light on (and help in understanding) particular aspects of the phenomena follow. Daily, Hankey, Olive and Jordan 10 examined friction losses in unsteady flows. Zielke | 68 | examined frequency dependent friction in transient pipe flow. Contractor |9| studied the reflection of water hammer waves from minor losses in devices such as orifices. Studies such as those of Henry, Grolmes, Fauske 21, Fauske 17 and Silbermann | 51 | on the subject of wave propagation in gas-liquid mixtures help in understanding the celerity decrease associated with water hammer column separation 66. The bubbles that arise during column separation are in nature cavitation bubbles and their effects are not observable under steady conditions. However, steady cavitating flows are obtainable and have been studied. Chivers |8|, Ripken and Killen |45| and Stepanoff |53| discuss the role of gaseous nuclei in cavitation inception. Holl 23 discussed the role of nuclei in cavitation. Hsieh |24| gives extensive formulation for bubble dynamics. However, most cavitation studies such as those above do not deal with the bubbles in an unsteady flow from a theoretical basis. Weyler's work was aimed at this point |66|. His work is based on Rayleigh's bubble model. References | 62, 65 | cover much of the basis of Weyler's theoretical work and offer a good background for discussions presented in this study.

2.2. Basic Laws of Fluid Mechanics for Water Hammer Applications

Conservation of mass and momentum for a one dimensional transient flow are considered. The following formulations follow to a large extent the presentation of Weyler |66|. The analysis assumes:

- 1. the fluid in the flow system is in liquid form. It is elastic and of a homogeneous density.
- 2. the pipe is constructed of a sectionally homogeneous, isotropic elastic solid in which the stresse never exceed the elastic limit of the material.
- 3. the velocity and pressure in the pipe are considered to be uniformly distributed over any cross section transverse to the pipe with the result that the flow can be treated as one dimensional, closed conduit flow.
- 4. the frictional resistance encountered with transient flow is assumed to be proportional to some power of the mean velocity in the cross section transverse to the flow.

Consider a continuum analysis |6, 38| with two independent variables: the time t and the distance along the axis of the pipe measured from an arbitrary fixed reference point x. It is assumed that the changes in the properties V, ρ , p across δx can be presented by the first two terms of a Taylor series expansion. With reference to Fig. 2, the continuity equation can be written as:

$$\frac{\partial}{\partial t} \left(\rho A \delta x \right) + \left(\rho + \frac{\partial \rho}{\partial x} \delta x \right) \left(A + \frac{\partial A}{\partial x} \delta x \right) \left(V + \frac{\partial V}{\partial x} \delta x \right) - \rho A V = 0 \tag{1}$$

Expanding equation (1), neglecting terms of the second order in δx , and dividing by ρA δx , we obtain

$$\frac{1}{\rho} \frac{\partial \rho}{\partial t} + \frac{V}{\rho} \frac{\partial \rho}{\partial x} + \frac{1}{A} \frac{\partial A}{\partial t} + \frac{V}{A} \frac{\partial A}{\partial x} + \frac{1}{\delta x} \frac{\partial \delta x}{\partial t} + \frac{\partial V}{\partial x} = 0$$
 (2)

Using total derivatives, equation (2) takes the form:

$$\frac{1}{\rho} \frac{d\rho}{dt} + \frac{1}{A} \frac{dA}{dt} + \frac{1}{\delta x} \frac{\partial \delta x}{\partial t} + \frac{\partial V}{\partial x} = 0 \tag{3}$$

where

$$\frac{\mathrm{d}}{\mathrm{d}t} = \frac{\partial}{\partial t} + V \frac{\partial}{\partial x} \tag{4}$$

Recalling the definition of the bulk modulus of elasticity K

$$K = -\left(\frac{dp}{d\psi/\psi}\right)_{s} = \frac{dp}{d\phi/\phi} \tag{5}$$

equation (5) can be written in the form:

$$\frac{\mathrm{d}\rho}{\rho} = \frac{\mathrm{d}p}{K} \tag{6}$$

Hence:

$$\frac{1}{\rho} \frac{d\rho}{dt} = \frac{1}{K} \frac{d\rho}{dt} \tag{7}$$

The second and third terms in equation (3) arise from the deformation of the pipe both radially and axially. They are therefore functions of the radial and axial stresses and strains in the pipe. It can be shown |2,63| that: *)

$$\frac{1}{A}\frac{dA}{dt} + \frac{1}{\delta x}\frac{\partial \delta x}{\partial t} = \frac{dp}{dt}\frac{D}{\delta}\frac{c(\mu)}{E}$$
(8)

where D is the pipe diameter, δ its wall thickness, E the pipe modulus of elasticity and $c(\mu)$ is a constant depending on the type of the support of the pipe as well as Poissons ratio of the pipe material. Defining a **

$$a = \sqrt{\frac{K/\rho}{1 + \frac{K D c(\mu)}{E \delta}}}$$

using equations (7) - (9), the second and third terms in equation (3) can be replaced by $(\frac{1}{\rho_B 2} - \frac{1}{K}) \frac{dp}{dt}$; thus equation (3) can be written as:

$$\frac{1}{\rho} \left(\frac{\partial p}{\partial t} + V \frac{\partial p}{\partial x} \right) + a^2 \frac{\partial V}{\partial x} = 0 \tag{10}$$

To write the continuity in a more suitable form, the piezometric pressure H (Fig. 2) is used. Since

$$p = \rho g (H - Z) \tag{11}$$

differentiation of both sides of (11) (and bearing in mind that ρ changes are very small compared with H changes) yields

$$\frac{\partial p}{\partial t} + V \frac{\partial p}{\partial x} = \rho g \left(\frac{\partial H}{\partial t} + V \frac{\partial H}{\partial x} + V \sin \alpha \right)$$
 (12)

where

^{*)} see also appendix B

^{**)} The choice of such a term makes it convenient to have the flow represented by a wave equation (with some further assumptions |40|). "a" would turn out to be the wave speed of propagation.

$$\frac{\partial Z}{\partial x} = -\sin \alpha$$

Thus the continuity equation takes the form

$$\frac{\partial H}{\partial t} + \frac{a^2}{g} \frac{\partial V}{\partial x} + V \frac{\partial H}{\partial x} + V \sin \alpha = 0$$
 (13)

Now we consider the momentum equation in the x direction. With reference to Fig. 3 which shows the same control volume shown in Fig. 2 and keeping the assumptions mentioned before in mind, the momentum equation can be written as:

$$\frac{\partial}{\partial t} (\rho V A \delta x) + (\rho + \frac{\partial \rho}{\partial x} \delta x) (A + \frac{\partial A}{\partial x} \delta x) (V + \frac{\partial V}{\partial x} \delta x)^{2} - \rho A V^{2}$$

$$+ \frac{\partial \rho}{\partial x} \delta x A + \tau_{o} \pi D \delta x - \rho A \delta x g \sin \alpha = 0$$
(14)

Expanding equation (14) and neglecting terms of the second order in δx and dividing by $\rho A \delta x$ we obtain for a circular pipe ($A = \frac{\pi}{L} D^2$):

$$V \left[\frac{1}{A} \frac{\partial A}{\partial t} + \frac{1}{\rho} \frac{\partial \rho}{\partial t} + \frac{\partial V}{\partial x} + \frac{V}{A} \frac{\partial A}{\partial x} + \frac{V}{\rho} \frac{\partial \rho}{\partial x} + \frac{1}{\delta x} \frac{\partial \delta x}{\partial t} \right]$$

$$+ \frac{\partial V}{\partial t} + V \frac{\partial V}{\partial x} + \frac{1}{\rho} \frac{\partial \rho}{\partial x} + \frac{\mu_{TO}}{\rho_{D}} - g \sin \alpha = 0$$
(15)

The set of terms within the brackets in equation (15) is the continuity equation as given by equation (2) and is therefore zero. Again using the piezometric head (11), equation (15) reduces to:

$$\frac{\partial H}{\partial x} + \frac{1}{g} \frac{\partial V}{\partial t} + \frac{V}{g} \frac{\partial V}{\partial x} + \frac{1}{g} \frac{\mu_{\tau_0}}{\rho D} = 0$$
 (16)

The shear stress at the wall is usually expressed as:

$$\tau_{o} = \rho f \frac{V|V|}{8} \tag{17}$$

where f is the Darcy Weisbach friction coefficient. Substituting from (16) into (18) we obtain:

$$\frac{\partial H}{\partial x} + \frac{1}{g} \frac{\partial V}{\partial t} + \frac{V}{g} \frac{\partial V}{\partial x} + \frac{f V V}{2 g D} = 0$$
 (18)

The absolute value sign is introduced into the frictional term so that it has the proper sign depending on the direction of flow.

2.3. Characteristics Method

The two equations (13) and (18) are solved simultaneously to obtain the head and velocity as functions of x and t. A commonly used method, for this solution of the two hyperbolic, quasi-linear, partial differential equations is the method of characteristics. The expressions of (18) and (13) are identified as follows:

$$\Gamma_{1} = \frac{\partial V}{\partial t} + V \frac{\partial V}{\partial x} + g \frac{\partial H}{\partial x} + \frac{f V |V|}{2 D} = 0$$
 (19)

$$\Gamma_2 = + \frac{a^2}{g} \frac{\partial V}{\partial x} + \frac{\partial H}{\partial t} + V \frac{\partial H}{\partial x} + V \sin \alpha = 0$$
 (20)

The two expressions Γ_1 and Γ_2 are combined linearly using an unknown multiplier λ .

$$\Gamma = \Gamma_1 + \lambda \Gamma_2 \tag{21}$$

or

$$\Gamma = \left[\frac{\partial V}{\partial t} + \frac{\partial V}{\partial x} \left(V + \frac{a^2}{g} \lambda \right) \right] + \lambda \left[\frac{\partial H}{\partial t} + \frac{\partial H}{\partial x} \left(V + \frac{g}{\lambda} \right) \right] + \lambda V \sin \alpha + \frac{f}{2D} V |V| = 0$$
(22)

Since the continuum analysis involves the assumption V = V(x,t) and H = H(x,t), we have:

$$\frac{\mathrm{dV}}{\mathrm{dt}} = \frac{\partial V}{\partial t} + \frac{\partial V}{\partial x} \frac{\mathrm{dx}}{\mathrm{dt}} \tag{23}$$

and

$$\frac{dH}{dt} = \frac{\partial H}{\partial t} + \frac{\partial H}{\partial x} \frac{dx}{dt} \tag{24}$$

Equation (22) can be written in the form:

$$\Gamma = \frac{dV}{dt} + \lambda \frac{dH}{dt} + \lambda V \sin \alpha + \frac{f}{2D} V |V| = 0$$
 (25)

if the following conditions are chosen

$$\frac{dx}{dt} = V + \frac{a^2}{g} \lambda = V + \frac{g}{\lambda}$$
 (26)

The solution of (26) gives:

$$\lambda = \pm \frac{g}{a} \tag{27}$$

which makes

$$\frac{\mathrm{dx}}{\mathrm{dt}} = V + a \tag{28}$$

For the case of λ = + $\frac{g}{a}$ equations (25) and (28) form a pair of ordinary differential equations called the C^+ characteristic equations

$$\frac{dH}{dt} + \frac{a}{g} \frac{dV}{dt} + V \sin \alpha + \frac{a}{g} \cdot \frac{f}{2D} V |V| = 0$$
 (29)

$$\frac{\mathrm{dx}}{\mathrm{dt}} = V + a \tag{30}$$

For $\lambda = -\frac{g}{a}$ the resulting pair along C takes the forms:

$$+ \frac{dH}{dt} - \frac{a}{g} \frac{dV}{dt} + V \sin \alpha - \frac{a}{g} \cdot \frac{f}{2D} V |V| = 0$$
 (31)

$$\frac{\mathrm{dx}}{\mathrm{dt}} = V - a \tag{32}$$

The reader has to bear in mind that in the foregoing x has two meanings. One gives the position of a material fluid element at time t, so that V = dx/dt, the other gives the position of the disturbance at time t in a (x,t)-plane, as given by Eq. (28). So one could write V = dx'/dt, where x' is again the position of a fluid element as determined by the flow velocity, and x" is the position of the disturbance at time t relative to the flowing fluid element. Hence dx"/dt = + a. For simplicity x = x' + x'' has been written, so that x satisfies the expression Eq. (28). In general C and C are curves on the x,t plane (Fig. 4) as V is variable. These curves are defined by the total differential expressions given by Equations (30) and (32) respectively. These characteristic curves represent the pathes along which infinitesimally small velocity and pressure head differences propagate. For a wide range of water hammer applications (including the current work) the fluid velocity is very much less than the wave speed. Thus, it is neglected in (30) and (32), the characteristic equations become:

for
$$C^{+}$$
 $\frac{dH}{dt} + \frac{a}{g} \frac{dV}{dt} + \frac{a}{g} \frac{f}{2D} V|V| + V \sin \alpha = 0$ (33)

$$\frac{\mathrm{dx}}{\mathrm{dt}} = + a \tag{34}$$

and

for
$$C^- \frac{dH}{dt} - \frac{a}{g} \cdot \frac{dV}{dt} - \frac{a}{g} \frac{f}{2D} V |V| + V \sin \alpha = 0$$
 (35)

$$\frac{\mathrm{dx}}{\mathrm{dt}} = -a \tag{36}$$

The characteristic curves are then straight lines with slopes + a and - a as given by equations (34) and (36), respectively. We note for a horizon-tal pipe $\alpha = 0$ and the last term in each of equations (33) and (35) vanishes.

2.4. Finite Difference Solution

The numerical solution of a water hammer problem is essentially the solution of the continuity and momentum equations in the forms given by (13) and (18) subject to initial and boundary conditions:

- a. conditions at t = 0, that is the steady conditions before transients start
- b. conditions representing hydraulic devices on the pipe line system such as reservoirs, valves etc.

The finite difference technique |58|, commonly used, assumes the first order finite difference approximation of the characteristic equations (33 - 36). With reference to Fig. 5, if H and V are known at points R and S on the x-t grid, then the values of H and V at point P can be approximated by:

c+ :

$$V_{P} - V_{R} + \frac{g}{a} (H_{P} - H_{R}) + \frac{f V_{R} |V_{R}| (t_{P} - t_{R})}{2 D} + \frac{g}{a} V_{R} \sin \alpha (t_{P} - t_{R}) = 0$$
 (37)

$$x_{p} - x_{R} = a (t_{p} - t_{R})$$
 (38)

and

C :

$$V_{P} - V_{S} - \frac{g}{a} (H_{P} - H_{S}) + \frac{f V_{S} |V_{S}| (t_{P} - t_{S})}{2 D} - \frac{g}{a} V_{S} \sin \alpha (t_{P} - t_{S}) = 0$$
 (39)

$$x_{p} - x_{s} = -a (t_{p} - t_{s})$$
 (40)

Equations (37) and (39) may be added and subtracted to obtain H_{p} and V_{p}

$$\begin{aligned} & v_{\rm P} = 0.5 \left[v_{\rm R} + v_{\rm S} + \frac{g}{a} (H_{\rm R} - H_{\rm S}) - \frac{f}{2D} v_{\rm R} |v_{\rm R}| (t_{\rm P} - t_{\rm R}) - \frac{f}{2D} v_{\rm S} |v_{\rm S}| (t_{\rm P} - t_{\rm S}) - \frac{g}{a} v_{\rm R} \sin \alpha (t_{\rm P} - t_{\rm R}) + \frac{g}{a} v_{\rm S} \sin \alpha (t_{\rm P} - t_{\rm S}) \right] (41) \end{aligned}$$

and

$$H_{P} = 0.5 \left[H_{R} + H_{S} + \frac{a}{g} (V_{R} - V_{S}) - \frac{a}{g} \frac{f}{2D} V_{R} |V_{R}| (t_{P} - t_{R}) + \frac{a}{g} (v_{R} - v_{S}) \right]$$

$$+\frac{a}{g}\frac{f}{2D}V_{S}|V_{S}|(t_{P}-t_{S})-V_{R}\sin\alpha(t_{P}-t_{R})-V_{S}\sin\alpha(t_{P}-t_{S})$$
(42)

If R and S represent known conditions at the same time level, then H and V at the later lime level of P can be solved for, directly. This can be carried out in progression. This in fact represents the principle of computer simulation for the solution of the problem. A grid on the x-t diagram (Fig. 5) is chosen. The pipe is divided into a number of equal length intervals Δx , the time interval of the grid is:

$$\Delta t = \frac{1}{a} |\Delta x| \tag{43}$$

with the H and V known at points at time t, H and V at the different locations at time t + Δt can be calculated using equations (37) and (39) or (41 - 42). Having obtained the values of H and V at t + Δt the solution repeats itself for t + Δt . Then it is continued till the desired time limit. It is necessary to build the boundary conditions into the finite difference solutions. This is done using the characteristic equations at the boundary. As two examples, we consider a valve as a left end boundary (at x = 0) and a reservoir as a right end boundary (at x = L).

a. valve as a left end boundary

The following relation between the pressure head drop across the valve and the flow velocity is assumed:

$$H_{us} - H_{p}(0, t + \Delta t) = \xi(t + \Delta t) \cdot \frac{V_{p}(0, t + \Delta t)}{2 g} \cdot |V_{p}(0, t + \Delta t)|$$
 (44)

where H is the pressure head upstream the valve

 H_{p} , (0, t + Δ t) is the pressure head at a point x = 0 at the time t + Δ t (just after the valve)

 V_p , (0, t + Δ t) is the velocity at point x = 0 at time t + Δ t

 $\xi(t+\Delta t)$ is the valve resistance, for its particular opening position at time $t+\Delta t$

When the valve is completely closed equation (46) is replaced by a dead end condition that is:

$$V_{p}(0, t + \Delta t) = 0$$
 (45)

Besides, the characteristics equations in the finite difference form along C (Fig. 6) are still valid. Thus equations (39 - 40) can be written:

$$V_{P}(0, t + \Delta t) - V_{S}(0 + \Delta x, t) - \frac{g}{a} H_{P}(0, t + \Delta t) - H_{S}(0 + \Delta x, t)$$

$$+ \frac{f}{2D} V_{S}(0 + \Delta x, t) |V_{S}(0 + \Delta x, t)| \Delta t - \frac{g}{a} V_{S}(0 + \Delta x, t) \sin \alpha \Delta t = 0$$
 (46)

and

$$\Delta x = |-a \Delta t| \tag{47}$$

Either (44) or (45) together with equation (46) is solved simultaneously, to obtain the head and velocity H_{p} , (0, t + Δ t) and V_{p} , (0, t + Δ t) knowing the values of the other conditions in the two equations from the preceding time step.

b. a reservoir as a right end boundary

If $_{\circ}^{\text{H}}$ is a constant value giving the level in the reservoir, the following relation is assumed

$$H_{p''}(L, t + \Delta t) = H_{Q}$$
(48)

Besides the characteristics finite difference equations along C⁺ (Fig. 6) are valid

$$V_{P''}(L, t + \Delta t) - V_{R''}(L - \Delta x, t) + \frac{g}{a} \left[H_{P''}(L, t + \Delta t) - H_{R''}(L - \Delta x, t) \right]$$

$$+ \frac{f}{2D} V_{R''}(L - \Delta x, t) |V_{R''}(L - \Delta x, t)| \Delta t + \frac{g}{a} V_{R''}(L - \Delta x, t) \sin \alpha \Delta t = 0$$
 (49)

and

$$\Delta x = a \Delta t$$
 (50)

Again, in this case equation (48) and (49) are solved simultaneously during the step by step computations.

2.5. <u>Illustrative Description of the Phenomena of Water Hammer and Water Column</u> Separation

In this section two simple examples demonstrating the sequence of events after sudden closure of a valve at the upstream end of a pipe are presented. In the first example conditions are assumed such that during the transients, the pressures in all points remain higher than the vapour pressure and only water hammer is observed. In the second case the conditions are chosen such that the pressure behind the valve reaches vapour pressure of the fluid resulting in water column separation together with water hammer.

Sequence of Events Following Sudden Closure of a Valve at the Upstream End of a Pipe-line

a. Water hammer only:

The case of instantaneous stoppage of a flow at an upstream valve in a single horizontal pipe is considered. Friction and minor losses are neglected. The instant the valve is closed, the fluid immediately adjacent to the valve is brought from velocity V_o to rest due to the depression developed at the face of the valve. As soon as the first layer (the one adjacent to the valve) is brought to rest the same action is applied to the next layer of the fluid bringing it to rest. In this manner a rarefaction wave is visualized travelling towards the downstream end of the pipe at some wave speed "a" and the amplitude of the pressure wave is large enough to apply just the impulse to the fluid to bring it to rest. The wave speed of the pressure wave propagation in the fluid depends on the elasticity of the fluid as well as the elasticity of the pipe wall material, its diameter, thickness and means of support. The amplitude of the pressure (rarefaction) wave is given by Joukowsky's law:

$$\Delta H = \frac{a \Delta V}{g}$$

Fig. 7a* shows in a stereogram the sequence of events following the sudden closure. Initially the pressure in the whole pipe is assumed to be the reservoir pressure (0.0). As can be seen from the figure the rarefaction wave travels from the valve to the reservoir in time $\frac{L}{a}$. At t = $\frac{L}{a}$ the whole pipe is at a lower pressure than that of the reservoir and the fluid is at rest in the whole pipe. With this unstable situation, the fluid starts to flow into the pipe at the reservoir end and the pressure rises to the reservoir pressure. This action propagates towards the valve at the upstream end of the pipe and it reaches there at time $\frac{2L}{a}$ (see Fig. 7). At that instant, the fluid in the whole pipe is moving with a velocity $-V_{0}$ and the whole pipe is at the reservoir pressure. The first layers of the fluid adjacent to the valve (dead end) now start to stop and a pressure wave starts to propagate towards the reservoir at the downstream end of the pipe. This action travels in the pipe from time $\frac{2L}{a}$ till $\frac{3L}{a}$ when it reaches the reservoir.

^{*)} Fig. 7^b shows pressure and velocity histories at different locations on the pipeline. Experimental results in the following chapters will be presented in a similar manner.

At that instant the unstable situation (due to the difference in the pressure between the fluid layer just adjacent to the reservoir and the reservoir pressure) will cause the fluid to flow outwards from the pipe (with velocity V_0) and the pressure drops to the reservoir pressure. This action travels towards the valve and reaches it at $\frac{4L}{a}$. At that moment the whole pipe is under the same situation as at time t = 0. The events explained above repeat themselves with a period $T = \frac{4L}{a}$. In actual systems, friction acts to reduce the energy to zero in few cycles.

b. Water hammer - water column separation:

In the case discussed above the different values (V_0 , a) where chosen such that the pressure at any part of the pipe did not drop to the vapour pressure of the fluid (P_v). In the case to be discussed here, conditions are chosen such that the resulting depression due to the instantaneous closure of the valve is large enough to cause the pressure at the valve to drop to the vapour pressure of the fluid. The sequence of events following the closure of the valve can be followed on the stereogram shown in Fig. 8a.

In the current example, the hypothetical method introduced by Escande | 15 | is used to demonstrate the events associated with water column separation. Escande assumed that during hydraulic transients if the pressure drops to the vapour pressure, a vapour cavity starts to form. The cavity is assumed to fill the whole cross sectional area of the pipe and its pressure remains at a constant value equal to the vapour pressure. As the pressure at the cavity is assumed to remain constant, water hammer waves that travel in the water column are assumed to reach a reservoir condition upon their arrival at the cavity. In the mean time, the arrival of the water hammer waves to the cavity result into changes in its size. With the assumption that the cavity fills the whole cross section of the pipe, the terminal velocity of the water column governs the growth and later the diminution till the collapse of the cavity.

In building up the diagram shown in Fig. 8a the values of V_0 and a as well as the vapour pressure P_v were assigned in a specific way. V_0 is chosen to be equal to $3v^*$ where $v = \left| \frac{gPv}{a} \right| **$ With reference to Fig. 8,

^{*)} This choice is arbitrary as will be explained later ***) Note Joukowksy's formula $\Delta H = \frac{a}{g} \Delta V$

as the valve is closed instantly, the fluid adjacent to it tends to stop. The depression impulse causes the pressure at the valve to drop to the vapour pressure. The result would be a creation of a reservoir at vapour pressure at the valve (filled with vapour) and the fluid layers adjacent to that created reservoir will encounter a drop in its velocity given by $\Delta V = -\frac{gP_V}{a}$ (the velocity becomes 2v). That drop in the velocity will propagate together with a rarefaction wave of an amplitude equal to the vapour pressure towards the reservoir, which it reaches at time $\frac{L}{a}$. At that instant the pressure in the pipe just adjacent to the reservoir is at the vapour pressure. This will cause a pressure wave to start propagation from the reservoir end and a further drop in the velocity of the fluid. (The velocity becomes V). This action will travel towards the vapour reservoir near the valve which it will reach at time $\frac{2L}{a}$. At that instant the pressure difference (the reservoir pressure and the vapour pressure) will cause a further drop in the velocity of the fluid adjacent to the vapour reservoir (the velocity becomes zero). Again a rarefaction wave together with the decrease in the velocity will travel from the vapour reservoir to the reservoir at the down-stream end during $\frac{2L}{a} < t < \frac{3L}{a}$. In the example shown in Fig. 8 the value of the initial velocity is such that the velocity drops to zero near the vapour reservoir at $t = \frac{2L}{a}$. Thus, at $t = \frac{3L}{2}$ the fluid is at rest in the whole pipe. But at that instant the unstable condition of lower pressure in the pipe adjacent to the reservoir causes the fluid to flow inwards in the pipe. Flow of the fluid would start at -v near the reservoir and the pressure would start rising to the reservoir pressure. This action will propagate towards the vapour reservoir which it reaches at $t = \frac{4L}{a}$. During the time interval o < t < $\frac{4L}{a}$ the vapour void has been growing to its largest size. A representative value of its largest size is $2v \frac{2L}{a}$. At the instant $t = \frac{4L}{a}$, the reservoir pressure arriving at the vapour reservoir will cause further increase in the value of the velocity at which the water adjacent to this reservoir is flowing in the negative direction making it -2v. A rarefaction wave now travels towards the reservoir and these two events reach the reservoir at $t = \frac{5L}{a}$. At that end, a further increase of the magnitude of the velocity at which the fluid is flowing in the negative direction and a rise of the pressure to the reservoir pressure starts to travel towards the vapour reservoir. (The velocity then is -3v). This action will continue to travel from the reservoir end to the vapour reservoir for $\frac{5L}{a} < t < \frac{6L}{a}$. In the meantime during the

interval $\frac{4L}{a}$ < t < $\frac{6L}{a}$ the velocity adjacent to the vapour void continued to be -2v. Thus resulting in a continuous diminishing of that vapour reservoir. Finally that reservoir size reaches zero at $t = \frac{6L}{a}$. Thus at that instant as the pressure reaches the reservoir pressure and the velocity is -3v, a pressure wave whose amplitude is $\frac{a.3v}{c}$ starts to propagate towards the reservoir as the fluid adjacent to the valve comes to rest. This action travels to the reservoir where it arrives at 7L. At that moment the fluid is at rest in the whole pipe and the pressure is at a high value. The water adjacent to the reservoir starts to flow outwards bringing the velocity to 3v and the pressure to the reservoir pressure. This action propagates towards the valve ending in the situation similar to the initial condition in the system at $t = \frac{8L}{a}$. The whole cycle repeats itself again. In practical systems friction causes damping away in few cycles. One closing remark here is that; in constructing Fig. 8a, the choice of the magnitude of the initial velocity was made in such a way that the duration of the growth and disappearance of the vapour reservoir is an integer multiple of $\frac{L}{a}$. In general this is not the case. However, the simplified conditions were chosen so as not to complicate the diagram and for the purpose of clarity of demonstration. Fig. 8b shows the pressure and velocity changes versus time at different locations along the pipeline with the initial steady velocities chosen 2.6v, 2.8v, 3v, 3.2v and 3.4v. Note that the case illustrated in the central part of Fig. 8b is the case described above.

3. EXPERIMENTAL STUDY

To study the transients occurring in typical cooling water systems of thermal power plants (Fig. 1) following pump failures it was felt that an experimental model should be built. In designing this model, the following main considerations were taken into account:

- 1. Pump failure was to be represented by a shut-off of a valve, that could be closed within a preselected closure time according to prescribed closing characteristics. This gave the possibility of simulating conditions resulting from pump failure of different types of pumps.
- 2. It was decided to carry out the investigation in three phases (Fig. 9):
 - I Testing of transients resulting from closure of a valve at the upstream end of a horizontal pipe
 - II Testing of transients resulting from closure of a valve in a horizontal line having a high (inverted U) vertical section (siphon)
 - III Testing of transients from closure of a valve upstream a line like that in II having in addition a condenser at top of the inverted U section.

The advantage of this staging approach was to gain gradual insight into the problem as it gets more complicated.

3. It was felt that it would be of great help to see through the walls of the model at many points of interest. Moreover, to avoid complications in the mathematical modeling resulting from use of different materials for the pipe system, it was decided to built the whole model from "plexiglass".

In addition to the above considerations some other points arose during the design of the model. These additional factors will be pointed out during the description of the model in the following section.

3.1. Water Hammer - Water Column Separation Experimental Circuit

Fig. 10 shows a view of the experimental model. In the system, water flows from the high level water reservoir (shown left in the picture) to the lower level water reservoir (at right) through a "plexiglass" pipe. The pipe can be arranged in different configurations as desired for carrying out different experiments (phases I - III Fig. 9). The platform at

the centre facilitates holding the siphon high section or the condenser model. The valve used to produce transient conditions is located at the foot of the high level reservoir (at the upstream end of the "plexiglass" pipe). The water leaving the low level reservoir collects in the sump via the return pipe (near the floor Fig. 10).

3.1.1. General description

A schematic diagram of the water hammer - water column separation experimental circuit is shown in Fig. 11. A "plexiglass" pipe connects a high level water reservoir and a low level water reservoir. The pipe has an inner diameter of 90 mm. The horizontal span of the pipe between the two reservoirs is 40 m. The pipe is built up from 2 m.segments attached together by flanges. The pipe can be arranged in different configurations as shown in Fig. 12.

These configurations allow testing of: horizontal line, siphons with different heights as well as condenser arrangements. The constant level in each reservoir can be varied using a funnel built into each. The water level difference (maximum 1.6 m) between the two reservoirs can be adjusted to obtain a specific steady flow velocity in the pipe. A ball valve is situated at the foot of the high level reservoir. The valve can be closed electrically with the help of a specially built servo-system. This system allows the closing of the valve according to prescribed closing characteristics and with different closure times. A return pipe leads the water leaving the low level reservoir to a 90°V-notch. The V-notch discharges in a sump. A pump raises the water from the sump to the high lever reservoir. The overflow of this reservoir returns back to the water-sump.

3.1.2. Details and data of main parts of circuit

"Plexiglass" pipe.1. *)

The pipe is built up of 2 m segments. These segments are attached together with flanges. The pipe is freely supported as can be seen in Fig. 13. The horizontal part of the pipe stands at 1.5 m elevation from the floor. Fig. 14 gives some useful constructional details of the pipe.

The pipe has an inside diameter 90 mm and an outside diameter of 100 mm. The celerity "a" of a pressure pulse through the pipe can be calculated from equation (9).

^{*)} Numbers between two points designate parts of the circuit in Fig. 11.

$$a = \sqrt{\frac{1}{\rho \left[\frac{1}{K} + \frac{c(\mu)}{E} \left(\frac{D}{\delta}\right)\right]}}$$
(9)

where: ρ is the water density; ($\rho = 980 \text{ kg/m}^3$)

K is the bulk modulus of elasticity of the water; $(K = 2.05 \times 10^9 \text{ N/m}^2)$

- $c(\mu)$ is a parameter depending on the mounting of the pipe, Poisson's ratio of the pipe material and the thickness to diameter ratio of the pipe; $(c(\mu) = 1.07)$ $(\mu = 0.075)^{***}$
- D is the inside diameter of the pipe; (D = 0.09 m)
- δ is the thickness of the pipe; (δ = 0.005 m)
- E is the modulus of elasticity of the pipe material; $(E = 2.5 - 3.5 \times 10^8 \text{ N/m}^2)$ $(3.2 \times 10^8)^{***}$

substitution of the different values of data in (9) yields a value: $a \approx 400 \text{ m/s}$

High level water reservoir.2.

The high level reservoir is 1.25 m in diameter. The height of this reservoir above the center line of the "plexiglass" pipe is about 2 m. As can be seen from Fig. 11, the pump .8. delivers water from the sump .7. to the high level reservoir. The water level in the reservoir can be changed by lowering or raising the funnel as shown in Fig. 15. This built-in funnel controls the required constant level of the water in the reservoir. A maximum level of 1.8 m above the center-line of the valve .4. can be reached. An additional control on the overflow above the funnel is provided by the valve .10. on the delivery of the pump. This valve is particularly useful to obtain small steady flow velocities in the "plexiglass" pipe. A maximum level increase of +20 mm in the water level in this reservoir was recorded during the transient tests of the investigation.

Low level water reservoir.3.

The low level reservoir is 1.25 m in diameter. The height of this reservoir above the center-line of the "plexiglass" pipe is about 1 m. The water level in the reservoir can be changed using a built-in moveable funnel (Fig. 16). A maximum level of 0.8 m above the center-line of the horizontal portion of the plexiglass pipe can be reached. The overflow of the funnel in this reservoir is the steady discharge through the "plexiglass"

^{**)} The values of data of pipe material properties used in calculation of "a" from equation (9) are discussed in section 3.3.4.

pipe. This overflow goes to a V-notch .6. via the return pipe .5. It was observed that the maximum change in level during the transients resulting from the closure of the valve was \pm 15 mm for all measurements of the investigation.

Valve and valve-steering system.4.

Fig. 17 shows the valve and its servo-motor. The electronic devices of the valve-steering system are shown in Fig. 18. A ball-plug valve is situated at the foot of the high level water reservoir at the upstream end of the "plexiglass" pipe. The valve was furnished by "Neue Argus G.m.b.H." (DIN 2633).

The valve steering system enables the closing of the valve according to the prescribed characteristics (angle of rotation versus time). An example of such chosen characteristics is shown in Fig. 19a. Fig. 19b shows the effective area of the valve versus the angle of closure. The steering system allows closing the valve within times of closure as short as 0.4 s.

Principle of Operation of the Valve Steering System:

With reference to Fig. 20, the angular position of the valve α is controlled by a proportional-error electronic servo-mechanism. The angular position for the valve is converted into an equivalent voltage $(E_0 = k \alpha)$ which is continuously compared with a voltage E_1 , representing the desired position. Any difference ϵ between these two voltages will cause the motor to rotate, thus moving the valve in such a way to reduce ϵ to zero. The dynamic response is controlled by the error amplifier A_3 and the tacho-generator TG feedback. The following paragraphs discuss the functions of the main components of the steering system (Fig. 20).

Selector switch S_2 allows the choice of three possible ways of programmed valve closure.

These are:

1. Function generator

A specially designed device that generates stepped function shown in Fig. 21. The number of steps can be as large as 10 steps. ΔV_n is adjustable voltage step between 0.01 V and 10 V. Δt_n is adjustable time step between 10^{-3} and 4 seconds. In Fig. 21, it can be seen that the valve open position (angle 0°) is equivalent to 0 V on the y axis while the valve closed position (angle 90°) corresponds to 10 V in the diagram. The function generator is used to produce desired (prescribed), angle-time closing characteristics

as the ones shown in Fig. 19. The desired curve is approximated by appropriate voltage and time steps.

2. R-C response

To simulate typical hydraulic conditions at a pump (resulting from its tripout) - that is a steep pressure change at the beginning of failure with a slower rate of change towards the end of the failure time - an exponential angle-time dependence is used. In this case, when S_{1a} is switched on, an E_{i} of the form E_{i} = 10 (1 - $e^{-t/R}1^{C}1$) is generated from start to stop. R_{1} can be selected from values between 10^{4} and 10^{6} Ohms. C_{1} has a fixed value of 10^{-5} Farad. Different times of valve closure are obtained by inserting the appropriate resistance R_{1} .

3. Manual

The valve is positioned by means of a potentiometer R_2 acting as a voltage divider E_1 = 0 - 10 V. This mode is particularly helpful when the valve is positioned at a partial closure position at steady conditions and transients resulting from completing the closure of the valve are investigated.

Buffer amplifier A₁

This amplifier acts like a buffer stage to insure that the programme (chosen by switch S_2) is not affected by the loading of the error amplifier A_3 . Besides, its gain is adjustable, allowing its use as a programme attenuator for minor adjustments.

Buffer amplifier A2

The voltage signal E_0 coming out of the position transmitter circuit goes into the buffer amplifier A_2 . A_2 isolates this circuit from A_3 to avoid nonlinearity due to loading effect of the operational amplifier. A_2 has an adjustable gain from 1-10, that enables the setting of the appropriate scaling factor. That is to say it is to be set to magnify E_0 to the same order to which E_1 is magnified when it leaves the buffer amplifier A_1 .

Operational-error amplifier A3

As the function generator and the R-C source provide only functions of positive voltage polarity reversed programming has to be carried out by some other means. Since only sign reversing of voltages is needed this is easily accomplished by an operational amplifier with reversing and non-reversing inputs (selector switch S_3). The ope-

rational amplifier is followed by an error amplifier (adjustable gain 1-10). The setting of this amplification factor influences in combination with the Tacho-generator feed back, the accuracy and response time of the servo system.

Power amplifier Ah

The output voltage of A_3 is proportional to the error signal causing the motor M to rotate slower or faster in the proper direction to minimize the error ϵ . Again the response time of the system depends on the Tacho-generator feed back setting of A_1 .

Motor M

The servo motor is of DC permanent magnet printed motor type, featuring extremely low inertia and linear current torque characteristics. The mechanical time constant of the motor is approximately 0.001 second.

Gearing (Motor-valve stem)

The gearing between the motor shaft and the valve stem uses a 36:1 reduction ratio. Backlash, being an important factor in the overall accuracy of the system, is minimized to less than 0.1°.

V Notch Weir.6.

The return pipe .5. leads to a 90° V-notch weir for the measurement of the steady flow discharge in the "plexiglass" pipe. The V-notch is built according to the recommendations of the "Organisation Internationale de Normalisation". The V-notch discharges in the water sump .7.

Secondary parts of the circuit

Pump .8. raises water from the sump .7. to the high level reservoir. The overflow of the high level reservoir goes back to the sump via return pipe .9. Auxiliary valve .11. on the downstream end of the plexiglass pipe is used for starting the siphon. This valve is the same type of the ball valve as that at the upperstream end of the pipe and can be closed manually. A vacuum pump .13. (shown in Fig. 22) is used for starting the siphon. It is also used for getting rid of the air accumulated on top of the siphon or the condenser before the valve is closed. This is necessary at low steady flow velocities. The circuit is a closed one with the water circulating in it originally tap water. All parts of the circuit were covered to protect the water from dust, etc. A filter .12. (shown in Fig. 23) is used for filtering the water of the circuit. The water stayed

rather clean and water was circulated through the filter only occasionally. Condenser model

Fig. 24 shows a diagramatic sketch of the condenser model. The condenser is built from "plexiglass". Condenser tubes are 20 mm inner diameter and 30 mm outside diameter. Twelve condenser tubes are arranged in one plane parallel to each other. This would allow high speed filming of transients if wanted. There are 8 points on the condenser tubes for possible attachments of piezoelectric pressure transducers. Normally two pressure transducers are used at a time and the other points are plugged. The condenser water boxes are 200 mm in diameter. The condenser model can be mounted in a vertical position as well as horizontally on the top of the siphon. The support of the condenser may be regarded as a free support. Figs. 25 and 26 show the means of support of the condenser when held in the vertical and the horizontal positions, respectively.

3.2. Instrumentation

The transients experimental data measured and recorded for the experimental study consist of:

- 1. Angular position of the valve during the closure time
- 2. Transient pressure changes at selected points on the "plexiglass" pipe system
- 3. Transient flow velocity changes at selected points on the pipe Fig. 27 shows the instrumentation pannel. A general schematic diagram of the instrumentation is shown in Fig. 28. Table 1 gives a listing of the different components of instrumentation, their manufacturer and their types.

Piezoelectric pressure transducers are mounted on the selected points of the pipe. They are mounted flush with the pipe walls. Fig. 29 shows the mounting of one pressure transducer. Signals of the piezoelectric transducers are amplified by the charge amplifiers before reaching the amplifiers of the recorders. The outgoing signals of these amplifiers are recorded on the Oscillomink recorders *. Selection of suitable pressure scales is done with the help of both the charge amplifiers and the galvoamplifiers (on the recorders) gains to display the signals with appropriate

^{*)} These recorders were replaced by two 7 channel visicorders in the latter stages of the investigation (galvanometers natural frequency 1650 c.p.s.).

scales on the paper. The galvanometers of each channel on the recorder have natural frequency of 1000 c.p.s. securing good dynamic response for the measured pressures. Paper speed of the recorders could be chosen among a set of speeds ranging from 2.5 mm/s. to 1000 mm/s. with paper speed fluctuations within + 2.5%.

The output signal of the angular position potentiometer (mounted on the valve stem) is amplified and then recorded on one channel of the available twelve channels of the two recorders. This signal also goes to the valve servo motor mechanism.

The output signal of the induction flowmeter (Fig. 30) is recorded on one channel (details of this flowmeter are discussed in section 3.3.2.). On each recorder a time signal is displayed. This signal comes from the 10 or 100 c.p.s. oscillator. It serves as a time check for the paper speed of the recorders. In addition, the displayed time signal undergoes a step shift at the starting of the valve closure. This serves as a zero time reference instant. When details of two particular signals are wanted to be studied, these two particular signals can be displayed on the two-channel storage oscilliscope. The particular part of interest can be conveniently displayed using appropriate external triggering delay through an Elesta type-timer and suitable sweep time.

Table 1
Instrumentation list

Device	Manufacturer	Type	Number	off
piezoelectric	Kistler	410B	6	
pressure				
transducer acceleration	Kistler	6031	2	
compensated	KIBOTEL	0031	-	
piezoelectric				
pressure transducer				
connecting cable	Kistler	1631	8	
charge amplifier	Kistler	5001	8	
angular position	Electric Corp.	400STD	1	
potentiometer				
induction flowmeter	(specially built)		2	
10 or 100 c.p.s. oscillator	(specially built)		1	
6 channel recorder	Siemens	Oscillomink	2	
storage oscilloscope	Tektronix	Model A293/A2 464B	1	
timer	Elesta	404D	1	
7 channel recorder	Honeywell	Visicorder	2	
with	, , , , , , , , , , , , , , , , , , ,	2206AC		
amplifiers	Honeywell	Accudata 107 DC-amplifier	14	

Table 1 gives a list of the instrumentation used. A schematic diagram showing the principle of pressure measurements and their recording on the recorders and the oscilloscope is found in Fig. 31.

3.3. Experiments

The experimental testing covered the following five types of measurements:

- 1. Steady conditions measurements. The purpose of these measurements was to determine the steady flow friction factor in the "plexiglass" pipe and the steady valve resistance for different partial closures of the valve.
- 2. Measurement of transient flow velocities. An attempt was made to adapt two systems for the measurement of transient flow velocity changes. A digital-displacement system (photographic system) and an induction flowmeter were used. This part of the experimental study resulted in preparing two dependable induction flowmeters that were used in performing the main measurements (Transient conditions 5.).
- 3. High speed filming of water column separation. Some techniques were developed to photograph the segment of the pipe system where water column separation occurred. As the phenomena occur at very high speed, visual observations were inadequate to obtain a physical understanding of what happened. With the high speed photography the movies obtained gave good insight into the phenomena and the sequence of events occurring during column separation.
- 4. Experimental evaluation of the elastic behaviour of the pipe wall material under transient conditions. These measurements consisted mainly of strain measurements on the outside surface of the pipe wall during the hydraulic transients.
- 5. Transient conditions: These measurements represent the main measurements of the study. In these measurements, pressure changes, velocity changes (using induction flowmeters) at selected points on the pipe line as well as valve angular position were measured and recorded. These measurements were carried out changing:
 - a. pipe configuration (horizontal line, siphons with different heights and siphons with the condenser model on top)
 - b. initial steady flow velocity in the pipe system
 - c. valve closure time

d. valve closure characteristics (angular rotation versus time)

3.3.1. Steady conditions measurements

These measurements were made on a horizontal line configuration in sets of readings for selected steady flow conditions (Fig. 32). Each set consisted of the row in table 2.

Table 2

Observations during steady flow tests

α .	H _A mm	H _B mm	h ₁₋₄ mm water	h ₂₋₃ water	h _{Vmm}	remarks

where: a is the angle of partial closure of the valve, degrees

- HA is the level of water in the high level water reservoir above the center-line of the "plexiglass" pipe, mm
- ${\rm H_B}$ is the level of water in the low level reservoir above the center-line of the "plexiglass" pipe, mm
- h_{1-4} is the pressure difference between points PT $_1$ and PT $_4$ as given by manometer reading in mm water (i.e. friction pressure loss between the two points)
- h₂₋₃ is the pressure difference between points PT₂ and PT₃ as given by manometer reading in mm water (i.e. friction pressure loss between the two points)
- h_{V} is reading of the level indicator of the 90 $^{\circ}V$ -notch weir.

The tabulated measured readings of table 2 were used to compute the results tabulated in table 3, yielding:

- the friction variation with the flow velocity in the pipe
- the steady valve resistance for different opening positions.

Table 3
Calculated results for steady flow tests

α	H _A -	- H _B	V	Re	f	Hfr	ξ

where: $H_A - H_B$ is the level difference between the two reservoirs v is the flow velocity in the pipe.

First the discharge Q is obtained from tables of the "Organisation Internationale de Normalisation" corresponding to h_v . Then v is calculated: $v = Q / \frac{\pi}{4} d^2$, where d is the inside diameter of the pipe (d = 90 mm). This yields values of the velocity accurate within 2%.

Re is Reynolds number Re = $\frac{vd}{v}$, where v is the kinematic viscosity (v = 10^{-6} m²/s).

f is the friction factor calculated from

$$h_{1-4} = f \frac{1}{d} \frac{v^2}{2g}$$

$$h_{2-3} = f \frac{1_{2-3}}{d} \frac{v^2}{2g}$$

 l_{1-4} and l_{2-3} being distances between points PT_1 - PT_4 and PT_2 - PT_3 respectively (Fig. 32)

H_{fr} is the friction head loss in the whole length of the pipe

$$H_{fr} = f \frac{L}{d} \frac{v^2}{2g}$$
, where

L is the total length of the pipe

is the valve steady resistance when fully open as given by $\Delta H \Big|_{O} = \xi_{O} \cdot \frac{v^{2}}{2g}$

$$\Delta H|_{o} = \left[(H_{A} - H_{B}) - H_{fr} - \frac{v^{2}}{2g} \right] / 2. *)$$

 ξ is the valve steady resistance for partial closure as calculated from ΔH = $\xi \; \frac{v^2}{2g}$,

$$\Delta H = \left[(H_A - H_B) - H_{fr} \right] - (1 + \xi_0) \cdot \frac{v^2}{2g}$$

The calculated results were plotted in Figs. 33 - 34. Fig. 33 shows the steady friction coefficient in the pipe versus the steady velocity of flow in the pipe. On the same graph results for a smooth pipe as obtained from Moody's diagram |59| are plotted. On Fig. 34 the steady valve resis-

^{*)} The last term between the square brackets accounts for the exit losses. Entry losses are neglected. The devision by 2 is because there were two similar valves one at each end of the pipe (Fig. 32).

tance for partial openings is shown versus α the angle of partial closure of the valve.

Comments

The measured friction factor values are larger than the values obtained from smooth pipe results (Fig. 33). This may be due to the effect of the flanges connecting the different segments of the pipe. The values of the valve steady resistance for angles larger than 75° (Fig. 34) could not be measured as the water velocities became too small to be measured with the maximum available head difference between the levels of the two water reservoirs. Also, it was found that the valve is practically completely closed at 82.5°.

3.3.2. Measurement of transient flow velocities

This section presents two methods for the measurement of transient flow velocities for water hammer applications. The first uses a digital-displacement system and the second uses an induction flowmeter. Measurements using both systems are presented followed by a comparison of the two methods.

Introduction

Literature lacks mention of any significant transient flow velocity measurement in experimental water hammer research. Although it is the flow velocity change that causes the pressure changes, the latter are the ones commonly reported by investigators in this area. During the course of the development of our investigation the measurement of transient flow velocity changes was motivated. It has been thought that such measurement would be very useful for the study and would complement the pressure measurements. This proved to be true as indicated in the conclusions of this section. Turbine, ultrasonic, thermal, ionization, laser, digital-displacement and induction devices represent the most commonly used systems for unsteady flow measurements |27|. The latter two systems were adapted for the measurement of transient flow velocity changes at a point on a horizontal pipe resulting from a closure of a valve on the line.

Photographic Measurement of Transient Flow Velocities

This system is based on digital-displacement principle. In this method, the transient displacement of a ball introduced in the water together with the time are used to obtain transient flow velocity changes, resulting from the closure of the valve. With reference to Fig. 35 the

following procedures and analysis are followed:

A. Experimental procedures

1. Camera and lighting set up

A Hitachi, high speed camera (type 16 HB-400) is placed to photograph a segment of the pipe in the vicinity of the point where transient flow velocity changes are to be measured. A stand carrying a 5 mm thick, light diffusing glass plate is placed behind this pipe segment. Illumination of the pipe segment is done indirectly through the glass plate by two (Kobold, Halogen 1000 Watt) high intensity lamps. A small motor is mounted on the glass plate. This motor drives a pointer whose position on the film serves as a time base at a speed of 600 r.p.m.

2. Introduction of a ball in the pipe

A ball of nearly the same density of the water is introduced in the steadily streaming water using a small ball injector mounted on the pipe upstream of the point where transient velocity changes are to be measured. The ball is approximately 8 mm in diameter, and it is prepared from two types of wax. **) The ball is carried with the steady streaming flow.

3. Valve closure

As the ball passes through a detecting ring mounted around the pipe at a point upstream of the point where transient velocity changes are to be measured, the photocells sense its passage and give a signal that automatically starts the closure of the valve. The closure of the valve would in turn result in a transient displacement of the ball. The detecting ring is movable and can be clamped on the pipe such that the transient displacement of the ball occurs within the range of view of the camera. Thus its position upstream the point of measurement of the transient velocity depends on the initial steady velocity of flow in the pipe as well as the valve closure time. Trials are made without starting the high speed camera and when the above condition is fullfilled visually, the following procedure is completed.

^{*)} Impression compound, manufactured by Kerr Manufacturing Co.,
Detroit, Michigan and Modelling wax no. II, Alston, produced by
the Dental Manufacturing Co. Ltd., London.

4. Sequence of steps for filming

- a) Setting up of camera and light arrangement is made.
- b) Steady conditions of flow in the pipe are reached.
- c) The recorder is started.
- d) The ball is introduced into the water.
- e) When the ball is seen passing a point some distance upstream of the detecting ring, the high speed camera is started manually. This is done to assure that the high speed camera has attained its running speed when the ball is within the range of view of the camera. A speed of 500 frames/second is used.
- f) Once the ball passes through the detecting ring the valve starts to close. This instant is displayed on the recorders. At the same instant time marks start on the film at a frequency of 1000 c.p.s.

B. Film data analysis

After developing the film it is displayed in a (Benson France, Boscar Model N/F) photo analyzer. For each frame, Fig. 36, the following data are obtained:

- Frame number
- co-ordinates of two marked reference points on the pipe (R1 and R2 in Fig. 36)
- ball center coordinates
- time pointer coordinates

These data are obtained on a punched tape. They are used as input data for a FORTRAN IV programme (appendix A). The output of this programme yields the required transient flow velocity changes. The main steps of this programme are as follows:

For each frame, the displacement of the ball along the axis of the pipe is obtained. The coordinates of the time pointer are used to obtain the time. Corrections for possible non-uniformity of the motion of the camera during the filming are allowed for, with the help of the co-ordinates of the two reference points (appendix A). Numerical differentiation of the ball displacement with respect to the time gives the required transient flow velocities. These results are plotted versus time.

Induction Measurement of Transient Flow Changes

The specially developed induction flowmeter is shown in Fig. 30. It uses the well known working principle of induction flowmeters. Briefly, under the action of magnetic field, an e.m.f. is induced in the moving liquid and its value is proportional to the speed of flow. The induced

e.m.f. is measured between two electrodes situated in the flow flush with the pipe wall inner surface. It is not our purpose to go deeply into the electronic aspects of the flow-meter; however, with reference to Figs. 30 and 38, some of its pecularities are listed below together with few comments. The thickness of the pipe wall is small (5 mm compared with the 90 mm diameter of the pipe). The conductivity of the tap-water (with its dissolved salts) is much higher than that of the "plexiglass" pipe material. The electromagnet is fed by 1800 c.p.s. current to obtain suitable quick response characteristics. Special care in the design was given to reduce the following two error signals:

- 1. The e.m.f. induced in the column of water between the two electrodes due to the alternating magnetic field. The water column acts in a way like the secondary turns of a transformer.
- 2. The stray signals owing to the inhomogeneities of the magnetic flux and to the capacitance between the windings of the electromagnet and the measuring electrodes.

The reduction of the first effect is achieved by special positioning of the different electronic components. The second effect is reduced by using the phase demodulator as the stray signals are phase shifted 90° with respect to the measuring signal. The flow-meter was calibrated with the V-notch weir using steady flows in the pipe.

Measurements and comparison of the two methods

Heights in the high level and low level reservoirs were adjusted to 1.32 m and 0.5 m above the centerline of the "plexiglass" pipe, respectively. Steady conditions of flow were reached. The value of the steady flow velocity in the pipe was measured using the V-notch weir. This value was 1.22 m/s. Transient flow velocity changes (at the points marked $V_{\rm h}I$ and $V_{\rm h}P$ on Fig. 39), resulting from the closure of the valve in 1 second, were measured, using both the photographic and induction systems simultaneously. The procedures of the photographic method explained in detail before were followed. Figs. 39 and 40 show the results obtained. Fig. 39 shows the following signals as extracted from the two recorders records.

- a. Valve angular position (The valve closure is completed in 1 second. The valve is closed linearly with time).
- b. Pressure at point PT (Fig. 39)
- c. Pressure at point PT (Fig. 39)

^{*)} A discussion of the different events occurring during a similar test is presented later on in section 4.5.

- d. Pressure at point PT3(Fig. 39)
- e. Pressure at point PT, (Fig. 39)
- f. Output signal of the induction flowmeter.

 The velocity scale is obtained from the steady calibration of the flower.

The velocity scale is obtained from the steady calibration of the flowmeter.

Analysis of the film and calculations yielded the velocity changes shown in Fig. 40. The calculated results are superimposed on the results obtained by the induction flowmeter.

As can be seen from Fig. 40, the results of the two methods compare reasonably well with each other. The variation of the velocity distribution across the cross sectional area of the pipe during the transients may result in some of the small discrepancies. Further differences in time (seen in Fig. 40) will arise on the following accounts.

- 1. The velocity changes are actually measured at two different points $(V_4I \text{ and } V_4P \text{ Fig. 35})$ that are 0.7 m.apart. Knowing that the average accoustic velocity in the pipe was about 450 m/s.,a little difference should be expected. However the order of the time discrepancy due to this factor is relatively very small.
- 2. The time base of the induction flowmeter results is based on the recorder paper speed which is accurate to within 2%, while the time base of the photographic method is the synchronous motor rotation.

With regard to the accuracy of the measurements, for the induction flowmeter results, the accuracy is defined mainly by the noise level in the output signal of the system. On this basis the values of the velocities presented here are accurate to within 2%. For the photographic system the following factors can contribute to errors in the measured results:

- the very small difference between the ball density and that of the water
- human error in lining up of the cross wires of the photoanalyzer during the photo analysis of the film
- the effect of refraction of light through the pipe wall may result in some error in the measurement of the ball displacement
- errors in the numerical differentiation |22|.

A comment can be added at this point, namely that the induction flowmeter gives a more complete picture of the velocity changes at the point of measurement during the whole time of the transient than the photographic system which only gives a part of this time. To obtain the whole time history, an excessively large area of viewing for the camera is needed when using the photographic system. The induction flow-meter measures the average velocity in the cross section of the pipe while the photographic sy-

stem measures local velocity changes. The photographic system provides velocity changes in the direction of the axis of the pipe. It would also permit measurement of velocity changes in the radial direction should this be of interest. The photographic system needs many arrangements and requires some expensive devices, e.g. camera, photo-analyzer. It is obvious that the induction flow-meter is much easier to use than the photographic system. The induction flow-meter needs to be calibrated (e.g. versus V-notch weir steady flows) with still some additional check necessary as regards the quick response characteristics, while the photographic system does not need to be calibrated. The above discussion may lead to the conclusion that the photographic system can be considered for refined laboratory use such as calibrating fast response characteristics of other velocity-meters, while the induction flow-meter can be used in more field and versatile applications.

Two induction flow-meters similar to the type described above have been used in carrying out the main measurements of the study (section 3.5.5.). The measured transient flow velocity changes proved to be very helpful and were of great use as can be seen in the following chapters.

3.3.3. High speed camera photographic study of water column separation

The purpose of these experimental measurements was to gain insight into the very rapid changes occuring during water column separation.

Techniques were developed for photographing a segment of the "plexiglass" pipe system where cavitation void took place using a high speed camera. Such films were made only during few tests as they were aimed at solely qualitative study of the phenomenon.

High intensity illumination of the segment of the pipe was produced indirectly using two (Kobold, Halogen 1000 Watt) high intensity lamps, through a diffuse transmitting glass plate as shown in Fig. 41. A Hitachi (type 16 HB-400) high speed camera was placed in front of the segment of the pipe where the cavitation void occurred (Fig. 41). Special attention to light intensity and lens shutter time was given to obtain a good quality movie. A film speed of 1000 frames per second was used. On Fig. 41, a small motor driving a time pointer in the back of the pipe, can be seen. The motor speed was 600 r.p.m. This time pointer served as a time base in the background of the filmed pipe segment. The instant the valve closure was started, time marks at 1000 c.p.s. began to appear on the film, marking a reference zero time. Prior to the starting of the closure of the valve to produce the transient conditions (see section 3.3.5.) light ad-

justments were completed and the filming was started.

After development of the film, it was displayed by a multi speed projector for the study of the results. At this stage care was given to the observation of the sequence of events occurring during formation and collapse of the cavitation void. Also, the films were studied in correlation with the obtained records of pressure and velocity measurements. These studies were of excellent value for the physical understanding of the column separation phenomenon. Section 4.5 will discuss in detail a study of a film made for column separation just behind the valve for a horizontal line configuration.

3.3.4. Experimental evaluation of the elastic behaviour of the pipe wall meterial Introduction

Strains in the pipe wall during transient conditions resulting from closure of a valve on a horizontal pipeline were measured. The measured strains were used together with transient pressure measurements to evaluate the elastic behaviour of the pipe wall during such hydraulic transient conditions. The assumptions commonly made in the derivation of the continuity equation for water hammer applications, chapter 2, are investigated in the light of the measurement.

It is known that because of the expansion and contraction of the pipe the speed of the pressure wave propagation is less than that of the sonic velocity in the liquid. This influence depends on the pipe characteristics and its means of support, and is usually built into the water hammer analysis in the way shown in appendix B. As can be seen from the derivations in appendix B a number of assumptions are made as regards the elastic behaviour of the pipe. In the analysis (appendix B) a term "a" is introduced. This term would give the speed of the pressure wave propagation as seen from the final forms of the partial differential equations commonly used to describe one dimensional transient flow |58|. In carrying out water hammer calculations, it is of great importance to use an accurate value for the speed of propagation of the resulting pressure waves.

During the course of the development of our investigation, a study of the elastic behaviour of the pipe in the experimental model was motivated in search for an answer to the following questions.

1) As it was essential for the study of the phenomenon of water column separation to have transparent pipe walls, therefore it was decided to build the model op "plexiglass" piping. Thus an evaluation of the

- "plexiglass" pipe behaviour under the stresses and strains occurring due to transient conditions would reflect the extent of any deviation from elastic behaviour that could be exhibited by the "plexiglass" (if any) on the experimental transient pressure measurements.
- 2) As transient experimental tests were started, an obvious trend of decrease in the speed of the pressure wave propagation with time was observed associated with water hammer, water column separation phenemena. Although such a trend was observed by previous investigators [2, 66], again the question was raised of how large the contribution (if any) of the pipe wall material to the trend was under such conditions.

A set of experiments designed for the evaluation of the elastic behaviour of the pipe under transient conditions was carried out. These experiments and their results are presented in the following parts. It is worth noting that the set of experiments chosen for this purpose was carried out on the model during typical transsient tests. This procedure was preferred to carrying out material stress-strain tests on samples of the pipe.

Transient conditions experimental test

A typical transient test was carried out in the following manner. Water levels in the high and low level reservoirs were adjusted to 0.99 m and 0.5 m, above the centerline of the "plexiglass" pipe, to obtain a steady flow velocity of 1 m/s. This value was checked using the V-notch weir. The output signals of the pressure transducers and the valve angular position displacement were recorded. Fig. 42 * shows the following signals:

- a. 10 c.p.s. time signal
- b. P₁, pressure at point PT₁, (Fig. 42)
- c. P, pressure at point PT, (Fig. 42)
- d. P3, pressure at point PT3, (Fig. 42)
- e. valve angular position (The valve closure was completed in 1 second. It was closed linearly with time).

Experiments to evaluate pipewall transient behaviour

To study the pipe stress-strain behaviour during transient conditions, a number of (Hottinger Baldwin Messtechnik, 6/120 La 11) straingauges were cemented on to the outside surface of the pipe at the location of pressure transducer PT₂ (see Fig. 42). The first strain gauge gave

^{*)} A discussion of the different events occurring during a similar test is presented later in section 4.5.

the circumferential strain while the second yielded the axial strain at the same cross section. The signals of the two strain gauges were recorded via two Hottinger Baldwin Messtechnik strain gauge instrument-amplifiers combination KWS (3S-5) Fig. 43 shows the mounted strain gauges. Fig. 44 shows the output signals of the two strain gauges together with the pressure Po during a transient test for the closure of the valve in 1 second for a steady flow velocity of 1 m/s. Note that these are practically the same testing conditions as the transient test shown in Fig. 42. In Fig. 44 pressure P_1 and the valve angular position are also shown. Fig. 45 shows a record of the oscilloscope which was taken during the same test whose results are shown in Fig. 44. It shows the parts of the pressure P_2 and circumferential strain ϵ_{c2} signals when the first peak of pressure occurred. The triggering time of the scope was set at 1.4 s. and the sweep time was 20 millisecond per division. The upper beam shows the pressure P, while the lower beam shows the tangential strain ε_{c2} . A similar test to the one whose results are presented in Fig. 44 was carried out for steady flow velocity of 1 m/s. and linear closure of the valve in 2 seconds. The results of this test are shown in Fig. 46.

Discussion of results

As can be seen from Figs. 44 - 46, the changes of the circumferential strain and the pressure P_2 with time agree very well, showing nearly no phase (time) deviation between the two signals. Also, the axial strain shows fairly good agreement with the pressure signal time-wise. The opposite signs of the axial strain to the circumferential strain can be easily understood from equations (B.6 - B.8) *) with $\sigma_{\rm x}$ = 0, that is the case for a free support condition. The very tiny peaks (marked A on Fig. 44) that appear on the axial strain signal are of very minor effect and can be attributed to stress waves in the walls resulting from end effects. In addition, the amplitudes of the strain signals and pressure P_2 at any time during the transient appear to have a linear dependence. These results suggest that the "plexiglass" pipe behaviour may be considered as an elastic one during such hydraulic transient tests. Thus any effect due to "plexiglass" hysteresis (if any) did not show an appreciable magnitude.

Also, in answer to the second question (introduction) it can be concluded, that the decrease of the speed of propagation of the pressure waves associated with the water column separation that was observed during

^{*)} B. refers to equations found in appendix B.

the transient tests (see e.g. Fig. 44) ** was due to changes within the fluid under such flow conditions and not due to the pipe wall behaviour.

It is interesting to try to see how the assumptions made in the commonly used one dimensional transient flow analysis (appendix B) really hold for such hydraulic transient tests. Considering the instantaneous internal pressure in the thin cylindrical shell P, and the circumferential strain at the same time and using equations B.7 and B.9, (for r = b) a value of the modulus of elasticity under such dynamic loading can be calculated. An average value of such dynamically determined modulus of elasticity was calculated for the "plexiglass" pipe to be $32 \times 10^8 \text{ N/m}^2$. This compares fairly well with a value found for static loading obtained from measured strain under different static heads (no flow in the pipe) using the same equations B.7 and B.9 for r = b. The latter value found to be $29 \times 10^8 \text{ N/m}^2$. The pipe manufacturer gave a value of E in the range of 25 - 35 x 10^8 N/m². Using the obtained value of the dynamically measured modulus of elasticity and the axial strain measurements together with equation B.8 an average value of μ = 0.075 was calculated. As can be seen from equation B. 12, the second and third terms in equation B. 1 have been replaced by a term proportional to $\frac{dp}{dt}$. This can be seen to be a valid assumption in view of the measurement results.

In an attempt to see the influence of the flanges used to connect the different segments of the pipe two strain gauges were cemented to measure the tangential and axial strains near the flanges, 0.05 m from the flange, that is 0.95 m from PT₂, which was a middle point in the center of 2 m segment of the "plexiglass" pipe. The obtained results when compared to results of the strain gauges mounted just opposite to the pressure transducer being in the middle of the 2 m pipe segment did not show any appreciable difference.

After the discussion above one may ask what is the value of speed of the propagation of a pressure wave in the pipe? A value of "a" can be calcu-

This observation can be clearly seen for example from the fact that t_{vr} is larger than $2t_{rr}$ (Fig. 44). t_{vr} being a period of complete cycle of a wave travelling between a dead end (the valve) and a reservoir (the low level reservoir), while t_{rr} is the period of a cycle of a wave travelling between a reservoir (at the vapour pressure, when the vapour cavity exists at the valve) and the reservoir at the downstream end of the pipe. The two simple examples considered in section 2.5. show that theoretically t_{vr} would be equal to $2t_{rr}$.

lated from equation B.15 using the data of the pipe R = 45mm, b = 50 mm, E (dynamically determined) = $32 \times 10^8 \text{ N/m}^2$, μ (dynamically determined) = 0.075 and K for water $2.05 \times 10^8 \text{ N/m}^2$, ρ = 102, ρ kg/m³. This yields a value a = 400 m/s.

Some tests were planned to measure the speed of propagation in the pipe experimentally. These tests were carried out in the following manner. The auxiliary valve (marked .11. on Fig. 11) was set in a nearly closed position and steady flow conditions were obtained in the pipe. This valve is normally used for service purposes. It only has a handle but no servomotor. That is why it was set near its fully closed position as the idea was to try to create a sudden closure condition. That was achieved by manually closing the valve its last 30° very fast. The pressure changes at a point close to the valve PTS (Fig. 42) during the resulting transient conditions were recorded. Fig. 47 shows such records for two different initial steady flow velocities in the pipe of 0.5 m/s. and 0.75 m/s. The value of the first pressure surge was used to calculate "a" using the relation $\Delta P = \frac{a}{g} \Delta V$. The average value obtained for "a" was 450 m/s. The above experimental procedures were chosen to avoid the influence of the occurrence of sub-atmospheric pressures occurring at the start of transients, resulting from the closure of the valve at the upstream end of the pipe. This might have some influence on the compressibility of the water. The use of the relation $\Delta P = \frac{a}{g} \Delta V$ was preferred to other possible ways of obtaining "a" by measuring the travel time of the pressure wave between two points on the pipe to avoid errors due to the rounding off of the wave front during its passage in the pipe. The calculated value of "a" using equation B.15 (400 m/s.) was found to be lower than the measured value being 450 m/s. This can be attributed to extra stiffness due to the flanges which suggests an equivalent $(\frac{R}{b-r})$ lower than 9, which is the value used in calculating the value 400 m/s. from equation B.15.

One more conclusion can be drawn from the above which may be of use in fluid engineering. For experimental measurement of transient pressures in pipe lines, the measurement of the strains on the outside surface of the pipe wall can yield indirectly the transient pressure changes in the pipe. Such a procedure would be useful in carrying out transient pressure measurements on existing pipelines without the necessity of drilling holes in them to fit pressure transducers. Also, this method would be adaptable to carry out transient pressure measurements in pipelines carrying hazardous fluids.

3.3.5. Transient conditions

The transient conditions measurements represent the main measurements of the study. They were carried out changing:

- a. pipe configuration (horizontal line, siphons with different heights, and siphons with condenser model on top)
- b. initial steady flow in the pipe system
- c. valve closure time
- d. valve closure characteristics (angular rotation with time) These factors were preselected before the testing. The experimental circuit configuration was prepared for the test. Points of interest for the pressure and velocity measurements were chosen. Experiments could be undertaken only after all electronic equipment had operated during a sufficiently long time to insure its stability and after all instruments check calibrations had been successfully accomplished. Adjustment of the water level in the two reservoirs to obtain the required steady flow velocity was then completed. Then, when steady flow in the circuit was assured, a visual check of existance of air liberated from the water in the system was made. When steady flow without air in the system was attained the recorders were started. Settings of valve steering system knobs were completed according to the selected characteristics of valve closure. Settings of oscilloscope and timer were finally made before the valve was closed. All the necessary data of each test were filled in on the experimental data sheet shown in Fig. 48. A diagramatic sketch of the principle of the measurements is shown in Fig. 31.

On certain laboratory tests high speed photography of cavitation void at selected points of interest was carried out. Photographic procedures were explained in section 3.3.3.

Once column separation had ceased and pressure waves had diminished the valve was opened and the recorded data were removed from the recording instruments and marked for subsequent identification. The system could be made ready for the next experimental run. It was found that the experimental results were very well reproduced. The experimental results are presented in the next chapters and compared with the calculated results obtained from computer simulation for the same testing conditions.

CHAPTER 4

4. COMPARISON OF EXPERIMENTAL MEASUREMENTS AND CALCULATED RESULTS USING CLASSICAL WATER HAMMER CALCULATIONS

In this chapter, calculated transient conditions are compared with measured results for hydraulic transients resulting from the closure of the valve upstream of the horizontal line. The comparison is aimed at evaluating the numerical solution of the problem using the finite difference characteristic method presented in chapter 2. This evaluation includes the study of different factors involved in carrying out these calculations regarding the choice of the input data for the computer programme as well as the principle of the calculations and technique. The study leads to findings discussed in the last section of this chapter. These findings form the foundation of the work presented in the following chapters.

4.1. Schematization of the Pipe System

Fig. 49 shows a schematic diagram of the horizontal pipe system, the pipe system in this case consists of a horizontal "plexiglass" pipe with valve at its left (upstream) end and a constant level reservoir at its right (down stream) end. When the valve is closed, the resulting transients in the system are to be investigated. The schematic diagram (Fig. 49) gives the principle for the mathematical simulation of the system used for the numerical calculations. With reference to Fig. 49 the following data are required for carrying out the water hammer calculations. They form the input data to the HOZ computer programme (appendix C):

D "D" **)

is the pipe inside diameter m

1 "CL" is the pipe length m

a "C" is the wave speed of a transient pressure pulse m/s.

HB "HO" is the level head above the centerline of the horizontal pipe m

f "F" is the Darcy-Weisbach coefficient of friction in the pipe

^{*)} Symbols between inverted commas represent names of the variables as they appear in the computer programmes

V	"VO"	is the steady flow velocity in the pipe m/s.
ξ,		is the flow resistance of the valve at time
		t = 0.
ΔH O	"HVO"	$\Delta H _{0}$ is the pressure drop given by $\xi_{0} \frac{o}{2g}$ across
		the valve at time t = o. "HVO" is read directly
		in the input data.
Pv	"PV"	is the vapour pressure of water corresponding to
		its temperature.

The description of the conditions during the closure of the valve is done using the following relation:

$$\Delta H \big|_{t} = \xi \big|_{t} \frac{V |V|}{2g}$$

where: $\Delta H \big|_{t}$ is the pressure drop across the valve at any time t during its closure

 $\xi|_{+}$ is the resistance of the valve at time t.

Thus the change of ξ with time during the valve closure has to be given as input data to the programme. This is done by specifying the valve closure time "TC" and reading in a number of resistance values "ZO (M)" that are used as a basis for interpolation of the resistances "ZZ (L)" representing $\xi|_{\pm}$. The choice of the data values is discussed in the following section.

4.2. Choice of Input Data for the Programme HOZ

The geometrical dimensions, i.e. D and 1, were specified (chapter 3). The celerity value was measured as described in section 3.3.4. The remaining input data were determined in view of the experimental data of the specific test which the calculated results were to be compared with. Thus, from the experimental data sheet the steady velocity of flow V was found as well as the level in reservoir $\mathbf{H}_{\mathrm{R}}.$ From Fig. 33 the value of f corresponding to V was obtained. Also the value ΔH was calculated. The value of the vapour pressure corresponding to the water temperature was found. For the valve closure data the closure time was found from the experimental records (the output signal of the potentiometer mounted on the valve stem). Then a number of time steps on the valve position record was chosen. The angle of closure corresponding to these time steps during closure were noted from the record. Then the corresponding resistances for these angles were found from the valve flow resistance angular position diagram Fig. 34. The obtained values were the resistance values "ZO (L)" needed for the input data.

4.3. Investigated Conditions

A number of experimental tests were completed. However the two tests shown in table 4 would suffice for the purpose of the discussions in this chapter.

Table 4
List of experimental measurements (for chapter 4)

Test number	steady flow	valve closure	type of	cavitation
	velocity	time	closure	void
	V _o m/s	S		occurance
6104 (Fig. 54)	1.0	2.0	linear	yes
6156 (Fig. 55)	0.75	1.0	linear	yes

The experimental data of the tests above are found in appendix H.

4.4. Comparison of Measurements and Calculated Results

When the first computer programme output results of the pressure history were compared to the measured pressure changes a very obvious damping in the experimental pressure peaks was not exhibited by the calculated results. So an attempt to modify the way that friction was allowed for in the calculations was made. Instead of a constant value of the friction factor, the form of friction factor dependence on velocity was adopted from the smooth pipe (f - Re Moody) diagram |57|, where Re is the Reynold number. This dependence of the friction factor on the velocity of flow was built into the programme HOZ by the function subprogramme "FRFA (VV,D)" (appendix C). No additional changes in the programme were attempted. The numerically calculated pressure histories that are presented in Figs. 54 - 55 were obtained using the programme HOZ in the form shown in appendix C.

Examination of Figs. 54 - 55 to compare the calculated results with the measured pressure changes yields the following observations:

^{*)} The measured values of the steady friction factor were approximated as 1.2 times the values of the friction factor in a smooth pipe (see Fig. 33). Note, that such procedure used data of steady conditions in a non-steady flow situation.

- 1. The calculated pressure peaks are higher than the measured ones.
- 2. The measured pressure changes show an evident diminishing with time that the calculated results do not exhibit.
- 3. There is a difference on the time base between the measured and calculated results.
- 4. The calculated results show pressure values less than the vapour pressure at some points of the line for some intervals of time in cases where a cavitation void occurs. Such pressures do not exist in the measured results.
- 5. The measured results show a decrease of the celerity towards the end of the transients *).
- 6. From the experimental results in the later cavitation voids, occurring near the valve, the pressure tends to increase ***), this can be explained by the fact that air dissolved in the water is released when underpressures are reached. This air remains free in the water even during the time compression waves exist in the pipe as the process of re-solution of the air in the water is a rather slow one.
- 7. We note that the points where the calculated pressure changes are presented, do not represent exactly the locations where the experimental pressure measurements were measured. This is because these points are the grid points closest to the locations where the actual experimental pressures were measured. Yet, the influence of this factor is of much smaller order than the discrepancies found between the measured and calculated results. Besides, the pipe length was divided into 10 Δx-intervals. However, when the grid interval size Δx was decreased by choosing a larger number of divisions no significant change in the picture of the calculated results was obtained.

^{**)} e.g. In Fig. 55 t_{vr} is larger than $2t_{rr}$. t_{vr} is a period with a valve (dead end) at the upstream end of the pipe and a reservoir at the downstream end of the pipe. t_{rr} is a period with a reservoir (cavity at vapour pressure) at the upstream end of the pipe and a reservoir at the downstream end of the pipe. Figs. 7 - 8 are helpful in understanding this point.

^{**)} e.g. In Fig. 55 pressure at B with respect to pressure A

4.5. Photographic Study of Water Column Separation during Transients in the Horizontal Pipe

Introduction

The study presented in this section comprises mainly a study of a high speed film taken for transient conditions occurring in a segment of the horizontal "plexiglass" pipe line, just downstream of the valve, following the closure of the valve. The film shows the events occurring during water column separation. The study is presented together with a discussion of pressure measurements during the resulting transient.

Transient Conditions Test

A typical transient test was carried out in the following manner. Water levels in the high and low level reservoirs were adjusted to 1.12 m and 0.5 m above the center-line of the "plexiglass" pipe, respectively, to obtain a steady flow velocity of 1 m/s. This value was checked using the V-notch weir. The output signals of the pressure transducers and the valve angular position displacement were recorded. Fig. 56 shows the following signals:

- a. valve angular position (the valve closure was completed in about 1.6 second)
- b. P₁, pressure at point PT₁ (Fig. 56)
- c. P2, pressure at point PT2 (Fig. 56)
- d. P3, pressure at point PT3 (Fig. 56)
- e. P_h, pressure at point PT_h (Fig. 56)
- f. 10 c.p.s. time signal

With reference to Fig. 56, it is seen that as the valve started moving towards its closed position about 0.2 second lapsed before pressure P_1 started to fall. This can be explained by the fact that the ball valve offered a small resistance to the flow at small angles of closure. The continued motion of the valve towards its closed position caused gradual deceleration of the flow through the valve. This resulted in propagation of rarefaction waves in the direction of the low level water reservoir at the downstream end of the pipe. Pressure P_1 continued to decrease till it reached the vapour pressure of water resulting in a formation of a vapour void at the valve. The phenomenon of water column separation was initiated. A cavitation void continued to grow and later diminished while small pressure waves travelled back and forth in the water column between the void and the low level water reservoir. Finally the cavitation void at the valve collapsed resulting in the first pressure surge. This pressure peak

travelled towards the low level water reservoir where it was released. When this release reached the valve (dead end) pressure P₁ felled instantly to the vapour pressure and column separation at the valve re-occurred. The resulting cavitation void grew and then diminished and this collapse resulted in the second pressure surge. Similar events to those causing the second pressure surge caused the third pressure surge. Also a clear damping of the pressure changes can be seen in Fig. 56.

Preparation of the High Speed Film

The high speed camera arrangement for photographing the segment of the pipe adjacent to the valve at the upstream end of the horizontal "plexiglass" pipe shown in Fig. 41 was presented in section 3.3.3. The set up was used to photograph a part of the pipe of (about) 300 mm length just downstream of the valve. After steady conditions of flow in the pipe at the desired flow velocity were reached the following steps were completed.

- a. Setting up of camera and light arrangement were made.
- b. The recorder was started.
- c. The high speed camera was started to photograph at 1000 frames per second.
- d. After about 1 second, the valve closure was initiated. This instant was displayed on the recorder. At the same instant time marks would start on the film at a frequency of 1000 c.p.s.. The waiting interval between the start of the camera and the initiation of valve closure (the 1 second period) was done to assure that the high speed camera attained its 1000 frames per second running speed when the events of the water column separation took place.

The valve completed its closure according to the prescribed closing characteristic and the events of water column separation were photographed. At the same time the transient pressure changes were recorded (Fig. 56).

Study of the High Speed Film

The discussion described here after gives a qualitative study of the high speed film obtained in the light of the transient pressure records (Fig. 56). Fig. 57 * shows twenty four different frames of the film. The approximate instant of each of these frames is marked on the pressure P_1 record shown in the figure. The time pointer can be seen on the different frames. The dark area on the right side of the pipe (seen in all fra-

^{*)} In Fig. 57, a single arrow line points to the region of small bubbles and a double arrow line indicates a main void.

mes) is due to the shadow of the piezo-electric pressure transducer mount. At the beginning of the valve closure, a very small drop in pressure P1 at the downstream end of the valve can be seen. This drop in pressure became larger as the valve continued moving towards its closed position. On the film the water could be seen to continue flowing without any observeable change. A typical frame of such a picture is I 1. This continued nearly to I 2, when a number of tiny bubbles started to appear very close to the valve. On the pressure record one sees a drop in the pressure P that marked the initiation of rarefaction waves propagating towards the low level water reservoir. At I 2 the pressure Po nearly reached the vapour pressure and apparantly some of the dissolved air in the water was liberated out of it. These air particles might be the nuclei for the formation of vapour bubbles. These bubbles were extremely small. I 3 shows the picture of such bubbles. At that moment the pressure P, had reached the vapour pressure and a whole lot of tiny bubbles filled the cross section of the pipe close to the valve (at left of the picture in I 3). These tiny bubbles, which filled the whole cross section, extended further along the pipe (nearly the length of the photographed segment of the pipe) with the pressure remaining constant at the vapour pressure. I 4 shows a larger portion of the pipe filled with these tiny bubbles. In the meantime the valve approached its fully closed position causing a diminishing rate of flow through the valve. This flow practically ceased by I 4. The tiny bubbles were seen to join each other forming larger bubbles as coalescence took place between adjacent bubbles, the resulting larger bubbles continued to grow (I 5). When a bubble reached a size large enough such that the difference between the internal pressure and the external pressure offset the surface tension pressure, which is inversely proportional to its size, the bubble reached an unstable condition. This resulted in formation of a vapour filled cavity. Two vapour cavities appeared near the top the pipe as shown in I 6. The two voids continued to grow and they joined together at I 7. As seen on I 7 a large void of vapour was contained in the cavity near the top of the pipe with a number of small vapour bubbles near the cavity. The pressure record continued to show the same vapour pressure value. Then, this vapour void started to diminish as can be seen on I 8. One can say that in the first part of the transient, the water in the pipe decelerated till it came to rest because of the difference in pressure between the reservoir and the vapour void (vapour pressure) as well as the resistance in the pipe. Later-on the water started moving towards the valve under the pressure difference between the low

level water reservoir and the vapour void at the valve. I 9 was just before the collapse of the vapour cavity was completed. The vapour cavity collapse resulted in a large pressure surge as seen on the pressure record. As the water in the pipe stopped along the length of the pipe, this pressure peak continued. I 10 shows no bubbles at all, but one cannot say if the minute air particles that came out of the water at the sub-atmospheric pressures had redissolved. Most probably they did not, as the diffusion process of gas particles in the water is a relatively slow one. The high pressure continued till all the water in the pipe came to rest ending with an unstable condition of higher pressure in the pipe than that in the water reservoir, thus water started flowing out of the pipe and the high pressure in the pipe started to be released. When the water just adjacent to the valve started moving towards the reservoir, an instantaneous reduction of the pressure at the valve to the vapour pressure resulted in formation of small bubbles near the valve (I 11). It is noted that these bubbles were larger than the ones seen when cavitation started on the previous occasion (I 2). These large bubbles gathered very quicky near the top of the pipe (I 12). Then, they formed a vapour void cavity on the top of the pipe (I 13). A small void appeared in front of the large void cavity on the top of the pipe (I 13). The main void cavity appeared to grow with still the little cavity ahead of this large cavity (I 14). A little later the two voids joined forming mainly one vapour cavity (I, 15). This cavity continued to grow. At nearly I 16 it started to diminish. That was because of the reversed direction of flow of the water column being towards the valve at that moment. I 17 shows a further diminishing of the void. I 18 shows the cavity just before it collapsed. I 19 shows the pipe segment after the collapse of the cavity had been completed. The collapse resulted in a pressure surge. This resulting pressure peak lasted for $\frac{2L}{c}$ at the valve. Once again a new void started when the pressure at the valve dropped to the vapour pressure. I 20 shows some small bubbles (larger than both previous times (I 2 and I 11) starting adjacent to the valve. It is thought that at that moment more air particles existed in a free form near the valves and that these act as nuclei for the vapour bubbles. These bubbles gather very rapidly to the top of the pipe and form a vapour cavity I 21. That vapour cavity continues to grow (I 22). Its size increased still further and then it started to diminish. I 23 shows the cavity whilst diminishing. Finally it collapsed at I 24.

Discussion of Water Hammer - Water Column Analysis in view of the photographic study

Among the first techniques to be used for predicting the resulting pressure surges resulting from water column separation associated with water hammer was the method used by Escande | 15 |. In reference | 15 | the graphical solution of transient flow in a pipe was adapted for the solution of the problem in the following manner. When the pressure reached the vapour pressure a bubble was located. The growth and, later, diminution of this bubble was followed in a tabular form as given by the velocity changes obtained from wave propagation in the water column. When the bubble size vanished, the normal graphical solution | 3 | procedures were continued. The above technique remained for a number of years as the commonly used method for the evaluation of pressure surges due to column separation. However, Li 31, 32 developed some mathematical models using rigid column theory approach for describing the combined water hammer - water column separation phenomena. In adapting digital computers for the solution of transient hydraulic flow problems involving water column separation essentially the idea used by Escande | 15 | has been utilized using a finite difference solution of the water hammer equations by the method of characteristics [58, 60]. In such numerical solutions, the viscous friction could be allowed for (making some assumptions regarding values of friction coefficients to be used in the calculations). Recently as more interest has developed in water column separation during transient conditions in hydraulic pipe-lines with low pressures, more effort to better description of the phenomena has been attempted. Siemons | 50 | developed a mathematical model for the transient flow resulting when vapour pressure is reached in a horizontal pipe. In his analysis, the commonly used finite difference solution of the continuity and momentum equations for the one dimensional unsteady flow, based on the method of characteristics is followed. When the pressure reaches the vapour pressure at a point a thin vapour cavity is located at top of the pipe. Flow under such cavity is assumed to be a one dimensional unsteady open channel flow. He used a number of assumptions regarding the shape of the cavity. Siemons' work did not include experimental verification. It was about the same time that Baltzer 2 used a similar approach. He used the same idea of dividing the pipe into parts where calculations were done using closed conduit analysis and other parts where open conduit analysis was used. He also introduced some assumptions regarding the tip edge shape of the cavity under which the open flow was assumed. This last assumption he introduced as a result of visual appeal

to the shape of the resulting column separation in a "plexiglass" pipe at the location of the column separation. The experimental results of Baltzer involved measurement of the depth of the resulting vapour cavity using a series of miniature wave gauges. However, he reported dissatisfaction with the performance of these gauges as regards calibration and dependability. He reported descrepancies in the transient pressure changes between those calculated and the measured. These descrepancies included both the values of the resulting surges as well as the time lapse between the pressure surges. A clear damping could be noticed in his experimental measurements |2|. Brown |5| presented some experimental transient measurements with water column separation resulting from a pump failure. In an attempt to modify the graphical solution for this problem to allow for the damping that he noticed in his experimental results, he assumed a number of pockets of air in the pipe and modified the solution to allow for such a model. He obtained a better agreement of the graphically obtained results with the experimentally measured results. However, the assumptions he made as regards the amount of air and the air pocket locations were made in view of the experimental results to get better agreement of the calculated and measured results.

Recently Weyler |66| introduced a new model for carrying out the calculations of transient one dimensional flow with pressures near the vapour pressure of the fluid. This mathematical model considers typical tiny bubbles to exist along the whole length of the pipe. He formulated an analysis of the dissipation involved during expansion and compression of a single bubble during the passage of rarefaction waves and compression waves in the pipe. Such approach was motivated by reported noise heard during the transient tests reported by Baltzer |2| in the pipe (opaque pipe). However, Weyler had to make some assumptions as regards what radius he should use for a typical bubble. Moreover, in attempting to compare the results of his mathematical model with experimental results he had to make some assumptions about the number of bubbles existing per unit length of the pipe. That he did by changing a certain parameter value to obtain best agreement of the predicted values with the experimental results. Following the above short survey we shall try to evaluate the different approaches in view of the photographic study and the experimental pressure results presented before.

As regards the use of Siemons' and Baltzer's approaches the characterization of the flow at the void as an open flow under a main cavity is questionable. Only for the durations between (I 7 - I 9), (I 15 - I 18) and

(I 22 - I 23), (see pressure record Fig. 57), could the flow be approximated to an open flow under a cavity. For a longer duration, during column separation the photographed flow shows more or less a two phase flow with different regimes. Another additional remark here is that the length of pipe where main vapour void accured was relatively very small with respect to the length of the pipe (0.2 m to 46 m). In view of the above qualitative study one may conclude that the approach of Siemons and Baltzer would not really describe the events of the phenomena in a precise way in similar hydraulic transient applications.

The loss of the momentum associated with the phenomena would be explained in a more representative way by such an approach as that of Weyler. This suggested the occurrence of changes in the fluid, considered as an intimate two phase mixture, along the whole length of the pipe, resulting in the momentum loss exhibited by the experimental results. Such damping can be seen in all experimental results of investigators in this area (see Fig. 55 as well)..

A further examination of the pressure records in Fig. 56, shows some changes (marked a) for the pressures at the points PT₂, PT₃, PT₄ which are away from the main void at the valve. These changes could be attributed to pressure changes in bubbles in the neighbourhood of the pressure transducers when the pressure waves pass such points. The visual observation of the pipe during the transient test along the whole length of the pipe suggest formation of very tiny bubbles during the transients. The above discussion suggests that: to obtain a better mathematical model for predicting pressure changes associated with water hammer - water column separation, changes occurring within the fluid along the length of the pipe should be accounted for; these changes result in a large momentum loss associated with the phenomena; the expansion and compression of the tiny bubbles forming (along the legnth of the pipe) during such transients play an important role in this respect.

A new mathematical model based on the above idea will be introduced in chapter 5.

Also an important observation that can be made from the study of the film is that the time of formation and growth of the vapour void to its largest size was longer than the time it took to decrease from its largest size till it collapsed (e.g. I 10 - I 16 with respect to I 16 - I 18 on the pressure record Fig. 57).

4.6. Significant Findings

- 1a. The measurements show that the pressure inside the cavity remains nearly constant. When attempts were made to have the first pressure transducer arranged on top and bottom sides of the cross section no significant difference in pressure records were found.
- 1b. When a vapour cavity exists near the valve, the pressure signals P_2 , P_3 , P_4 show small pressure peaks. The time interval between two successive peaks is $\frac{2L}{3}$.
- 1c. The study of the film shows that during the formation of the first cavitation void, a large number of bubbles fill the whole cross section near the valve. This lasts for the time-interval (I 3 I 5) during which the pressure at the valve remains at the vapour pressure value.

In view of the above remarks it seems that the assumption of a single cavity under which an open flow is assumed to represent water column separation |2| is not quite right. For the first cavitation void, the film shows that this does not happen. The first two remarks show that a use of a constant pressure at the valve at the vapour pressure value as a boundary condition during the occurrence of column separation is quite reasonable.

- 2a. The damping associated with the water column separation phenomena show actually an appreciable loss of momentum.
- 2b. Referring to the experimental results (Figs. 54, 55, 56), an exponentially decaying trend in pressures with time can be seen.

This observation was of great importance in building the new mathematical model to describe flow during such transients (chapter 5). In this model, the momentum loss is exhibited along the whole pipe. No special attention was given to the mechanics of the formation or collapse of the cavitation void.

In carrying out the numerical calculations the cavitation void can still be dealt with as a reservoir at the vapour pressure and it will be considered as part of the boundary condition in the manner used in this chapter.

3. Also, as can be seen through the previous discussions it was felt that efforts should be made to prepare more representative and accurate values for the input data to be used in the calculations. This

^{*)} e.g. marked C in Figs. 55 and 56.

involved basically the values to be used for celerity and valve resistances during closure. How this was accomplished will be discussed in chapter 6.

5. NEW MATHEMATICAL MODEL

From the ideas discussed in the last chapter, it is evident that the dissipation influence associated with water column separation should be built in the analysis in a more representative form. Thus referring back to the basic flow equations formulated in chapter 2, the following newly deviced model is proposed. The equation of continuity is used in the same form (13) with an additional simplification by neglecting the last two terms in the equation.

Thus the equation takes the form:

$$\frac{\partial H}{\partial t} + \frac{a^2}{g} \frac{\partial V}{\partial x} = 0 \tag{51}$$

As pointed out is section 4.6., experimentally an exponential decay of the pressure-waves has been observed. This suggests a linear resistance law. Therefore, without going into the actual physical processes taking place, we assume from a practical engineering point of view, that the phenomena can be predicted on the assumption of a linear resistance-law. With this assumption the momentum equation (18) can be written in the form:

$$\frac{\partial H}{\partial x} + \frac{1}{g} \frac{\partial V}{\partial t} + \frac{c}{g} V = 0 \tag{52}$$

In equation (52), c is a combined momentum loss factor. The idea behind the choice of such simple form for the wall shear term will become clear after some further mathematical manipulations of equations (51) and (52) are presented. Eliminating V from equations (51) and (52), we obtain:

$$\frac{\partial^2 H}{\partial t^2} + c \frac{\partial H}{\partial t} - a^2 \frac{\partial^2 H}{\partial x^2} = 0 \tag{53}$$

Similarly eliminating H from equations (51) and (52) we obtain:

$$\frac{\partial^2 V}{\partial t^2} + c \frac{\partial V}{\partial t} - a^2 \frac{\partial^2 V}{\partial x^2} = 0 \tag{54}$$

Equations (53) and (54) are of the same form. They are hyperbolic, linear, second order, partial differential equations. To explore the mathematical solution of these equations, initial and boundary conditions have to be specified.

We proceed just for the sake of illustration, by considering as an example the following problem | 19|.

$$\frac{\partial^2 u}{\partial t^2} + \frac{\partial u}{\partial t} - \frac{\partial^2 u}{\partial x^2} = 0 (55)$$

$$u(x,0) = g(x)$$
 (56)

$$\frac{\partial \mathbf{u}}{\partial t} (\mathbf{x}, 0) = 0 \tag{57}$$

$$u(0,t) = u(\pi,t) = 0$$
 (58)

In the problem above, equation (55) is of the same kind as (53) or (54). Using the well known separation of variables technique, a solution of the form:

$$u(x,t) = \sum_{n=1}^{\infty} A_n e^{-\frac{t}{2}} \sin(n x) \cos\{(\sqrt{n^2 - \frac{1}{4}})t\}$$
 (59)

is obtained for this problem.

The mathematical solution shows the exponential damping trend that was exhibited in the experimental measurements as pointed out in the last chapter. By analogy with the solution (59) of equation (55), the solution of (53) or (54) will have an exponential term with an exponent $(-\frac{ct}{2})$.

It is also useful at this moment to note the equation of motion of a single mass element with a linear damping rate

$$m \ddot{x} + c \dot{x} + k x = 0$$
 (60)

as a number of similarities do exist between (53) or (54) and (60). Note that the value of c to be used in carrying out the analytical solutions of equations (53) and (54) to describe the flow has to be found. This is done experimentally using the logarithmic decrement technique, and will be explained in the following chapter. The above note about the equation of motion of the single mass system gives the reasoning behind the choice of such a technique.

The analytic solution of equations (53) and (54) describing the transient flow (with the associated cavitation bubbles) subject to the boundary conditions is carried out using a finite difference solution.

5.1. Finite Difference Solution

Writing H or V as function u whose solution is u (x,t), the finite difference approximations (with reference to Fig. 58) may be written, neglecting terms of higher orders than the second, as |19|.

$$u_2 = u(x_1,t_1) + \Delta x \frac{\partial u(x_1,t_1)}{\partial x} + \frac{(\Delta x)^2}{2} \frac{\partial^2 u(x_1,t_1)}{\partial x^2}$$
 (61)

$$u_3 = u(x_1,t_1) + \Delta t \frac{\partial u(x_1,t_1)}{\partial t} + \frac{(\Delta t)^2}{2} \frac{\partial^2 u(x_1,t_1)}{\partial t^2}$$
 (62)

$$u_{4} = u(x_{1},t_{1}) - \Delta x \frac{\partial u(x_{1},t_{1})}{\partial x} + \frac{(\Delta x)^{2}}{2} \frac{\partial^{2} u(x_{1},t_{1})}{\partial x^{2}}$$
 (63)

$$u_5 = u(x_1,t_1) - \Delta t \frac{\partial u(x_1,t_1)}{\partial t} + \frac{(\Delta t)^2}{2} \frac{\partial^2 u(x_1,t_1)}{\partial t^2}$$
 (64)

choosing

$$\Delta x = a\Delta t \tag{65}$$

and using the approximation

$$\frac{\partial u(x_1, t_1)}{\partial t} = \frac{u_3 - u_5}{2\Delta t} \tag{66}$$

Substituting from (61 - 66) in both (53) and (54), the finite approximation relations (67) and (68) are found.

$$H_{3} = \frac{\left[(H_{2} + H_{4}) - (1 - \frac{\Delta t \cdot c}{2}) \cdot H_{5} \right]}{(1 + \frac{\Delta t \cdot c}{2})}$$
(67)

$$V_{3} = \frac{\left[(V_{2} + V_{14}) - (1 - \frac{\Delta t \cdot c}{2}) \cdot V_{5} \right]}{(1 + \frac{\Delta t \cdot c}{2})}$$
(68)

Grid system

To obtain a numerical solution of equations (53) and (54) describing the flow, a grid system similar to the one used in chapter 2 is devised in Fig. 59. Referring to the grid notation (Fig. 59), the following finite difference equations are used for a progressive step by step numerical solution:

$$H_{P} = \frac{\left[(H_{R} + H_{S}) - (1 - \frac{\Delta t \cdot c}{2}) H_{Q} \right]}{(1 + \frac{\Delta t \cdot c}{2})}$$
(69)

$$V_{p} = \frac{\left[(V_{R} + V_{S}) - (1 - \frac{\Delta t \cdot c}{2}) V_{Q} \right]}{(1 + \frac{\Delta t \cdot c}{2})}$$
(70)

For the initial and boundary conditions

a. To evaluate H and V at the first time interval Δt, the momentum loss coefficient is neglected. This is done on the basis that at the first time step the influence of cavitation bubbles associated with water column separation effect does not exist. In this case, equations (53) and (54) reduce to the wave equation and we practically have a first Cauchy problem |19|. The finite solution of which takes the form:

$$H_{p} = \frac{1}{2}(H_{p} + H_{q}) \tag{71}$$

$$V_{\mathrm{P}} = \frac{1}{2}(V_{\mathrm{R}} + V_{\mathrm{S}}) \tag{72}$$

b. To evaluate H and V at x = 0, that is a left end boundary condition Fig. 6, the influence of the momentum loss coefficient is neglected and the characteristic equation along C^- (46) takes the form:

$$V_{P'} - V_{S'} = \frac{g}{a} (H_{P'} - H_{S'})$$
 (73)

c. To evaluate H and V at x = L, that is a right end boundary condition Fig. 6, again the influence of the momentum loss coefficient c is neglected and the characteristic equation along C^+ (49) takes the form:

$$V_{P''} - V_{R''} = -\frac{g}{a} (H_{P''} - H_{R''})$$
 (74)

Equations (69 - 74) give the finite difference equations needed for the solution of Water Hammer - Water Column Separation Problems using the newly devised mathematical model. In the following three chapters, calculations based on this analysis are presented for different cases:

- a) for a horizontal line (chapter 6)
- b) for a siphon (chapter 7)
- c) for a condenser system (chapter 8)

CHAPTER 6

6. TRANSIENTS RESULTING FROM CLOSURE OF THE VALVE AT THE UPSTREAM END OF THE HORIZONTAL PIPE

In this chapter, the transient conditions resulting from the closure of the valve at the upstream end of the horizontal pipe are investigated. The study covers the influence of the following factors: the initial steady flow velocity, the valve closure time and the valve closing characteristic (angle of closure versus time during valve closure). The resulting conditions are examined as regards both the water hammer and water-column separation phenomena. The mathematical model together with the numerical solution method described in chapter 5 are used for the prediction of the resulting pressures. As was pointed out in chapter 4 a careful choice of data values for the input to the computer programme is essential. The bases for the selection of the celerity, momentum loss coefficient and valve resistance values necessary for carrying out the numerical calculation are discussed in detail. The calculated results are compared with measurements.

6.1. Typical Experimental Test

A typical experimental test is found in section 4.5. Fig. 56 represents the experimental results of this typical test.

6.2. Schematization of the Line

The same scheme that was discussed in chapter 4, was used (Fig. 49).

6.3. Choice of Input Data for the Programme HZD

The same grid (Fig. 50) which was described in chapter 4 and used for programme HOZ in appendix C was adapted for the presentation of the x-t plane for programme HZD. Programme HZD, (appendix D) was used for the calculation of the resulting pressure changes during transient conditions. The programme was based on the new mathematical model that was introduced in chapter 5 and its main steps are presented in appendix D. The following parts discuss in detail the choice of the essential data values needed for calculations using programme HZD. Specifically:

- 1. Celerity
- 2. Valve dynamic resistances during its closure
- 3. Celerity change with time
- 4. Momentum loss coefficient.

For the purpose of the following discussions some experimental measurements were performed. Such experiments are described through the following discussions.

1. Celerity

In section 3.1.2., with the knowledge of the pipe geometrical and material data a value of a = 400 m/s was calculated.

To obtain a measured value of the celerity that is not influenced by the cavitation bubbles occuring along the pipe (as subatmospheric pressures exist during the transients), a lot of tests were carried out closing the auxiliary valve at the downstream end of the pipe suddenly. Results of such tests were presented in section 3.3.4. (Fig. 47). A value of 450 m/s for the celerity was found.

Note that this value represents the celerity at the start of the transients when there were no cavitation bubbles in the water. Experimental measurements exhibited a slower wave speed of propagation near the end of the transients and this fact is discussed later in part 3.

2. Dynamic resistance of the valve

In chapter 4, a number of valve resistances obtained from steady measurements corresponding to the angular position of the valve were used as valve resistances during its closure. In an attempt to examine how good such values would be, it was decided to try to obtain actual dynamically determined valve dynamic resistances. This was only possible because the induction flowmeter described in chapter 3 had been developed. The experimentally determined dynamic resistances were obtained, using a set of measurements. In these measurements the pressure changes very close to the valve were recorded. One induction flowmeter was placed as close as possible to the valve, that is after the first 2m segment of the pipe. Records of the pressure and the velocity downstream of the valve, together with the valve angular position during its closure were made for a number of linear valve closures.

The closure times ranged from 0.5 to 4.0 seconds. An example of these measurements is shown in Fig. 60. The records were used to obtain a digital presentation at a number of time increments of the signals H_1 , V_1 and

the angle α . Then using the relation (75), the valve dynamic resistances were calculated.

$$H_{us} - H_1 = \xi(\alpha) \frac{V_1^2}{2g}$$
 (75)

where: H is the pressure head upstream of the valve (head in high level reservoir)

- H₁ is the pressure head at a point just downstream the valve at a particular instant
- V₁ is the velocity at a point just downstream of the valve at the particular instant
- α is the angle of opening of the valve at the same particular instant
- ξ is the dynamic valve resistance corresponding to angle

The obtained values of the dynamic resistances are plotted versus the valve angular position in Fig. 61.

The values of the resistances obtained from steady flow measurements (Fig. 34) are also shown in the figure. Note in Fig. 61, that for measurements number 5176, 5178 and 5071 values of the valve dynamic resistances at the large angles of closure are not shown. They could not be found, as water column separation occurred just behind the valve in these cases. The location of the induction flowmeter being about 2m from the valve at which water column separation occurred, it was not possible to measure V_1 in cases when water column separation took place. The operation of the induction flowmeter necessitated its positioning away from locations where cavitation voids occur during transient tests.

Examination of the results shown in Fig. 61 yields the following conclusion. **) If the representation of the flow through the valve during its dynamic closure $\Delta H = \xi(\frac{V^2}{2g})$ is used, then the valve resistance angular valve position dependence obtained from steady measurements would represent the dynamic resistance for the range of our testing conditions to a reasonable accuracy.

Furthermore it was felt that the linear interpolation procedures used in programme HOZ (appendix C) may be yielding unsmooth changes of the instantaneous valve resistances required for the calculations of the valve boundary conditions and it was decided to replace these linear interpola-

^{*)} In general one might expect a departure from steady characteristic when the times involved are comparable with times following from the Strouhal number |49|.

tion procedures in the following manner. The measured steady flow valve resistances versus angle of closure (data Fig. 34) were fitted with polynomials. **) Two Tchebichef polynomials were necessary. The first covered the range of α between $0-60^{\circ}$ and the second covered α between $48-82.5^{\circ}$. The computed coefficients of the two Tchebichef polynomials are listed in table 6. (see appendix D).

3. Celerity change with time

Preliminary measurements showed a decrease of the celerity associated with water column separation phenomena at the end of the transients. This was noted by Weyler |66| as well. A number of tests aimed at a better understanding and evaluation of this fact was carried out. No particular test is presented to give the following results but the results to be discussed in this part are clear from the experimental results presented in this chapter.

It was found that the celerity gradually decreases from a = 450 m/s at the beginning of the transients to a lower value, as low as 420 m/s, at about 4 seconds from initiation of the closure of the valve. This feature was true of all experimental measurements for the hydraulic transients in the horizontal line configuration in an approximate sense. Tests covered linear closure of the valve in times between 0.4 - 4 seconds for a range of steady flow velocities between 0.3 - 1.45 m/s. The above range covered cases where water column separation took place as well as cases where it did not. The above decrease in the celerity may be explained by occurrence of very small bubbles in a large portion of the length of the pipe as sub-atmospheric pressures were reached. These bubbles were very small.

Some effort was made to visualise these bubbles. A small "plexiglass" box that was filled with water could be mounted around the pipe at different locations (Fig. 62). Such arrangement minimized light reflections on the circular surface of the pipe, thus a clearer view to the water under flow could be achieved. Visual observations, using this system showed occurrence of small bubbles at large number of locations during transient conditions. The observed bubbles were very tiny and they rose very quickly to the top of the pipe. It is thought that these bubbles are air bubbles freed from the water as the pressure dropped to sub-atmospheric pressures. The assumption that these bubbles were of a gaseous type can be explained

^{*)} Tchebichef polynomials were chosen as their convergence was reasonable.

by the slow nature of the above observation as the air freed out of the water takes a relatively long time to re-dissolve. A supporting observation to this last postulate is that some air pockets could be seen at top of the pipe at the end of the transients. This could be clearly seen when the valve was re-opened to establish the steady flow conditions for the subsequent experiment. Attempts were made to make high speed films of these bubbles, but unfortunately these attempts did not succeed because of photographic difficulties. Observations made through out the testing indicate that the original size of a typical bubble was smaller than the 0.3mm which is the typical size Weyler assumed in his study 66. The occurence of such bubbles could also be seen from the pressure signals during the transient conditions as has been indicated before in section 3.3.3.. It is due to the occurrence of these bubbles during the transients that decrease of the celerity with time is observed. Fig. 63 shows a plot of the change of pressure wave propagation speed in a two phase mixture under a homogeneous bubble regime with the void fraction 21. It is seen that a very small amount of vapour in the flow, line I in Fig. 63, (in our case gas) would cause a large decrease in the celerity. Weyler | 66 | did not incorporate the decrease of the celerity in his mathematical model but he had noted it in commenting on his measurements. For the numerical calculations, we will assume a linear celerity decrease relative to time, quantitatively a drop from 450 to 420 m/s in 4 seconds. A supporting fact for such an assumption is that the time of overpressure duration in the pipe is relatively small to cause resolution of the gas bubbles, knowing that such a process is a slow one. Another point is that in case of very small bubbles the surface tension force is of a very large order thus the stability of such bubbles would be hindered only under relatively large pressure difference between the outside of the bubble and its inside. It is noted that this assumption is based on imperical results. It is justified to a large extent by the reasoning discussed above. Besides, it provides a reasonable simplification of a complex phenomenon for engineering purposes.

4. Momentum loss coefficient

As has been discussed in chapter 4, the exponential decay of the pressures with time exhibited by the experimental measurements results is analogous to the exponential term in the mathematical series solutions of equations (53) and (54). It was decided to use the logarithmic decrement technique to obtain experimentally, a representative value of the momentum

loss coefficient c. Fig. 64 shows the principle of such procedures..

As the speed of the pressure wave propagation was found to decrease with time during the transient, the period of a complete cycle T (Fig. 64) increased with time. Besides, when a vapour void existed at the valve the pressure wave travel frequency was twice that when no vapour void existed at the valve.

**

This can be explained by the fact that when a vapour void existed, the water column was separating two reservoirs while when there was no vapour void at the valve we had a situation of a valve at one side (dead end when it was completely closed) and a reservoir at the other side of the water column. This could be seen clearly in the illustrative examples presented in section 2.5.. An approximate relation between c and the travel time of the pressure wave T was found:

$$c = \frac{0.6}{m} \tag{76}$$

where: $T = \frac{4L}{a}$ when there was no vapour void at the valve $T = \frac{2L}{a}$ when a vapour void existed at the valve.

Note that the data values above are based on the pipeline system and the range of measurements described before.

The rest of the data necessary for programme HZD are essentially the diameter of the pipe, its length and the steady conditions. These data were chosen in the same manner described in section 4.2. for programme HOZ.

6.4. Comparison of Experimental Measurements and Calculated Results

Table 7 gives a list of test conditions for the experimental measurements presented in Figs. 65 - 70.

Table 7

List of experimental conditions for chapter 6 (horizontal line)

Test Number		Time of closure of the valve s	Type of valve closure(angle-time)	Column se- paration at the valve	Fig.
6154	0.75	2.0	linear no		65
6155	0.75	1.0	linear	yes	66
6156	0.75	0.5	linear	yes	67
6104	1.0	2.0 line		yes	68
6105	1.0	1.0	linear	yes	69
6106	1.0	0.5	linear	yes	70

^{*)} e.g. see A with respect to B in Fig. 66

Table 8 contains a listing of data used as input data for the computer programme HZD. These data represent conditions that resulted in the experimental test results of the measurements listed in Table 7.

Table 8

Input data for programme HZD

Management Nambara		6154	6155	6156	6104	6105	6106
Measurement Number "MESNUM"		0154	0155	0190	0104	010)	0100
"CL" pipe length	m	40	40	40	40	40	40
"D" pipe diameter	m	0.09	0.09	0.09	0.09	0.09	0.09
"C" celerity	m/s	450	450	450	450	450	450
"VO" steady velocity	m/s	0.75	0.75	0.75	1.0	1.0	1.0
"F" steady friction factor		0.0202	0.0202	0.0202	0.0188	0.0188	0.0188
"HVO"steady head loss in valve	m.water	0.03	0.03	0.03	0.05	0.05	0.05
"HO" low level reservoir head	m.water	0.5	0.5	0.5	0.5	0.5	0.5
"PV" vapour pressure	m.water	-10.	-10.	-10.	-10.	-10.	-10.
"TC" valve closure time	S	2.0	1.0	0.5	2.0	1.0	0.5
"DECS" celerity decrease rate	m.s ⁻²	7.5	7.5	7.5	7.5	7.5	7.5

"NF" calculations done using "NF" = 11

Pressure history plots correspond to "N" = 1, 2, 4, 6, 8, 10

Velocity history plots correspond to "N" = 2, 9

Satisfactory agreement of the numerically calculated pressure and velocity changes with the experimental measurements for test number 6154 can be seen from Fig. 65. These results represent pressure and velocity changes resulting from linear closure of the valve in 2 seconds for an initial steady flow velocity of 0.75 m/s.

The order of pressure values as well as the time intervals between pressure changes obtained in the numerical results agree with measured results.

For the results presented in Fig. 66, giving the calculated and measured results for valve closure time of 1 second for initial steady flow of 0.75 m/s, good agreement of both results could be seen. However the calculated results gave smaller pressure peaks at the end of transients which is perhaps due to larger value of the momentum loss coefficient than the actual one.

For results shown in Fig. 67, i.e. pressure and velocity changes during experimental test number 6156, the first calculated pressure peaks compare fairly well with their counter parts in the experimental measurements. The latter parts of the changes do not agree so well showing lower calculated results than the measured ones.

Reasonable agreement of the calculated pressure results with the experimental measurements for experimental test conditions of valve closure time of 2 seconds and steady flow velocity of 1 m/s. are exhibited in Fig. 68.

The calculated and measured results for tests 6105 and 6106 Figs. 69 - 70 agree fairly well during the first part of the transient with a less extent of agreement in the latter parts, where calculated results show more damping than the measurements.

In comparing the calculated results with the experimental measurements one must keep the following facts in mind.

- a The possible errors in the measurements of the steady flow velocity that can amount to \pm 2.5%. This will certainly have an influence on the results.
- b The calculated pressure results shown in Figs. 65 70 are at certain nodes (corresponding to N = 1, 2, 4, 6, 8, 10). These nodes would correspond to certain distances from the valve. On the other hand the experimental pressure measurements are at points PT₁, PT₂ ----- PT₆. The corresponding distances are not exactly the same.
- c The same influence of difference in location of points of velocity measurements and the nodes used for calculations must be realized.
- d As regards the time base of comparison, the time base of the measured results is affected by the accuracy of the paper speed of the recorder (+ 2%).
- e Temperature changes of the water cause change of vapour pressure.

 However, the vapour pressure for calculations was taken -10m (water) in all calculated results. When programme runs with vapour pressure values corresponding to the temperature of the water were made a

- better agreement was always found. In addition, the value of the vapour pressure is influenced by the barometric pressure.
- f The valve closure was not 100% reproducable in the long run. That is to say that at the beginning of the investigation it was a little different from towards its end (because of some rusting).
- g If the time of waiting to estiblish steady flow velocity was not long enough, some air bubbles could be still in the line and this would have some influence on the experimental results. However, in performing the experimental tests, an extra care was given to this factor to eliminate such influence on the results.

A closing remark could be added at this point that the calculated results agree fairly well with the measured results for a large range of conditions. The selected test conditions (table 7) are selected among a wide range of measurements covering steady flow velocities of 0.4 to 1.4 m/s and valve closure times of 0.5 to 4 seconds. The prediction of the results using the numerical calculation procedures discussed in this chapter yields results that are of enough accuracy for engineering applications.

CHAPTER 7

7. TRANSIENTS RESULTING FROM CLOSURE OF THE VALVE AT THE UPSTREAM END OF THE SIPHON

In this chapter, the transient conditions resulting from the closure of the valve at the upstream end of the siphon system are investigated. The study covers the influence of the following factors; the value of the initial steady flow velocity, the valve closure time and the siphon height. The resulting conditions are examined regarding both the water hammer and water-column separation phemonema. The mathematical model together with the numerical solution method described in chapter 5 are used for the prediction of the resulting pressures. The choice of data values for the input to the computer programme is discussed. The calculated results are compared with the corresponding experimental measurements.

7.1. Typical Experimental Tests

Two typical tests are presented in this section. In the first, the hydraulic transients resulting from the closure of the valve caused water column separation at the top of the siphon only. In the second, a faster closure of the valve resulted in water column separation at two locations, one just behind the valve and one at the top of the siphon. Figs. 71 and 72 show pressures and velocities at different locations as recorded during the experimental tests.

For the test whose results are shown in Fig. 71, a steady flow velocity of 1.42 m/s was established in the pipe system. The head at the low level water reservoir and the higher level water reservoirs were 0.35m and 1.66m respectively. The valve was closed in 5 seconds linearly with time. Fig. 71 shows the recorded pressure signals P_1 , P_2 , P_3 , P_4 , P_5 , P_6 and velocity signals V_A and V_B . It also shows the valve angular position during its closure. The sequence of events as can be deduced from the experimental results can be described as follows. As the valve started to close, water started to slow down near by the valve. This would result in a decrease in the pressure near the valve. We note that the resulting deceleration of the water was a small one at the beginning of the closure and it increased towards the fully closed position.

As can be seen from the records the valve closure resulted in a decrease in pressure P₁ and rarefaction waves proceeded towards the low level reservoir. They arrived at P_2 , P_3 and P_4 which showed pressure drops in turn. As the pressure at P_4 during steady conditions was rather low (approximately -8m) P_4 very soon reached vapour pressure and water column separation occurred at the top of the left bend of the siphon. The pressure at P_4 remained for some time at the vapour pressure as could be seen from the record. During this time one could say that two water columns existed. The first was between the valve and the cavitation void at the top of the siphon and the other one between the cavitation void and the low level water reservoir. We will refer to the first column as the left column and to the second one as the right column. In the left column small pressure waves travelled between the two ends and damped away. The velocity V_A showed a slowing down of the column to practically zero velocity. In the meantime P_5 , P_6 showed pressure drops that remained nearly constant for some time. Note, that the pressure drop in P_5 was larger than in P_6 .

The velocity signal V_B shows that the right column slowed down to complete rest and then it started moving in the opposite direction. This was due to the pressure difference between the downstream water reservoir and the cavitation void. The above events caused the growth and later the diminution of the cavitation void and finally it collapsed. This resulted in a pressure surge as registered first by P_h . The resulting pressure wave travelled in two directions, one towards the valve and the other towards the low level water reservoir. Successive pressure rises in P_3 , P_2 and P_1 are seen in Fig. 71.

Furthermore, the following logic could be stipulated from the velocity signals V_A and V_B . As the collision occurred the terminal velocity of the right column in the direction of the valve would decrease while the stationary left column started to move in the direction of the valve. The collapse pressure surge travelled in the two columns. One may summarise the results of the collapse of the cavitation void as follows.

- a. Travel of the pressure surge in the left column towards the valve, together with additional velocity change (increase in magnitude as it was standing still) in the direction of the valve.
- b. Travel of the pressure surge in the right column towards the low level water reservoir together with drop in the magnitude of the velocity at which it was moving in direction of the valve.

The first changes a. could be seen from P_3 , P_2 and P_1 and V_A . Later when the velocity change reached the valve (a dead end) an additional surge

^{*}) Approximately at time 4.8 s (Fig. 71)

resulted as the water stopped and this travelled from P_1 to P_2 and P_3 .

In the meantime, for the second changes b. the pressure surge travelled from P_4 to P_5 and then to P_6 . When that pressure wave reached the low level water reservoir it was released and this release was shown first by P_6 . Then this release reached P_4 at about the same time that the pressure wave resulting from the stoppage of the water in the left column at the dead end reached P_4 . Thus the release together with that pressure wave practically made P_h remain at unchanged value.

At that moment, the left column had practically stopped. Then the right column stopped resulting in a pressure wave proceeding from P_{l_1} to P_{l_2} and P_{l_3} . As can be seen from the records, all the water stopped in the whole pipe length ending in a non-equilibrium situation at the reservoir. This resulted in the start of water flow outwards of the pipe together with a release of the pressure. This in turn propagated towards the valve. This situation ended with the water adjacent to the valve flowing outwards and causing the pressure at the valve P_{l_1} to drop nearly to vapour pressure. This resulted in a rarefaction wave moving towards the low level water reservoir thus arriving at the top of the siphon. The pressure at top of the siphon reached vapour pressure and a vapour void started to form. From that moment, again, two columns could be indentified: one between the valve and the vapour cavity at top of the siphon and the other between the vapour void at the top of the siphon and the low level water reservoir.

In the left column pressure and velocity changes kept travelling and fading out. In the right column, pressure and velocity changes kept propagating resulting in stopping of the column and later reversing its motion towards the valve. That ended with the collapse of the vapour cavity on top of the siphon and resulted in the pressure surge first shown by P_4 . Similar events to those explained before re-occurred and the pattern of pressure and velocity changes repeated themselves with damping resulting in smaller amplitudes of the resulting changes.

Fig. 72 shows the different pressure and velocity changes at a number of locations on the siphon system resulting from linear closure of the valve at the upstream end of the pipe in 2 seconds for an initial steady flow velocity of 1.42 m/s. Again, the elevation of the siphon was 8m above the horizontal part of the pipe. In this case the closing of the valve resulted in column separation at the valve and at top of the siphon. The order of occurrence of the events could be found following similar logic to that followed in case of the test results presented in Fig. 71 and discus-

sed above in examining the experimental results shown in Fig. 72. Fig. 73 also shows water column separation at the left side *) of the top of the siphon during transient test conditions similar to those of Fig. 72.

7.2. Schematization of the Line for Programme WHN

The siphon system was schematized by a line between a valve at its upstream end and a reservoir at its downstream end. One point on the line was assumed to be at the higher elevation of the pipe. A vapour cavity could be located at that point if the pressure there reached the vapour pressure.

7.3. Choice of Input Data for the Programme WHN

The same grid (Fig. 50) which was used for programmes HOZ and HZD was adapted for the presentation of the x-t plane. Programme WHN (appendix E) was used for calculating the resulting pressure changes during transient conditions in the siphon system due to the closure of the valve. The programme steps are similar to those used previously in HZD with additional steps allowing for location of a cavitation void at an intermediate point on the grid representing the high point location, if the pressure at that point reached vapour pressure. This addition is explained in detail in appendix E.

The input data required in this case are mainly those explained previously in chapter 4 representing geometrical characteristics of the pipe, steady flow, valve closure time, valve resistance during closure, plus grid data. In addition to these, celerity change with time and momentum loss coefficient data were needed. Also, the grid point where the high point was assumed and the elevation of the high point above the centerline of the valve were required.

The choice of these data needed for the programme was discussed in detail in chapters 4 and 6. However, still to be considered is what values of celerity change with time and momentum loss coefficient could be used. Were these values the same as those found in section 6.3. (in case of the horizontal line)? To answer this question an examination of a wide number of experimental measurements, covering changing the parameters, initial

^{*)} Marked C on the schematic diagram of the siphon in Fig. 72.

steady flow velocities, valve closure time and elevation of the siphon was completed. An evaluation of the quantitative data for the decrease of the celerity with time yielded the following results. The average value of the celerity rate of decrease was found to be $7.5 \, \text{m/s}^{-2}$. This is the same value that was found for the rate of celerity decrease during the experimental tests of the horizontal pipe system (section 6.3.). As regards the value of the momentum loss coefficient using the logarithmic decrement technique (section 6.3.), it was found, that the ratio of the head amplitudes (y_2/y_1) Fig. 64) * remains approximately constant. This yielded an approximate relation between c the momentum loss coefficient and T the time of a complete period of wave travel

$$c \simeq \frac{0.69}{T} \tag{77}$$

In the above equation the value of T depends on the situation as follows

- I a closed valve (dead end) at the upstream end of the pipe and the low level reservoir at the downstream end of the pipe, $T = \frac{4L}{a}$.
- II a valve dead end at the upstream end of the pipe and a cavitation void (reservoir at vapour pressure) at a high point at the mid point of the pipe length, $T = \frac{2L}{a}$.
- III a cavitation void at the upstream end of the pipe and another cavitation void at a high point amid the pipe-line length (reservoir reservoir condition), $T = \frac{L}{a}$.
- IV a cavitation void at a high point amid of the pipe-line and the low level reservoir (reservoir reservoir condition), $T = \frac{L}{a}$.

Note that as "a"decreases with time T increases, resulting in smaller values of c towards the end of the transients. An additional remark may be made here, that equation (77) results in larger values of c than those given by (76), (in the case of the horizontal line section 6.3.). This may be due to the fact that in the siphon flow system, water passes a high part where the pressures are below the atmospheric pressure. This gives the possibility of air being released from the water. As mentioned before it is the freed air bubbles that form the nuclei of cavitation bubbles that occur along the pipe during the transient conditions and these bubbles are responsible for a large part of the dissipation exhibited.

^{*)} In considering the values of y₂, y₁ and T in Fig. 64, during the complete period T, the situation at both the valve and the high point must remain the same (existence of cavitation voids).

In the programme WHN (appendix E), relation (77) was used to calculate the momentum loss coefficient. Additional statements were built into the programme to assign the value of T according to the situation as described in the above four cases.

Also, among the data read in are the different elevations of the node points above the centre line of the valve "ELV(N)". These values are necessary for the calculations to assure that the pressure at the different locations does not fall below the vapour pressure (see appendix E).

7.4. Comparison of Experimental Measurements and Calculated Results

Table 9 gives a list of test conditions for the experimental measurements presented in Figs. 74 - 79.

Table 9

List of experimental test conditions for chapter 7 (siphon system)

Test Number	steady velocity m/s	valve closure time s	type of valve closure	column separa- tion at valve	elevation of siphon top	column separa- tion at top of siphon	Fig.
8008	1.14	4	linear	linear no 8.0		yes	74
8011	1.21	2	linear	yes	8.0	yes	75
8016	1.00	2	linear	yes	8.0	yes	76
8018	1.00	1	linear	yes	yes 8.0		77
2034	1.14	2.5	linear	yes	5.0	yes	78
2043	1.00	1.5	linear	yes	5.0	yes	79

Table 10 contains a listing of data used as input data for the computer programme WHN. These data whould represent the conditions that resulted in the experimental test results of the measurements in table 9.

Table 10

Input data for programme WHN

"MESNUM" Measurement number	8008	8011	8016	8018	2034	2043
"CL"pipe length m	55.14	55.14	55.14	55.14	49.14	49.14
"D"pipe diameter m	0.09	0.09	0.09	0.09	0.09	0:09
"C"celerity m s ⁻¹	450	450	450	450	450	450
"VO"steady velocity m s ⁻¹	1.14	1.21	1.00	1.00	1.14	1.00
"F"steady friction factor	0.0182	0.0180	0.0188	0.0188	0.0182	0.0188
"HVO" steady head loss in the valve m wate:	r 0.01	0.01	0.01	0.01	0.01	0.01
"HO"low level re- servoir head m water	r 0.5	0.5	0.5	0.5	0.5	0.5
"PV"vapour pres- sure m wate	r -10	10	-10	-10	-10	-10
"TC" valve clo- sure time s	4	2	2	1	2.5	1.5
"DECS"celerity _2 decrease rate ms	7.5	7.5	7.5	7.5	7.5	7.5
"ZHP"elevation of siphon m	8	8	8	8	5	5
ELV (1)	0.0	0.0	0.0	0.0	0.0	0.0
ELV (2)	0.0	0.0	0.0	0.0	0.0	0.0
ELV (3)	0.0	0.0	0.0	0.0	0.0	0.0
ELV (4)	0.0	0.0	0.0	0.0	0.0	0.0
ELV (5) elevation of nod	e 3.8	3.8	3.8	3.8	1.40	1.40
ELV (6) points in m	8.0	8.0	8.0	8.0	5.0	5.0
ELV (7)	3.8 .	3.8	3.8	3.8	1.40	1.40
ELV (8)	0.0	0.0	0.0	0.0	0.0	0.0
ELV (9)	0.0	0.0	0.0	0.0	0.0	0.0
ELV (10)	0.0	0.0	0.0	0.0	0.0	0.0
ELV (11)	0.0	0.0	0.0	0.0	0.0	0.0

"NF" calculations done using "NF" = 11

"NHP" location of high point at "N" = 6

Pressure history plots correspond to "N" = 1, 2, 4, 6, 7, 9

Velocity history plots correspond to "N" = 2, 10

Fig. 74 shows satisfactory agreement of the calculated and measured results. Both the first two pressures peaks (magnitude and timing) agree fairly well, less degree of agreement is seen at the later parts with smaller changes in the calculated results than those in the measurements.

The comparison of the calculated results with the measurements for test number 8011 (Fig. 75) yields reasonable agreement of the pressure and velocity histories for the first five seconds. Some deviation between the calculated results and the measured changes is exhibited in the duration of the third cavitation void (marked C in Fig. 75) showing longer duration of the void in the measured results than in the calculated results. This fact is also seen for the fourth cavitation void as well (D in Fig. 75). It is believed that the air bubbles that formed in the vertical legs of the siphon tend to collect at the highest point (they could be seen rising during the tests). These form some pockets of air at the top of the siphon where the cavitation occur. As more air collected with time, this air apparently played a role in the formation and diminution of the void. This can be seen from the smaller steepness of the pressure surges at the top of the siphon (see marks E₁, E₂, E₃, E₄ on P₄ in Fig. 75). In Fig. 76, fair agreement of the pressure and velocity changes given by calculated results with the measurements can be seen. However, it is believed that the initial steady flow velocity in the experiments was a little higher than 1 m/s. Again, less agreement at the latter part of the transient is seen in Fig. 76.

Fig. 77, shows satisfactory agreement of the calculated results with the measurements for the first 2.5 s with less agreement for the later time. It is believed that during this test some air pocket existed at the top of the siphon before the test was carried out. This caused longer duration of the cavitation voids at the top of the siphon and the influence of the air discussed before was manifested.

The above results are for the 8m siphon system. The following comparison is done for results for the 5m siphon. Note that the results shown in Figs. 78 and 79 (5m siphon) fade more quickly than those shown in Figs. 74 - 77. The comparison of the measured and calculated results in Fig. 78 show reasonable agreement both in magnitudes of changes and in their timing.

In Fig. 79 the measured and calculated results agree fairly well with small deviation in the later part of the transient.

CHAPTER 8

8. TRANSIENTS RESULTING FROM CLOSURE OF THE VALVE AT THE UPSTREAM END OF THE CONDENSER SYSTEM

In this chapter, the third phase of the investigation is presented. Transient conditions resulting from the closure of the valve at the upstream end of a siphon with a condenser model mounted on the top of the siphon are investigated. The study covers the influence of the following factors:

- the valve closure time
- the elevation of the condenser model above the centre-line of the horizontal part of the pipe as well as the position of the condenser model (whether held vertical or horizontal).

The resulting conditions are examined regarding both water hammer and water column separation phenomena. The mathematical model together with the numerical solution method described in chapter 5 are used for the prediction of the resulting pressures. The calculated results are compared with measurements.

8.1. Typical Experimental Tests

Figs. 80 and 81 show experimental measurements of pressure and velocity changes for two different tests. For test number 180 (Fig. 80) the initial steady flow velocity was 1.11m/s and the valve was closed linearly in 3.4 seconds. The highest point of the condenser model was at an elevation of 5.6m above the centre-line of the horizontal part of the pipe. The results (in Fig. 80) show that column separation occurred only at the top of the condenser. (P, approaches P,). The results shown in Fig. 81 are for the same steady flow velocity and the condenser held in the same vertical position, but the valve was closed in a shorter closure time (1 second). These conditions resulted in column separation at two location: at the valve and at the top of the condenser. Fig. 82 shows a view of water column separation at the top of the condenser during transient tests produced under conditions similar to those of test number 181. (Fig. 81) The upper photograph shows the upper-most section of the upstream water box, where water column separation occurred with the condenser model held in the vertical position. See C on the scheme of the condenser system shown in Fig. 81. The lower photograph shows water column separation at the same location (the upperstream water box) with the condenser held in a horizontal position (testing conditions similar to those of test number 181).

Examination of Figs. 80 and 81 demonstrate the sequence of occurrence of events during the transients. The same discussion presented in the description of the siphon experimental measurements (section 7.1.) applies to a large extent. It is worth noting at this point the following visual observations of water column separation at the top of the condenser.

Water column separation was seen to take place at the top of the upstream water box of the condenser during most of the tests (under conditions that caused the pressure to drop to vapour pressure in the condenser). Comparing the size of the main cavities which were seen during tests performed for the same steady velocity and valve-closure time but with the condenser model held at different elevations, the sizes of cavities occurring at higher elevations were larger than those occurring with the condenser model held at lower elevations. During tests with the condenser model held at 9.1m level (above the horizontal main part of the pipe line), the cavitation void could be seen extending in the condenser pipes and in some instances at the top of the down stream water box.

8.2. Schematization of the Condenser Configuration for Programme WCN

Fig. 83 shows a diagrammatic sketch of the condenser configuration as adapted for the numerical calculations using programme WCN. The system was schematized by a line between a valve at the upstream end of the pipe and a reservoir at its downstream end. One point on the line was assumed to be at a higher elevation and to have a restriction representing the condenser. The restriction was assumed to have a resistance equal to that offered by the condenser for steady flows. Also, vapour void could be located at the upperstream side of the restriction if the pressure there reached the vapour pressure.

8.3. Choice of Input Data for the Programme WCN

The grid that was used for previous programmes (Fig. 50) for the presentation of the x-t plane was adapted for this programme WCN. Programme WCN (appendix F) was used for calculating the resulting pressure changes in the condenser system due to the closure of the valve. The programme steps are similar to those of HZD and WHN with some modification (the reading of input data for the restriction resistance and to complete cal-

culations at the restriction). This additional modification is discussed in appendix F.

The input data required in this case were mainly those used previously representing geometry, steady flow, closure time, valve resistance during closure, plus grid data. In addition to these, celerity decrease with time and momentum loss coefficient data were needed. Also, the grid point where the restriction was to be located, the elevation of the restiction and the resistance of the restriction. In addition, the deceleration of the downstream water column (if water column separation at top of the condenser occurred) had to be read in with the input data. The choice of most of the data needed for programme WCN as discussed in the previous programmes HZD and WHN. However, the choice of some of the data warrants some comments. In choosing the length of the pipe system, an equivalent length of the condenser had to be assumed representing the average path of the water into it. This length is 4.785m as can be deduced from the dimensions of the condenser model (Fig. 24). For the celerity rate of decrease, the value of 7.5m s⁻² which was found for both the horizontal and siphon measurement (chapters 6 and 7) seems to hold for the measurements of the condenser system, as well. As for the celerity itself, the speed of the pressure wave propagation in the pipe is different from that in the condenser. Besides, the speed of pressure wave propagation in the condenser pipes is different from that in the water boxes. The nature of the interaction of these speeds is a complicated one. The use of a value of 450 m/s as a representative value of the celerity in the system implies the negligence of the influence of the lower celerity in the condenser model. This may be justified on the basis that the equivalent length of the condenser is much smaller than the pipe length.

Another basis for obtaining an equivalent celerity for the system was proposed as follows: measuring the celerity at a later time in the transients (when the pressures have faded out) and calculating the equivalent speed of propagation of a pressure wave at the beginning of the transients with the aid of celerity decrease rate. This procedure yielded a value of 410 m/s for the celerity. For the momentum loss coefficient the relation found in the case of the siphon, relating c to the travel time of the waves, was found to hold in the case of the measurements of the condenser as well. Thus, the same relation (76), was used in the programme.

For carrying out calculations of the combined cavitation void and restriction, representing the conditions occurring in the condenser the following data had to be chosen "HCONDS", "ZCONDS", "NCONDS" and "ACR". The

elevation "HCONDS" of the combined cavitation void-restriction above the centre-line of the horizontal main part of the pipeline was assumed to be the elevation of the highest point of the condenser model above the centreline of the valve (that is the centre-line of the horizontal main part of the pipe). This procedure was chosen as the value "HCONDS" and is particularly important in checking whether pressures reached vapour pressure or not. This in turn is of large importance in starting a cavitation void in the numerical calculations. The value "ZCONDS" represents the resistance offered to the flow of the condenser model treating the condenser as a restriction. The restriction resistance $\xi_{\rm cond}$ was found relating the head drop across the condenser to the flow velocity in the pipe under steady flow conditions. For the calculations that are presented in the following section a value of ξ_{cond} equal to 10.5 was used. That value was chosen as a representative value though measurements showed some dependence of ξ_{cond} on the velocity (measurements under steady flow conditions). Fig. 84 shows the variation of $\xi_{\rm cond}$ with the steady flow velocity. "NCONDS" is the node location designating the combined cavitation void-restriction. As the total number of position nodes "NF" was chosen as 21, two values of "NCONDS" were used. In simulating tests for small condenser elevations (3.1m and 5.6m) a value of 10 for "NCONDS" was used. This was done in view of the visual observation that water column separation was seen to occur at the upperstream water box during tests at these elevations. On the other hand for tests with 8.1m and 9.1m condenser elevations "NCONDS" was chosen 11, as during these tests water column separation at the top of the condenser was seen to spread into the condenser top not only at the upstream water boxes, but also in the direction of downstream box (see section 8.1.). In carrying out the calculations of the combined cavitation-restriction when column separation occurred, a value for the deceleration of the downstream column was needed as part of the data: "ACR". "ACR" represents the deceleration rate of the water column between the cavitation void at the top of the condenser and the low level reservoir (when a vapour void exists at the top of the condenser). A representative value of it could be obtained from the slope of signal $V_{\rm R}$ in the measured results (marked B in Fig. 81). This value was also calculated considering the motion of the water column under the pressure difference between the low level reservoir and the vapour pressure at the top of the condenser and allowing for the mass of the water in the condenser being combined with this column.

8.4. Comparison of Experimental Measurements and Calculated Results using Programme WCN

Table 11 gives a list of test conditions for the experimental measurements presented in Figs. 85 - 93.

Table 11

List of experimental test conditions for Chapter 8

test number	steady velo- city m/s	valve clo- sure time s	type of valve closure	column se- paration at valve	elevation of condenser model m	column separation at top of condenser	Fig.
c3063	1.0	1.0	linear	yes	3.1 vertical	yes	85
C3064	1.0	2.0	linear	yes	3.1 vertical	yes	86
c3065	1.0	4.0	linear	no	3.1 vertical	no	87
C2019	1.0	2.0	linear	yes	5.6 vertical	yes	88
C1003	1.0	2.0	linear	yes	5.6 horizontal	yes	89
C5094	1.0	1.0	linear	yes	8.1 vertical	yes	90,93
c6109	1.0	2.0	linear	yes	9.1 vertical	yes	91,94
C6107	1.0	1.0	linear	yes	9.1 vertical	yes	95

Table 12 contains a listing of data used as input data for the computer programme WCN. These data would represent conditions that resulted in the experimental measurements of tests listed in table 11.

Table 12

Input data for Programme WCN

"MESNUM" Measurement number	c3063	C3064	C3065	C1003	C2019	C5094	C6109
"CL"system length m	45.5	45.5	45.5	53.0	50.5	55.5	57.5
"D"pipe diameter m	0.09	0.09	0.09	0.09	0.09	0.09	0.09
"C"celerity m/s	410	410	410	410	410	410	410
"VO"steady velo- city m/s	1.0	1.0	1.0	1.0	1.0	1.0	1.0
"F"steady friction factor	0.0188	0.0188	0.0188	0.0188	0.0188	0.0188	0.0188
"HVO"steady head loss in the valve m.water	0.0052	0.0052	0.0052	0.0052	0.0052	0.0052	0.0052
"HO"low level re- servoir head m.water	0.3	0.3	0.3	0.3	0.3	0.3	0.3
"PV"vapour pres- sure m.water	-10.0	-10.0	-10.0	-10.0	-10.0	-10.0	-10.0
"TC"valve closure time s	1.0	2.0	4.0	2.0	2.0	1.0	1.0
"ACR"deceleration of downstream co- lumn m.s ⁻²	2.0	2.0	2.0	1.5	1.5	0.74	0.4
"DECS"celerity de- crease rate m.s-2	7.5	7.5	7.5	7.5	7.5	7.5	7.5
"HCONDS"elevation of condenser m	3.1	3.1	3.1	5.6	5.6	8.1	9.1
"ZCONDS"resistance of condenser	1.0.5	10.5	10.5	10.5	10.5	10.5	10.5
"NCONDS" location of combined cavi- tation void-res-							
triction	10	10	10	10	10	11	11
ELV (1)	0.0	0.0	0.0	0.0	0.0	0.0	0.0
ELV (2)	0.0	0.0	0.0	0.0	0.0	0.0	0.0
ELV (3)	0.0	0.0	0.0	0.0	0.0	0.0	0.0
ELV (4)	0.0	0.0	0.0	0.0	0.0	0.0	0.0
ELV (5) elevation of nod	e 0.0	0.0	0.0	0.0	0.0	0.0	0.0
ELV (6) points in m.	0.0	0.0	0.0	0.0	0.0	0.0	0.0
ELV (7)	0.0	0.0	0.0	0.0	0.0	0.0	0.0
ELV (8)	0.0	0.0	0.0	0.3	0.3	1.1	1.9
ELV (9)	0.1	0.1	0.1	2.9	2.9	3.9	4.7
ELV (10)	2.7	2.7	2.7	5.4	5.4	6.7	7.5

Table 12

(cont'd)

"MESNUM" Measurement number	C3063	C3064	c3065	C1003	C2019	C5094	c6109
ELV (11)	3.1	3.1	3.1	5.6	5.6	8.1	9.1
ELV (12)	2.7	2.7	2.7	5.4	5.4	6.7	7.5
ELV (13)	0.1	0.1	0.1	2.9	2.9	3.9	4.7
ELV (14)	0.0	0.0	0.0	0.3	0.3	1.1	1.9
ELV (15)	0.0	0.0	0.0	0.0	0.0	0.0	0.0
ELV (16)	0.0	0.0	0.0	0.0	0.0	0.0	0.0
ELV (17)	0.0	0.0	0.0	0.0	0.0	0.0	0.0
ELV (18)	0.0	0.0	0.0	0.0	0.0	0.0	0.0
ELV (19)	0.0	0.0	0.0	0.0	0.0	0.0	0.0
ELV (20)	0.0	0.0	0.0	0.0	0.0	0.0	0.0
ELV (21)	0.0	0.0	0.0	0.0	0.0	0.0	0.0

"NF" calculations done using "NF" = 21

Pressure history plots correspond to N = 1, 3, 9, 11, 13, 19

Velocity history plots correspond to N = 3, 19

The calculated pressure and velocity changes based on the data supplied to the programme WCN to simulate the resulting conditions of test number C3063 compare fairly well with the measurements (Fig. 85). This covers both the time history and the magnitudes of the pressure changes. The drop in the registered pressure P_1 (marked D in Fig. 85) is due to the reflection of the steep pressure wave encountered upon its arrival at the condenser.

A comparison of the calculated results and the measurements for test number C3064 shows reasonable agreement (Fig. 86). There is however some deviation in the duration of the second cavity at the valve as can be seen from signal P_1 and the pressure P(N=1) (marked E in Fig. 86). Again the reflection of steep pressure wave fronts encoutered upon their arrival at the condenser can be seen on the pressure signal P_1 (marked D in Fig. 86).

Fig. 87 shows excellent agreement of the calculated and measured results. The agreement in the time periods is remarkable. Note, that in this case no water column separation occurred either at the valve or at the top of the condenser.

The results presented in Fig. 85 - 87 are for transient tests with the condenser model held at an elevation 3.1m, the steady flow velocity was 1 m/s for all three tests but the valve time of closure was changed 1, 2 and 4 seconds respectively. These results suggest that the schematization of the condenser system in the way described in section 8.2. together with the numerical calculations performed using programme WCN would yield reasonable results to predict transients under similar conditions. Fig. 88 shows the predicted pressure and velocity changes compared with the measurements for number C2019. The test conditions were: steady flow velocity 1 m/s valve closure time 2 seconds with the condenser held in the vertical position at an elevation 5.6m. The calculated results show smaller amplitudes for the pressure changes than the measurements. The duration of the second cavitation voids at the condenser top C, and at the valve Co show some discrepency. However, for the later part of the histories, after 3.8 seconds the predicted history changes seem to agree well if the duration of the second cavitation void in the calculations is supposed to have lasted 0.15 seconds longer. For a horizontal condenser at an elevation of 5.6m, test number C1003 is for steady flow velocity 1 m/s and valve closure time equal to 2 seconds. The discrepency between the calculated and measured values stemmed from an earlier collapse of the cavitation at the top of the condenser (in the calculated results) than in reality (see C in Fig. 89). Some deviation between the calculated and measured results can be seen at about 2.4 seconds (see E in Fig. 89). This resulted in difference of the duration of the second cavitation void at the condenser top (see F in Fig. 89). Again the latter part of the calculated pressure changes (later than 3.8 seconds) would compare well with the measurements if the time base was shifted 0.25 seconds which is the time discrepency in the duration of the second cavitation void.

In comparing the calculated and the measured results of test number C5094 (Fig. 90), the first part of the pressure and velocity histories up to about 3 seconds compare reasonably well. However, the second cavitation void at the top of the condenser as exhibited in the calculation is too short when compared with the measured one (see E in Fig. 90). This of course resulted in large deviations between the calculated and measured results from that moment on. Note that this test was for an elevation of the condenser of 8.1m.

Fig. 91 shows the calculated and measured results for test number C6109. The test was carried out for a vertical condenser at an elevation

of 9.1m. During the first part of the transients the calculated and measured results compare reasonably. However, after the first pressure peak large deviations between the calculated and measured results start to appear (see E in Fig. 91).

The comparisons of the calculated and measured results of Figs. 88 -91 as mentioned above have shown a discrepancy between the calculated and the measured results that starts after the collapse of the first cavitation void at the top of the condenser. This discrepancy was manifested at the higher elevations 9.1m and 8.1m. This deviation motivated the re-examination of the schematization of the system in the manner described in section 8.2. In this reconsideration of the system, the experimental measurements suggest that when large cavitation voids form (also if their time duration is long) the system may be more appropriately represented by a siphon system. That is to say, the influence of the flow in the condenser is not playing an important role under such conditions. In other words, when large cavitation voids exist at the top of the condenser the condenser may be better presented by a reservoir at the vapour pressure rather than a combined cavitation void (reservoir at vapour pressure)-restriction. Fig. 92 shows a comparison of two tests. C5094 is transient test for a condenser system Vo = 1 m/s, valve time closure 1 second and condenser elevation 8.1m. Test number 8018 is for the same steady velocity and time of closure, but for a siphon system with the height of the siphon 8m. The measured pressure and velocity signals shown in Fig. 92 were redrawn from the records for the demonstration of the following point. The trends of the measured results for the two tests are basically the same. The small difference of the slopes exhibited by the velocity signal Vp (marked B in Fig. 92) suggests that the mass of the water in the condenser has an influence. That is to say, when a cavitation void exists at the top of the condenser, the two columns between the valve and the cavitation void and the low level reservoir include some of the masses of the water in the condenser. With the above ideas in mind, it was decided to use programme WHN, which was used for the prediction of transient conditions in a siphon system, for condenser systems with high elevations. Little modifications of programme WHN were made. These modifications are explained in appendix F. Programme WHN in the modified form was used to predict conditions for the tests C5094, C6107 and C6109 (see table 11 for testing conditions). Table 13 shows the different data supplied for the modified version of programme WHN.

Table 13

Input data for the modified version of programme WHN

Measurement number	C5094	c6109	c6107
"CL"pipe length m	55.5	57.5	57.5
"D"pipe diameter m	0.09	0.09	0.09
"C"celerity m/s	450	450	450
"VO"steady velo- city m/s	1.0	1.0	1.0
"HVO"steady head loss in the valve m.water	0.0052	0.0052	0.0052
"PV"vapour pres- sure m.water	-10.0	10.0	-10.0
"TC"valve closure time s	1.0	2.0	1.0
"DECS"celerity de- crease rate m s ⁻²	7.5	7.5	7.5
"HHP"elevation of condenser m	8.1	9.1	9.1
"ZCONDS"resistance of condenser (for steady flow)	10.5	10.5	10.5
"NHP"location of high point	6	6	6
ELV (1)	0.0	0.0	0.0
ELV (2)	0.0	0.0	0.0
ELV (3)	0.0	0.0	0.0
ELV (4)	0.0	0.0	0.0
ELV (5)	3.9	4.7	4.7
ELV (6)	8.1	9.1	9.1
ELV (7)	3.9	4.7	4.7
ELV (8)	0.0	0.0	0.0
ELV (9)	0.0	0.0	0.0
ELV (10)	0.0	0.0	0.0
ELV (11)	0.0	0.0	0.0

Note, that a celerity of 450 m/s was chosen rather than 410 m/s. This was chosen on the basis that in longer duration of the time of the transients the condenser is dealt with as a reservoir at the vapour pressure. Thus the interaction of different speeds of propagation in the condenser and the pipe should be disregarded. Figs. 93 - 95 show comparisons of the calculated and measured results.

In Fig. 93 a good agreement between the measured and the calculated results could be seen. The time discrepency in the duration of the cavitation voids at the top of the condenser is believed to be due to air collection at the top of the condenser.

Fig. 94 shows a reasonable agreement of the calculated and measured results. The dip in pressure signal P_1 (marked R in Fig. 94) are due to reflections encountered upon the arrival of steep wave fronts to the condenser. The calculated results do not show such dip. Such difference is not of a significant order as can be seen in the figure. There is some deviation of the duration of the cavitation voids duration at the top. However, this is believed to be due to the fact that air collects at the top of the condenser when small pressure exist. Note that the duration of low pressures is relatively long during the transients. Moreover, air is even freed out of the water at steady conditions and collects at the top of the condenser because of the relatively small pressures. This air is affecting the mechanics of growth and collapse of the cavitation void at the top of the condenser. This fact could be seen clearly when experimental tests were repeated.

In the comparison of the calculated results of test number C6107 to the measurements the trends seen in the previous case could be seen as well.

To sum up the results obtained in this section, it may be concluded that the calculations based on the combined cavitation-restriction schematization are suitable for predicting transients in the condenser system for small elevations while for condenser systems with high elevations a siphon schematization would yield better results.

CHAPTER 9

9. CONCLUSIONS

A better understanding of the phenomena of water hammer and water column separation has been achieved in this study. The range of the experimental testing conditions covers a wide variety of conditions which are typical for those occurring in a lot of engineering applications.

Simulation of the typical cooling water system was obtained by an excellent testing facility. Simulation of pump failure conditions was simulated by the closure of a valve according to preselected closure characteristics (angle versus time). The system uses an electronically controlled servo-motor. Such a system would surely help other investigators in similar applications.

Transient flow velocity changes during the resulting hydraulic transients were successfully measured using two different methods namely the photographic and the induction flowmeter system. These transient flow velocity changes are the first measurements to be added to literature.

The high speed camera photographic study of water column separation gives a very interesting study of water column separation. It throws some light on the phenomenon and contributes to its further understanding. The experimental study of the elastic behaviour of the pipe wall material is an interesting one. The results show that the "plexiglass" pipe behave elastically during such hydraulic transient conditions. One conclusion of this study was that it is possible, for some applications, to measure transient pressure changes indirectly through the measurement of the strains on the outside wall of the pipe.

Experimental measurements are presented in this dissertation. These include transient pressure changes at a few locations along the pipe as well as flow transient velocity changes at two locations on the pipe. The set of measurements carried out for each test condition gives a complete picture of the transient conditions. Literature lacks such complete experimental measurements. The measurements completed in this form have an educational value as well.

A lot of investigators in this area try to avoid the complication of description of boundary conditions by using sudden closure of the valve. In this study we have managed to describe flow conditions in the valve

during the hydraulic transients.

To focus the attention on the sources of deviation of the classically calculated results (using method of characteristics) from the experimental measurement is of great use to investigators.

Attention was given to the role of the cavitation bubbles occurring when the pressure in the pipe drops to subatmospheric pressures. These bubbles contribute to the decrease in celerity with time during the transients. They also contribute to a large momentum loss associated with the phenomena. Examination of the nature of this influence has been considered.

A new mathematical model was proposed for the representation of the flow conditions under hydraulic transient conditions involving such cavitation bubbles.

A finite difference method of solution was developed for solution of water hammer - water column separation problems subject to the boundary conditions representing different hydraulic devices.

The photographic study gave a basis for the mathematical modelling of vapour void growth and collapse. The assumption of the resulting void to fill the whole cross section of the pipe was used successfully for all cases of water column separation.

The comparison of the calculated results with the experimental measurements shows a sufficent degree of agreement for engineering purposes in a great number of test situations. The agreement covers both magnitudes of the pressure peaks and the time intervals between the pressure peaks.

The developed method of calculation is useful in considering transient conditions for hydraulic systems having small pressures at steady conditions. The procedures are not very complicated but, as said, yield satisfactory results.

It is worth noting that in the numerical calculations based on the new mathematical model two main parameters were used: the celerity rate of decrease with time and the momentum loss coefficient. The idea behind the selection of these two quantities is discussed in chapter 6. Besides, appropriate procedures for the determination of the values of these two parameters from transient pressure measurements were also introduced. These procedures were applied to a wide range of experimental conditions. These two parameters are appropriate and could be found from experimental results, unlike parameters used by previous investigators which are diffi-

cult to determine (e.g. the number of nuclei per unit length of the pipe, the typical radius of cavitation bubbles occurring along the pipe-line during the transients |66|). It is believed that data of both the celerity rate of decrease and the momentum loss coefficient for conditions different from those reported in this study could be obtained in the near future. A first step in this direction would be the examination of available measurements in the literature.

A study of the factors affecting the values of these two quantities would be an interesting one. Examination of the influence of a number of factors on these values may prove to be useful. First, the frequency at which a pressure wave travels in the system (depending on the pipe length and the celerity). Ralations (76) and (77) relating c to T are in fact a first step in this direction. Note, that these two relations are only applicable to the system used. Further, air content in the water (saturated water - deareated water), the distribution of dissolved air and free air in the water, water temperature and previous history of the water (if it was subjected to high pressures prior to the transients)may also be considered.

It is felt that better description for presentation of hydraulic devices in water hammer calculations is needed. The development of the induction flow meter and measurements of transient flow velocities facilitate obtaining such goals. In this study an example of such effort was presented in considering how to represent conditions at the valve in the boundary conditions necessary for the calculations. Similar work is suggested for hydraulic devices as pumps, different types of valves etc.

A study of the viscous friction dependence on the frequency of velocity changes should be of interest to investigators in this area. It is believed that with the availability of the laser doppler velocimeter, measurements of velocity profiles for pulsating flow could be achieved and data of viscous friction factors could be obtained.

As regards transient conditions occurring in the cooling water systems of thermal power plants as a problem that could cause constructional damage, the developed calculation should allow designers of such systems to evaluate how serious the resulting conditions may be.

It is believed that through careful choice of pump failure characteristics and check valves closure characteristics in these systems, large surges could be avoided.

During the course of experimental testing of this investigation, it was observed that a very useful measure to suppress the resulting pressure surges associated with water column separation was the introduction of atmospheric air in the system at the point where water column separation would normally occur. This gives a very effective means for avoiding the large pressure surges if introduced at the right location and moment.

One aspect of this problem that should be considered is what sort of vibration problems the hydraulic transients could cause to the power station structure in general and the turbine-condenser in particular.

BIBLIOGRAPHY

- 1. Allievi, L., <u>Theory of Water Hammer</u>, (translated from Italian by E.E. Halmos for the A.S.C.E., 1925), Rome, Italy, printed by R. Garoni 1913.
- 2. Baltzer, R.A., A Study of Column Separation Accompanying Transient Flow of Liquids in Pipes, Ph. D. Thesis, University of Michigan, Ann Arbor, Michigan, 1967.
- 3. Bergeron, L., <u>Water Hammer in Hydraulics and Wave Surges in Electricity</u>, John Wiley and Sons Inc., New York, 1961.
- 4. Bird, R.B., W.E. Stewart, and E.N. Lightfoot, <u>Transport Phenomena</u>, John Wiley and Sons Inc., New York, 1960.
- 5. Brown, R.J., "Water Column Separation at Two Pumping Plants", <u>Trans</u>actions of A.S.M.E., Journal of Basic Engineering, 1968, p. 521 531.
- 6. Butler, H.W., <u>Irreversible Thermodynamics</u>, Lectures Notes, West Virginia University, Morgantown, West Virginia, 1966.
- 7. Carslow, H.S., and J.C. Jaeger, <u>Operational Methods in Applied Mathematics</u>, Dover Publications Inc., New York, 1963.
- 8. Chivers, T.C., "Air Content Effect on Advanced Cavitation in a Centrifugal pump", Cavitation State of Knowledge, A.S.M.E., 1970.
- 9. Contractor, D.N., "The Reflection of Water Hammer Pressure Waves from Minor Losses", <u>Transactions of A.S.M.E.</u>, <u>Journal of Basic Engineering</u>, 1965, p. 445 452.
- 10. Daily, J.W., W.L. Hankey, R.W. Olive, and J.M. Jordaum, "Resistance coefficients for Accelerated and Decelerated Flows through Smooth Tubes and Orifices", Transactions of A.S.M.E., Paper No. 55-SA-78, 1955.
- 11. De Hes M., "Water Hammer in a Closed Circuit Analysis with a Hybrid Computer", A.I.C.I. Conference, München, 1970.

- 12. Dijkman, H.K., and C.B. Vreugdenhil, "The Effect of Dissolved Gas on Cavitation in Horizontal Pipe Lines", <u>Journal of Hydraulic Research</u>, Vol. 7, No. 2, 1969, p. 301 314.
- 13. Duc J., "Negative Pressure Phenomena in a Pump Pipe Line", <u>Sulzer Technical Review</u>, 3/1959, p. 3 11.
- 14. Duc J., "Negative Pressure Phenomena in Pump Pipe Lines",

 International Symposium of Water Hammer in Pumped Storage Projects,

 A.S.M.E., Chicago, 1965, p. 154 167.
- 15. Excande, M.L., "Arrêt Instantane du débit d'une Conduit Forcée avec Cavitations", Proceedings, I.A.H.R. Symposium on Cavitation and Hydraulic Machinery, Sendai, Japan, 1963, p. 113 124.
- 16. Fanelli, M., "Il Modello Idraulico dell'Impianto dell'Aqua di Circolazione Relativo alla Cantrale Termica di la Casella", <u>E.N.E.L.</u>, <u>Direzione Studi e Ricerche, Centro Ricercha Idraulica e strutturale</u>, 2113/70 DSR, Milan, Italy, 1970.
- 17. Fauske, H.K., "Critical Two Phase Flow", <u>Advanced Heat Transfer</u>, Edited by B.T. Chao, University of Illinois Press, Urbana, 1969, p. 263 276.
- 18. Gayed, Y.K., and M.Y.M. Kamel, "Mechanics of Secondary Water Hammer Waves", Proceedings, The Institute of Mechanical Engineers, London, Vol. 173, 1959.
- 19. Greenspan, D., <u>Introduction to Partial Differential Equations</u>, McGraw Hill Bokk Company, New York, 1961.
- 20. Halliwell, A.R., "Velocity of a Water Hammer Wave in an Elastic Pipe", Proceedings, A,S.C.E., Vol. 89, No. HY4, 1963, p. 1 20.
- 21. Henry, R.E., M.A. Grolmes and H.K. Fauske, "Propagation velocity of Pressure Waves in Gas-Liquid Mixtures", Concurrent Gas-Liquid Flow, Edited by E. Rhodes and D.S. Scott, Plenum Press, New York, 1969, p. 1 18.

- 22. Hildebrand, <u>Introduction to Numerical Analysis</u>,
 McGraw Hill Book Company, New York, 1956, p. 64 68.
- 23. Holl, W.T., "Nuclei and Cavitation", Transactions, A.S.M.E., <u>Journal</u> of Basic Engineering, 1970, p. 681 688.
- 24. Hsieh, D.Y., "Some Analytical Aspects of Bubble Dynamics", Transactions, A.S.M.E., Journal of Basic Engineering, 1965, p. 991 1005.
- 25. Jansa, B., "Surge and Water Hammer Problems in the Cooling Water Systems of Large Thermal Power Plants", <u>Transactions</u>, part 1, I.A.H.R., Symposium Stockholm, 1970, J1, p. 1 8.
- 26. Joukowsky, N.E., <u>Water Hammer</u>, (translated by D. Simin from Memoires of the Imperial Academy of St. Petersburg, Russia), American Water Works Association, New York, Vol. 23, 1898, p. 341 424.
- 27. Katys, G.P., Continuous Measurement of Unsteady Flow, translated from Russian by D.P. Burrett), Pergamon Press, London, 1964.
- 28. Kovats, A., "Fluid Transient Conditions in Condenser Cooling Water Systems", A.S.M.E. paper 70-WA/FE-25.
- 29. Lai, C., A Study of Water Hammer Including Effect of Hydraulic Losses, Ph.D. Thesis, University of Michigan, Ann Arbor, Michigan, 1961.
- 30. Le Conte, J.N., "Experiments and Calculations on the Resurge Phase of Water Hammer", <u>Transactions</u>, A.S.M.E., Vol. 39, 1937, p. 691 694.
- 31. Li, W.H., "Mechanics of Pipe Flow Following Column Separation", Proceedings, A.S.C.E., Vol. 88, No. EM4, 1963, p. 97 - 118.
- 32. Li, W.H., and J.P. Walsh, "Pressure Generated by Cavitation in a Pipe", Proceedings, A.S.C.E., Vol. 90, No. EM6, 1964, p. 113 133.
- 33. Li, W.H., "Thermal Effect on Growth and Collapse of Cavities",

 Proceedings, I.A.H.R., Symposium on Cavitation and Hydraulic Machinery, Sedai, Japan, 1963, p. 1 16.

- 34. Liepmann, H.W., and A. Roshko, <u>Elements of Gas Dynamics</u>, John Wiley and Sons, Inc., New York, 1966.
- 35. Lister, M., "The Numerical Solution of Hyperbolic Partial Differential Equations by the Method of Characteristics", Mathematical Methods for Digital Computers, Edited by A. Ralston and H.S. Wilf, John Wiley and Sons, Inc., New York, 1960, p. 165 179.
- 36. McDonald, A., and J.A. Pilkington, "Pressure Surges in Condensor Cooling Water Systems", The British Hydromechanics Research Association,
 The 9th Members Conference, september 1967.
- 37. Magrab, E.B., and D.S. Blomquist, <u>The Measurement of Time Varying Phenomena: Fundamentals and Applications</u>, Notes, The Catholic University of America, Washington D.C., 1969.
- 38. Ness, N., <u>Dynamics of Viscous Fluids</u>, Notes, West Virginia University, Morgantown, West Virginia, 1966.
- 39. Parkin, B.R., and R.W. Kermeen, "The Roles of Convective Air Diffusion and Liquid Tensile Stresses During Cavitation Inception", Proceedings

 I.A.H.R. Symposium on Cavitation and Hydraulic Machinery, Sedai, Japan,

 1963, p. 17 35.
- 40. Parmakian, J., <u>Water Hammer Analysis</u>, Prentice Hall Inc., New York, 1955.
- 41. Rayleigh, L., "On the Pressure Developed in a Liquid During the Collapse of a Spherical Cavity", <u>Philosophical Magazine</u>, London, Vol. 34, 1917.
- 42. Reddick, H.W., and F.H. Miller, Advanced Mathematics for Engineers, John Wiley and Sons Inc., New York, 1957, p. 110, 114, 139 143.
- 43. Rich, G.R., "Water Hammer Analysis by the Laplace Mellin Transformations", Transactions, A.S.M.E., July, 1945, p. 361 376.
- 44. Richard, P.T., "Water Column Separation in Pump Discharge Lines", Transactions, A.S.M.E., Vol. 78, 1956, p. 1297 1306.

- 45. Ripken, J.F., and J.M. Killen, "Gas Bubbles: Their Occurance, Measurement and Influence in Cavitation Testing", <u>Proceedings I.A.H.R., Symposium</u> on Cavitation and Hydraulic Machinery, Sedai, Japan, 1963, p. 37 56.
- 46. Scarborough, E.C., and K.A. Webb, "Cooling Water System for Torrens Island Power Station Operating Characteristics at Pump Start Up and Shut Down: Water Hammer", Mechanical and Chemical Engineering, Transactions, The Institution of Engineers, Australia, 1968, p. 11 77.
- 47. Shapiro, A.H., The Dynamics, and Thermodynamics of Compressible Fluid Flow, Editor Ronald, New York, 1953.
- 48. Sharp, B.B., "Cavity Formation in Simple Pipes due to Rupture of the Water Column", Nature, London, Vol. 185, 1969, p. 302 303.
- 49. Schlichting, H., <u>Boundary Layer Theory</u>, Translated from German by J. Kestin, sixth edition, McGraw Hill Book Company, New York, 1968.
- 50. Siemons, J., "The Phenomenon of Cavitation in A Horizontal Pipe Line due to a Sudden Pump Failure", <u>Journal of Hydraulic Research</u>, Vol. 5, 1967., No. 2, p. 135 152.
- 51. Silberman, E., "Sound Velocity and Attenuation in Bubble Mixture Measured in Standing Wave Tubes", <u>The Journal of the Acoustical Society of America</u>, Vol. 29, No. 8, 1957.
- 52. Sommerfield, A., Partial Differential Equations in Physics, Academic Press, New York, 1949, p. 52 55.
- 53. Stepanoff, A.J., "Cavitation Properties of Liquids", Transactions, A.S.M.E., <u>Journal of Engineering of Power</u>, 1964, p. 195 200.
- 54. Stephenson, D., "Water Hammer Charts Including Fluid Friction", Proceedings, A.S.C.E., Vol. 88, 1962, p. 79 112.
- 55. Streeter, V.L., and C. Lai, "Water Hammer Analysis Including Fluid Friction", Proceedings, A.S.C.E., Vol. 88, 1962, p. 79 112.

- 56. Streeter, V.L., "Valve Stroking to Control Water Hammer", Proceedings A.S.C.E., Vol. 89, No. HY2, 1963, p. 39 66.
- 57. Streeter, V.L., "Water Hammer Analysis in Pipes", Proceedings, A.S.C.E., Vol. 90, No. HY4, 1964, p. 151 172.
- 58. Streeter, V.L., and E.B. Wylie, <u>Hydraulic Transients</u>, Mc Graw Hill Book Company, New York, 1967.
- 59. Streeter, V.L., <u>Fluid Mechanics</u>, 3rd edition, McGraw Hill Book Company, New York, 1962.
- 60. Tanahashi, T., and Kashara, E., "Analysis of the Water Hammer with Water Column Separation", <u>Bulletin</u>, J.S.M.E., Japan, Vol. 12, No. 50, 1969, p. 206 214.
- 61. Tanahashi, T., and Kasahara, E., "Comparison between Experimental and Theoretical Results of the Water Hammer with Water Column Separations", Bulletin, J.S.M.E., 1970, p. 914 925.
- 62. Tek, M.R., "Two Phase Flow Handbook of Fluid Mechanics, edited by V.L. Streeter, McGraw Hill Bokk Company, New York, 1961, Chapter 17.
- 63. Timoshenko, S., Strength of Materials, Part II, Van Nostrand Inc., New York, 1939, p. 528 583.
- 64. Van Wylen, G.J., and R.E. Sonntag, <u>Fundamentals of Classical Thermodynamics</u>, John Wiley and Sons Inc., New York, 1965.
- 65. Wallis, G.B., and Collier, J.G., <u>Two Phase Flow and Heat Transfer</u>, Notes, Thayer School, Dartmouth College, Hanover. N.H.
- 66. Weyler, M.E., An Investigation of the Effect of Cavitation Bubbles on Momentum Loss in Transient Pipe Flow, Ph. D. Disseration, University of Michigan, Ann Arbor, Michigan, 1969.

- 67. Wood, D.J., "Water Hammer Analysis by Analog Computers", <u>Proceedings</u>
 A.S.C.E., Vol. 93, No. NH1, 1967.
- 68. Zielke, W. "Frequency Dependent Friction in Transient Pipe Flow", Ph. D. dissertation, University of Michigan, Ann Arbor, 1960.

APPENDIX A

Digital Calculations of Velocities from Photo-analyzer Data

Photo Analyzer Data:

When displaying the film in the photo-analyzer, the start of the appearance of the 1000 c.p.s. time marks on the film marks the instant the valve starts to close. Thus, this first time mark should show the zero time reference (frame number 0). As the ball does not appear on the film at its beginning (the ball is still moving upstream towards the range of viewing of the camera), the film is scanned at a fast rate through the photo-analyzer, only counting how many turns the time pointer is completing till the ball starts to appear on the film relative to its first position on frame number 0. A frame is selected at this moment for starting recording the necessary data of the film being analyzed. This particular frame would be number 1. The time lapse between frames number 0 and 1 is calculated using the counted turns the time pointer completes and the electric motor speed. Starting from frame number 1, the film is scanned every five frames in the photo-analyzer. For each frame, the following data are obtained.

- frame sequential number
- coordinates of two marked reference points on the "plexiglass" pipe wall (R1 and R2, Fig. 37)
- ball centre coordinates
- time pointer coordinates

These data are obtained on a punched tape and they are the input data for the computer programme presented in the following section. The output of this programme is the required transient flow velocity changes.

Digital Computer Programme PDV:

A computer programme written in FORTRAN IV which is run on IBM System/ 360 is used. The main steps of the programme are:

- 1. Reading input data. These data consists mainly of two groups:
 - a.
- the time lapse between frames number 0 and 1 "TSTART" *)
- the physical distance between the two reference points R1 and R2

^{*)} Names between two inverted commas give the variable name in the computer programme

on the "plexiglass" pipe wall "DIST"

- the physical length of the radius of rotation of time pointer "RAD"
- the total number of frames analyzed "KOUNTF"

b. For each frame:

- frame sequential number "N"
- coordinates of reference point R1 (Fig. 37)
 "RX1, RY1"
- coordinates of reference point R2 (Fig. 37)
- coordinates of the ball centre "BXX, BYY"
- coordinates of the time pointer tip

all the above coordinates are read in with reference to the photo-analyzer screen coordinates (X-Y, Fig. 37) and are in Boscar units.

2. Calculations of ball displacement.

In this step of the programme, the displacement of the ball along the axis of the "plexiglass" pipe and perpendicular to it are calculated. These displacements, "X(I), Y(I)" are calculated with respect to the x-y coordinate system, that is a frame coordinate system rather than the X-Y system. This is done to eliminate any influence of inaccuracy of the film feed either in the camera during filming or in the photo-analyzer during the film analysis. With reference to Fig. 37, the following relations are used to account for the translation and rotation between the two axis systems

$$x_B = (X_B - X_{R1}) \cos \alpha + (Y_B - Y_{R1}) \sin \alpha$$
 A.1

$$y_{B} = (X_{B} - X_{R1}) \sin \alpha + (Y_{B} - Y_{R1}) \cos \alpha$$
 A.2

where

$$\alpha = \tan^{-1} \left(\frac{Y_{R2} - Y_{R1}}{X_{R2} - X_{R1}} \right)$$
 A.3

Finally the displacement scale factor is obtained knowing the actual distance between the two reference points R1 and R2.

3. Calculation of time.

The time increment between two successively analyzed frames is obtained calculating the angle "ANG" (β in Fig. 37) between two positions of the time pointer in the two frames (the dotted and complete positions on

Fig. 37). This is done using the coordinates of point t "TXX, TYY" and knowing the syncronous speed of the electric motor (600 r.p.m.) together with the radius of the pointer "RAD" and equation A.4:

$$\frac{\beta}{2} = \left(\sin^{-1}\frac{\frac{tt_b}{2}}{r}\right)$$
 A.4

The time "T(I)" is then calculated knowing the frame sequential number and the time lapse between frames 0 - 1 "TSTART".

- 4. Numerical calculation of displacement derivatives with respect to time |22|. The "DGT3" subroutine of the system/360 scientific subroutine package is used for the differentiation of the tabulated values "X(I), T(I)".
- 5. Using the CALCOMP plotter, the calculated values of the transient velocity changes "V(I)" are plotted versus time with the suitable scales.

A complete listing of the computer programme PDV is found in the section of computer programme listings (Part II).

APPENDIX B

On the Pipe Wall Deformation

In the derivation of the continuity equation for one-dimensional transient flow, equation B.1 |2,58,66| is quite familiar, (see chapter 2).

$$\frac{1}{0}\frac{d\rho}{dt} + \frac{1}{A}\frac{dA}{dt} + \frac{1}{\delta x}\frac{\partial \delta x}{\partial t} + \frac{\partial V}{\partial x} = 0$$
B. 1

In general, a solution of a water hammer problem requires finding the pressure and the velocity changes as function of the two independent variables x and t. Thus, the dependent variables in equation B.1 are to be expressed in pressure terms. The first term in equation B.1 gives the influence of the compressibility of the liquid and can be expressed using the bulk's modulus of the fluid K by

$$\frac{1}{\rho} \frac{d\rho}{dt} = \frac{1}{K} \frac{d\rho}{dt}$$
B.2

The second term in equation B.1 gives the change of the cross sectional area with time, while the third term gives the influence of the axial deformation. These two terms clearly depend on the strains in the pipe. These in turn depend upon the physical characteristics of the pipe as well as the resistance to deformation imposed by the particular manner in which the pipe is supported. Having

$$\frac{dA}{dt} = \frac{d\varepsilon_c}{dt} (2\pi R) R = 2 A \frac{d\varepsilon_c}{dt}$$
B.3

or

$$\frac{1}{A}\frac{dA}{dt} = 2\frac{d\varepsilon_c}{dt}$$

Equation B.4 gives the second term in equation B.1 in terms of the rate of change of the circumferential strain. On the other hand the third term in equation B.1 can be written as

$$\frac{1}{\partial x} \frac{\partial \delta x}{\partial t} = \frac{d\varepsilon}{dt}$$
B.5

It should be noted that this term only appears in the equation when the means of the support of the pipe allows axial deformation. To build up the influence of the pipe characteristics and its support conditions in the desired forms of the partial differential equation relating p,V to x

and t, the strain rates of changes $\frac{d\varepsilon}{dt}$ and $\frac{d\varepsilon}{dt}$ are expressed in terms of stress rates of change using the following basic equations

$$\varepsilon_{r} = \frac{1}{E} \left[\sigma_{r} - \mu(\sigma_{c} + \sigma_{x}) \right]$$
 B.6

$$\varepsilon_{c} = \frac{1}{E} \left[\dot{\sigma}_{c} - \mu(\sigma_{r} + \sigma_{x}) \right]$$
B.7

$$\varepsilon_{x} = \frac{1}{E} \left[\sigma_{x} - \mu(\sigma_{r} + \sigma_{c}) \right]$$
 B.8

The consideration of stress distribution in a thin cylindrical shell |63| in case of free support conditions (that is the case of the pipe system used in the experimental model), whose inner surface r = R. is subject to pressure p and whose outside surface (r = b) subject to pressure = 0, yields the following stress distribution relations:

$$\sigma_{c} = \frac{p R^{2}}{b^{2} - R^{2}} \left(1 + \frac{b^{2}}{r^{2}}\right)$$
B.9

$$\sigma_{r} = \frac{p R^{2}}{b^{2} - R^{2}} \left(1 - \frac{b^{2}}{r^{2}}\right)$$
 B.10

and

$$\sigma_{x} = 0$$
 B.11

Substituting from equations B.9 - B.11 for the stress terms in equations B.6 - B.8 at r = R and using B.2 - B.5, equation B.1 takes the form

$$\frac{dp}{dt} \left[\frac{1}{K} + \frac{2}{E} \left(\frac{R^2}{b^2 - R^2} \right) \left(1 + \frac{b^2}{R^2} - 2\mu + \mu \frac{b^2}{R^2} \right) \right] + \frac{\partial V}{\partial x} = 0$$
B. 12

introducing c(µ)

$$\frac{\mathrm{dp}}{\mathrm{dt}} \left[\frac{1}{K} + \frac{1}{E} \left(\frac{2R}{b - R} \right) c(\mu) \right] + \frac{\partial V}{\partial x} = 0$$
B. 13

where

$$c(\mu) = \frac{R}{b+R} \left[1 - 2\mu + \frac{b^2}{R^2} (1 + \mu) \right]$$
B.14

Halliwell |20|, following a different procedure arrived at a value of c = 1 instead of equation B.14.

The usual formulation |58| continues from B.13 with further introduction of a term "a" (with D = 2R and δ = b-R)

$$a = \sqrt{\frac{1}{\rho \left[\frac{1}{K} + \frac{c(\mu)}{E} \left(\frac{D}{S}\right)\right]}}$$
B. 15

The term "a" in this form turns out to be the wave speed of propagation for a pressure pulse as the final equations obtained describe a wave phenomenon. It suffices for out purpose to carry out the analysis up to this point. For the completion of the analysis and, as regards the momentum equation derivation, to arrive at the commonly used partial differential equations in water hammer applications, the reader is referred to chapter 2.

APPENDIX C

Numerical Computations for Transients in a Horizontal Line Based on Method of Characteristics

Programme HOZ is a FORTRAN IV programme that is run on IBM system/360. The programme carries out calculations necessary to predict transient pressure and velocity changes resulting from the closure of the valve upstream the horizontal pipe. The transient conditions calculations are based on the finite difference characteristics equations discussed in chapter 2. Water-column separation is assumed to occur just behind the valve when the pressure downstream of the valve reaches vapour pressure. One void of vapour is assumed to fill the cross section of the pipe and is assumed to grow, with its pressure remaining the same - that is the vapour pressure of the water corresponding to its temperature. Pressure waves continue to travel in the water column between the vapour void at one end and the water reservoir on the other end. Pressure and velocity changes in this column are calculated using the finite difference characteristics equations. In the meantime the arrival of these waves at the vapour void results in its growth and later in its diminution. Finally the void volume becomes zero, thus the water column is between the valve and the reservoir rather than between the vapour void and the reservoir. The above discussion is the principle of building up the water-column separation as a boundary condition in the digital calculations. How this is done, is explained in detail in the following steps.

The main steps of the programme are:

1. Read input data of valve resistance during closure: a number of values "MZ". *) These values "ZO(L)" are selected to give a dependable basis for the calculation of the interpolated instantaneous resistances of the valve to be calculated in step 6. In step 6 the instantaneous resistances are calculated to be used for the left end boundary condition. The value "ZVCL" is a large value representing the valve resistance when nearly completely closed.

Table 5 gives a list of valve resistances (obtained from steady measurements).

f x) Names between inverted commas give the variables names in the computer programme

Table 5

Valve resistances for linear closure of the valve *)

step number	Valve resistance $\xi(\alpha)$ "Zo(M)"	step number	Valve resistance $\xi(\alpha)$ "Zo(M)"
1	0.1	22	16.40
2	0.13	23	20.50
3	0.19	24	26.00
4	0.24	25	34.00
5	0.32	26	44.00
.6	0.41	27	54.00
7	0.59	28	60.00
8	0.72	29	93.00
9	0.94	30	135.00
10	1.20	31	200.00
11	1.50	32	300.00
12	1.60	33	460.00
13	2.30	34	650.00
14	2.95	35	1183.00
15	3.80	36	2484.00
16	4.34	37	6780.00
17	5.70	38	25200.00
18	6.70	39	50000.00
19	8.00	40	185000.00
20	10.00	41	475000.00
21	13.00	42	1000000.00

The first step corresponds to the open position of the valve. The 42nd step corresponds to a practically closed position of the valve (found experimentally to be at 82.5°).

^{*)} The tabulated values are extracted from the results obtained in section 3.3.1. and represented in Fig. 34 for a linear (angle-time) valve closure.

2. Read input data of the horizontal line. These data include "MESNUM", the sequential number designated to the experimental test number, with which calculated results are to be compared.

"C" the celerity of transient pressure pulse (m/s).

"VO" the initial steady velocity of flow in the pipe (m/s).

"TC" the nominal time of closure of the valve (s)

"HVO" pressure drop across the valve during steady conditions (m.water)

"HO" the level in the water reservoir at the downstream end of the pipe (m.water)

"F" the Darcy-Weisbach friction coefficient in the pipe corresponding to the steady flow velocity

"D" the inside diameter of the pipe (m)

'PV" the vapour pressure of water corresponding to its temperature (m.water)

3. Read calculations data

These are data necessary to build up the grid of the x-t diagram used for numerical calculations of water hammer (Fig. 50).

"NF" is the number of position nodes. That is the number of Δx intervals plus one

"MF" is the total number of time increments for which the calculations are to be completed.

- 4. Read the numbers designating locations on the x-t grid, where calculated pressure changes with time are plotted as output of the programme. These locations are selected according to the actual positions of the pressure transducers on the pipe.
- 5. Calculation of steady conditions in the pipe. These conditions consist of the values of "H(N,M), V(N,M)", for "M = 1". These calculations essentially use the Darcy-Weisbach expression.

$$\Delta H = \frac{f}{D} \Delta x \frac{V_0^2}{2g}$$

- 6. Interpolation procedures to calculate instantaneous valve resistances during its closure. "ZZ(K)" are obtained using linear interpolation between the values "ZO(L)" which are read in step 1. Fig. 51 shows the principle of these procedures.
- 7. Water hammer calculations.

 Solution of the finite difference characteristic equations described in chapter 2 is carried out progressively to obtain "H(N,M), V(N,M)" along

the length of the pipe at a certain time (i.e. for a particular "M") knowing the values at the preceding "M". The calculations are repeated incrementing "M" to "M + 1" in the programme. If "N" is equal to "1", the left end boundary condition is to be satisfied. That is the valve-cavitation void condition. If "N" is equal to "NF" the right end boundary condition has to be satisfied. On the other hand for the intermediate points for which "N" is neither equal to "1" nor to "NF" the finite difference characteristic equations are solved. Fig. 50 shows the finite difference notations used for building up the calculations grid.

a. Left end boundary condition:

This is a valve-cavitation void combined boundary condition. The valve boundary condition described in section 2.4. is used. However, if the pressure at the valve becomes less than the vapour pressure, then vapour pressure is assumed at the valve. The cavitation void is assumed to fill the whole cross sectional area of the pipe. The size of this void "BS" at any time "M" depends on the bubble growth "BG". The bubble growth is found from the velocities for its two sides. "VBL" the left side velocity, is defined from the flow equation through the valve when it is open, or is zero when the valve is completely closed. The right side velocity "VBR" is found from the C characteristic equation. When cavitation void is formed, its growth and diminution is followed and when the bubble size "BS" reaches zero then the valve boundary condition is used again. Fig.52 shows schematically the left end valve-cavitation void boundary condition.

b. Right end boundary condition:

In this case the reservoir boundary condition described in section 2.4. is used. Fig. 53 shows the right end reservoir boundary condition.

- c. Non boundary grid points:
 - For the intermediate points of the grid (Fig. 50) the finite difference characteristic equations presented in section 2.4. are solved simultaneously.
- 8. Writing output data. The output data mainly are pressure heads and velocities at different times "H(N,M), V(N,M)".
- J. Plotting of transient pressure and velocity changes at selected points on the pipe. These are points prechosen and identified in step 4. The computed values of pressure and velocity changes are plotted versus

time with the suitable scales using the CALCOMP plotter.

A complete listing of the programme HOZ is found in the listings of programmes (part II).

APPENDIX D

Numerical Computations for Transients in a Horizontal Line Based on the New Mathematical Model.

Programme HZD is a FORTRAN IV programme that is run on IBM system/360. The programme carries out calculations necessary for predicting transient pressure and velocity changes resulting from the closure of the valve at the upstream end of the horizontal pipe.

The transient conditions calculations are based on the new mathematical presentation of the flow and its finite difference solution described in chapter 5. The principle of building up the cavitation void that takes place near the valve if the vapour pressure is reached, is the same one that is used in programme HOZ (appendix C). The main steps of the programme are essentially the same as those of HOZ except for steps 1,6 and 7. The variables names assigned to the different parameters used in the calculations are the same as those of programme HOZ. A summary of the programme main steps follows:

1. The values of the two Tchebichef polynomials coefficients representing the valve resistance-angular valve position during its closure are assigned. The values of these coefficients are listed in Table 6.

Table 6

Computed Tchebichef polynomials coefficients representing valve resistance-angular position of the valve *)

For α 0 - 60°		For α 48 - 82.5°
Q (1) = 3.4845363745E Q (2) = 5.9455550667E Q (3) = 3.8761413203E Q (4) = 2.1035439852E Q (5) = 1.0192314314E Q (6) = 4.4316219652E Q (7) = 1.4281122695E Q (8) = 3.2727171997E Q (9) =-3.4798289640E Q(10) =-2.7324098151E Q(11) =-9.7082300198E	+ 01 + 01 + 01 + 01 + 01 + 00 + 00 - 02 - 01 - 01	E (1) = 1.5171599770E + 05 E (2) = 2.8264739567E + 05 E (3) = 2.2864336661E + 05 E (4) = 1.6031482768E + 05 E (5) = 9.6743620005E + 05 E (6) = 4.9549807881E + 05 E (7) = 2.1027203679E + 05 E (8) = 7.1102304836E + 05 E (9) = 1.8055376508E + 05 E (10) = 3.1710297590E + 05 E (11) = 3.6239602605E + 05

*) In fitting the measured data of ξ - α (Fig. 34) by the Tchebichef polynomials accuracy of 10^{-10} for the coefficients values was chosen. This accuracy is rather high but as the computing time was relatively small, it was decided to choose such high accuracy although the values of ξ and α themselves does not have such degree of accuracy.

- 2. Read input data of the horizontal line.

 Similar to HOZ appendix C, except for an additional reading of the celerity time dependent factor "DECS".
- 3. Read calculations data (similar to programme HOZ, appendix C).
- 4. Read the numbers designating locations on x-t grid where pressure histories are to be plotted (similar to programme HOZ, appendix C).
- 5. Calculations of steady conditions in the pipe (similar to programme HOZ, appendix C).
- 6. Instantaneous valve resistance "ZZ(M)" during its closure for all time steps till it is closed are calculated from the Tchebichef polynomials, using the values of Tchebichef polynomials coefficients assigned in step 1.
- 7. Water hammer calculations

These calculations are carried out incrementing time. For each time step, before the water hammer calculations are performed, the value of the celerity at this time level is calculated with the help of the celerity decrease rate "DECS". Also, the momentum loss coefficient "CDW" is calculated using the relation found in section 6.3. Note that in the calculation of "CDW" two possibilities are allowed for:

- 1. no vapour void at the valve
- 2. a vapour void at the valve.

The value of "CDW" in the second case is twice that in the first case (see section 6.3.).

At the first time step, i.e. "M = 2", the calculation of H and V along the pipe are based on equations (71 - 72). (see chapter 5.)

For "M" > 2, if "N" is equal to 1, the left end boundary condition is to be satisfied namely the valve-cavitation void. If "N" is equal to "NF" the right end boundary condition has to be satisfied. For intermediate locations "N" \neq "NF", calculations based on the finite difference equations (59 - 70)(chapter 5) are performed. The left end boundary condition is a valve-cavitation void combined boundary condition. The valve boundary condition described in section 2.4. is used. However, if the pressure at the valve becomes less than the vapour pressure, then vapour pressure is assumed at the valve. The cavitation void is assumed to fill the whole cross sectional area of the pipe. The size of this void "BS" at any time "M" depends on the bubble growth "BG". The bubble growth is found from the velocities at its two sides. The

left side velocity "VBL" is defined from flow equation through the valve when it is open or is zero when the valve is completely closed. The right side velocity "VBR" is found from the C characteristic equation. The growth of the vapour void is assumed to be "BG" = "(VBR-VBL)". On the other side when the bubble is diminishing the equivalent "BG" is replaced by 1.2 * "(VBR-VBL)". *) The cavitation void growth and diminution is followed and when the bubble size "BS" reaches zero then the valve boundary condition is used again. Fig. 52 shows schematically the left end valve-cavitation void boundary condition.

For right end boundary condition, the reservoir boundary condition described in chapter 5 is used. Fig. 53 shows the right end reservoir boundary condition.

For non boundary grid points, viz. the intermediate points of the grid (Fig. 50) the finite difference characteristic equations presented in chapter 5 are used.

Some conditional statements are used in the programme to impose some conditions when the calculated results are found to be in contradiction to realistic conditions. These statements were necessary for the following circumstances:

- At the beginning of the valve closure the calculated valve resistances are small. This results in a slight increase of the velocity at the beginning of the valve closure when calculated from the finite difference.
- Also, at the beginning of the transients the numerical finite difference relations at the reservoir boundary yielded slight increase in the velocity. As both the above conditions are not realistic and they were never observed in the experimental measurements, conditional statements were built into the programme to force the value of the velocity equal to the initial steady flow velocity if the computed one is found to be larger than the initial steady velocity.

^{*)} The factor 1.2 can be seen as a parameter used to allow for the observation noted in the photographic study of the film (section 4.5.), namely a faster rate of diminution of the void than that of its growth. (This fact can be also seen from the velocity measurements V_A in the experimental results of Figs. 65 - 70). Thus, the parameter used above was proposed to build this physical observation into the equivalent size growth of the vapour void. The value 1.2 was found by trial.

- Also, if the computed head at intermediate grid points is found to be less than the vapour pressure, it is replaced by the vapour pressure. This was done in view of the fact that the experimental measurements did not exhibit pressure heads less than vapour pressure.
- 8. Writing output data. The output data mainly are pressure heads and velocity at different times "H(N,M), V(N,M)".
- 9. Plotting of transient pressure and velocity changes at selected points on the pipe. These are points prechosen and identified in step 4. The computed values of pressure and velocity changes are plotted versus time with the suitable scales using the CALCOMP plotter.

A complete listing of programme HZD is found among the computer programmes listings (part II).

APPENDIX E

Numerical Computations for Transients in the Siphon System Based on the New Mathematical Model.

Programme WHN is a FORTRAN IV programme that is run on IBM system/360. The programme carries out calculations necessary for predicting transient pressure and velocity changes resulting from the closure of the valve at the upstream end of the siphon pipe system. The transient conditions calculations are based on the new mathematical presentation of the flow and its finite difference solution described in chapter 5.

In principle WHN is a modified HZD programme that allows a location of a high point at an intermediate location. If the pressure at that point reaches vapour pressure, a cavitation void is located "BSHP" and the growth and diminution of the void "BGHP" is followed in a similar way to the case of the cavitation void occurring at the valve, which was discussed in appendix D. The variable names assigned to the different parameters used in the calculations are the same as those in the previous programmes HOZ and HZD. A summary of the programme main steps follows:

- 1. The values of the two Tchebichef polynomials coefficients representing the valve resistance-angular valve position during its closure are assigned. (Table 6).
- 2. Read input data of the siphon line; similar to HZD plus reading of the number designating the grid point where the high point is located "NHP" and the elevation of the high point above the level of above the centre line of the valve "ZHP". Also, the elevations "ELV(N)" of the different nodes "N" above the valve centre line are read in.
- These steps are the same as in Programme HZD (appendix D)

 6.
- 7. Water hammer calculations
 In principle these are the same as those of HZD (appendix D) with the addition of the possibility of locating a cavitation void at "NHP" if the pressure at this grid point reaches vapour pressure. Thus, the pressure at that point is compared when calculated at the successive time

steps with vapour pressure and if the pressure reaches vapour pressure a cavitation void is located. Its size is given by "BSHP" and its growth "BGHP". The pressure at this grid point when the cavitation void exists is kept at the constant value of the vapour pressure. The cavitation void (bubble) side velocities, "UBL(M)" the left side velocity and the right side velocity "UBR(M)", are calculated using the characteristic equations along C and C respectively. When a vapour void exists the head is kept equal to the sum of the vapour pressure plus the elevation of the high point. To follow the growth and diminution of the void at the high point similar steps to those used in appendix D are adopted. However, as was seen from the experimental results *), the duration of the void growth is longer than the duration of the diminishing phase of the void. Besides, the motion of the water columns is affected by dissipation, causing a decrease in magnitudes of the velocities of the two columns. It becomes evident that during the diminishing phase, the "VBR-VBL" has a larger equivalent value on "BSHP" than that during the growth phase. This fact was also observed in a high speed camera film taken for column separation at the top of the siphon. From the high speed film of the water column separation at the top of the siphon two different situations could be recognized: during the formation of the cavitation void some small bubbles were seen to be rising to the top main cavity. On the other hand, during the diminishing phase, there was only a decreasing main cavity. These two different situations are believed to cause the observed different durations (formation and diminution) of the cavitation void. This observation is accounted for in the numerical calculations in the following manner. During the diminishing phase of the void at the high point (UBR(M) is negative), "BGHP" is assumed to be "SBHPF" times "UBR(M) - UBL(M)". This factor is assumed to have the simple form

"SBHPF" = "1.2 + 0.05 * ZHP"

This form is a simple form and shows that the value of this factor increases with the increase of the elevation of the siphon. The bubble (void) size "BSHP" is followed each time step till it vanishes. Once it vanishes, conditions at the grid point "NHP" are found in the same way

 $[\]star$) This can be seen clearly from the velocity measurements V_A and V_B in Figs. 71 - 79. Attention must be focused on the duration for which V_B is negative compared with the time it is positive.

as the other intermediate points (see step 7, appendix D).

The writing of output data and its plotting are the same as those found in steps 8 and 9 in appendix D. A complete listing of the programme WHN is found among the computer programmes listings (part II).

APPENDIX F

Numerical Computations for Transients in the Condenser System Based on the New Mathematical Model.

Programme WCN is a FORTRAM IV programme that is run on IBM system/360. The programme carries out calculations necessary for predicting transient pressure and velocity changes resulting from the closure of the valve at the upstream end of the condenser configuration. The transient conditions calculations are based on the new mathematical presentation of the flow and its finite difference solution described in chapter 5. In principle, WCN is a modified WHN that allows for a location of a restriction at an intermediate grid point. Also, a vapour cavitation void can be located at the upstream side of the restriction if the pressure there drops to vapour pressure (see Fig. 83). A cavitation void can be located and the growth and diminution of the void is followed in a similar manner to that used before. The variable names assigned to the different parameters used in calculations are the same as those used before in HZD and WHN. The programme main steps are:

- 1. The values of the two Tchebichef polynomials representing the valve resistance angular valve position during tis closure are assigned (Table 6).
- 2. Reading of input data of the condenser system. This step is similar to that in case of WHN with additional reading of "NRES" which is the grid location where the restriction is assumed. "ZCONDS" is the value of resistance used to present the condenser as a restriction satisfying the following relation

$$\Delta H = \xi \frac{V^2}{2g}.$$

"HCONDS" is the elevation of the condenser above the level in the low level water reservoir. "ACR" is the deceleration of the downstream column if water column separation at top of the condenser occurs.

- These two steps are the same as in HZD and WHN.
- 5. Calculation of steady conditions in the pipe is done in a way similar to the procedures used in WHN. At "N = NRES", the pressure drop across the restriction $\Delta H = \xi \frac{V^2}{2g}$ is allowed for. At that location pressure on

- the upstream side of the restriction is "PU(M)" while "PD(M)" represents the pressure on the downstream side ("M = 1").
- 6. Instantaneous valve resistances during its closure for all time steps till it is completely closed are calculated from the Tchebichef polynomials. This step yields the values of "ZZ(M)".

7. Water hammer calculations

In principle these are the same as those calculation procedures used in HZD and WHN with addition of the possibility of locating a cavitation void at the upstream side of the resitriction at the location "NRES" if the pressure there "PU(M)" reaches vapour pressure. Normally, at "N=NRES" the flow velocity in the resitriction "VVV(M)" is to satisfy the following relation "PU(M) - PD(M) = (ZCONDS/2.0*G)*VVV(M)**2" if the flow is in the positive direction. If the flow is in negative direction"PD(M) -PU(M) = (ZCONDS/2.0*G)*VVV(M)**2" is used instead. Beside one of the above equations the characteristic equation on C is used to relate "PU(M)" and "VVV(M)" while the characteristic equation along C is used to relate "PD(M)" to "VVV(M)". If "PU(M)" reaches "PV + HCONDS" a vapour bubble upstream of the restriction is located. Then "PU(M)" is kept constant at that value and the growth and the void size "BGU" and "BSU" are followed. "VLU(M)" is the left side velocity of the vapour void while "VRU(M)" is vapour void velocity at the right side (the downsteam side). The bubble size of the vapour void "BSU" is followed and when it vanishes the normal calculations are resumed. This is done in the same manner used in programme WHN.

The writing of the output results as well as the plotting of the calculated results are done in the same way used in steps 8 and 9 in programmes HZD and WHN. A listing of programme WCN is found in part II.

The modified version of computer programme WHN for use to predict transients in the condenser system based on a siphon schematization of the system allows for the following.

- a. reading the steady flow resistance in the condenser ξ_{cond} .
- b. calculation of steady pressures at different locations assuming the total pressure drop in the condenser to occur at the high point "NHP".
- c. to allow for the mass of the water boxes that is to be combined with the two water columns existing when a vapour void is located, two factors being used "FAL" and "FAR". These two factors give the ratio of the mass of both the left column and the right column in reality to the length of

the columns in the calculations (half the total length "CL"). They are used to adjust "PV" the vapour pressure at the cavitation void at the top of the siphon to "PL" and "PR". This would account for the influence of the mass of the water in the condenser on the motion of the two water columns occurring during the existence of the vapour cavitation void at the top of the siphon. The values of "FAL" and "FAR" are assigned in two different cased. First, for high elevations of the condenser, water column separation was in both the two water boxes. With reference to the scheme of the condenser system shown in Fig. 92, the left column is OQ including the mass of water in the water box and in the right column SR (without the mass of the right water box). In the second case, for lower elevations of the condenser, water column separation occurred at the top of left water box. In this case the left column is OQ (including the mass of water in the left water box) and the mass of the right water column is RS plus the mass of the water in the right water box (see Fig. 92).

The slight modifications in the listing of programme WHN are found in part II.

APPENDIX G

List of Experimental Measurements Data

Experimental measurements data as extracted from the data sheets (Fig. 48) for all tests presented in this study are listed below.

test number	date	air tem-	baro-	water tem-		steady co	onditions		valve	closure	remarks	rec	recorder data		
		pera- ture	pres- sure MBar	pera- ture °C	high level reser- voir mm water	low level reser- voir mm water	V notch reading mm	steady flow velo- city m/s	valve closure time s	valve closure type		pres- sure scale 10 mm equal	velo- city scale 10 mm equal	paper speed mm/s	
							Horizo	ntal Lir	ie						
6154 6155 6156 6104 6105 6106 5102 5052 5176 5178 5071	7- 4-71 7- 4-71 7- 4-71 7- 4-71 7- 4-71 7- 4-71 15-12-70 15-12-70 31-13-70 31-12-70	19 19 19 19 19 19 16.5 16.5 7		18.8 18.8 18.8 18.8 18.8 17 17 9.2 9.2 9.2	772 772 772 985 985 845 945 1185 770 770	457 457 457 495 495 495 465 460 473 473 511	151.6 151.6 151.6 164.1 164.1 164.1 163.9 173.2 150.5 170.5	0.75 0.75 0.75 1.0 1.0 1.0 1.19 0.759 0.739 1.17	2.0 1.0 0.5 2.0 1.0 0.5 4.0 4.0 1.0 0.5	linear linear linear linear linear linear linear linear linear linear		10*) 10 10 10 10 10 10 2 2 2	0.5***) 0.5 0.5 0.5 0.5 0.5 0.25 0.25 0.25 0.25	50 50 50 50 50 50 100 100 200 500 250	54-65 55-66 67 68 69 70 60-61 61 61
8001 8005 8008 8011 8016 8018 2034 2043	2- 7-71 2- 7-71 5- 7-71 6- 7-71 12- 7-71 9- 7-71 1- 9-71			17.2 17.2 18.0 19.0 20.6 20.6 18.5 18.5	1665 1665 1490 1490 1180 1180 1360 1115	350 350 505 505 505 505 505 500 500	181.7 181.7 170.4 173.4 163.9 163.9 172.7 164.0	1.42 1.42 1.14 1.21 1.0 1.0 1.14	5.0 2.0 4.0 2.0 2.0 1.0 2.5 1.5	linear linear linear linear linear linear linear	siphon 8 m 8 m 8 m 8 m 8 m 8 m 5 m 5 m	10 10 10 10 10 10 10	0.5 0.5 0.5 0.5 0.5 0.5	50 50 50 50 50 50 50 50	71 72 74 75 76 77–92 78

^{*)} m water

^{* *)} m/s

test	date	air tem-	baro-	water tem-	steady conditions			valve	closure	remarks		rec	order d	ata	Figs.	
		pera- ture °C	pres- sure MBar	pera- ture oc	high level reser- voir mm water	low level reser- voir mm water	V notch reading mm	steady flow velo- city m/s	valve closure time s	closure closure time type			pres- sure scale 10 mm equal	velo- city scale 10 mm equal	paper speed mm/s	
				THE SEC			Conden	ser Syst	em						2010	37,51
180	7-10-71	21.9		19.6	1660	320	169.0	1.11	2.0	linear	vertical 7A-8G	5.6m*)	10	0.5	50	80
181	7-10-71	21.9		19.6	1660	320	169.0	1.11	3.4	linear	vertical 7A-8G	5.6m	10	0.5	50	8
c 3063	22-10-71	21.6		21.1	1352	329	163.8	1.0	1.0	linear	vertical 7A-8G	3.1m	10	0.5	50	85
C 3064	22-10-71	21.6		21.1	1352	329	163.8	1.0	2.0	linear	vertical 7A-8G	3.1m	. 10	0.5	50	86
C 3065	22-10-71	21.6		21.1	1352	329	163.8	1.0	4.0	linear	vertical 7A-8G	3.1m	10	0.5	50	8
C 2019	7-10-71	21.9		19.6	1411	310	163.9	1.0	2.0	linear	vertical 7A-8G	5.6m	10	0.5	50	88
C 1003	27- 9-71	21.5		17.7	1450	310	163.9	1.0	2.0	linear	horizontal 7A-8G	3.1m	10	0.5	50	89
C 5094	29-10-71	21.1	1028	20.0	1447	306	163.9	1.0	1.0	linear	vertical 7A-8G	8.1m	10	0.5	50	90-92
C 6109	10-11-71	19.8	1022	19.0	1477	307	163.9	1.0	1.0	linear	vertical 7H-8G	9.1m	10	0.5	50	91-94
C 6107	10-11-71	19.8	1022	19.0	1477	307	163.9	1.0	2.0	linear	vertical 7H-8G	9.1m	10	0.5	50	95

^{*)} The notation 7A designates the location of the pressure transducer P7 in the condenser at location A Fig. 24.

ABSTRACT

The general aspects associated with transient conditions in the cooling water systems of thermal power plants which result from the pump trip out are examined. This covers the nature of the resulting hydraulic transients as regards water hammer and water column separation. Attention is foccussed on the problem and the dangers involved. The need for a dependable means of prediction of the resulting pressure changes for the design of modern power plants is pointed out. The simulation of a typical cooling water system for experimental study of such transient conditions is discussed with reference to a staging approach for carrying out the investigation. That is carrying out the study in three phases: transients in a horizontal line, transients in a siphon and transients in a siphon with a condenser model at its highest point. Different features of the experimental circuit and the instrumentation are presented. These includes the simulation of the conditions resulting from a pump failure by closing a specially built valve. Description of different types of experimental tests is then explained. These cover steady flows measurements to obtain friction factors for steady flow in the pipe and the valve resistance. Two methods were adopted for the measurements of transient velocity changes for hydraulic transients. The first was a photographic (digital-displacement) method while the second used a specially built induction flowmeter. The obtained transient velocity changes are new and proved to be very useful for the study. An experimental evaluation of the behaviour of the pipe wall material under the examined hydraulic transients is presented. This proved that the "plexiglass" pipe may be considered to be behaving elastically under loading conditions associated with the transients. The obtained results suggest that transient pressure changes in some cases could be obtained indirectly by measurements of strains on the outside surface of the pipe wall. This could be particularly useful in case of pipes carrying hazardous fluids. The use of high speed photography to examine the events of water column separation is reported. A study of a high speed film taken for water column separation at a part of a pipe just behind a valve situated at the upstream end of a horizontal pipe is covered. This part throws some light on the sequence of events occurring and contributes to the understanding of the phenomenon of water column separation. Pressure and velocity changes during a large number of tests are reported. Test conditions were changed varying the steady flow in the system, the valve closure time, the configuration of the system (horizontal pipe, siphon, a

siphon with a condenser model at its top) as well as the elevations of the high point in the system (in case of the siphon and the condenser systems). Numerical prediction of transient pressure and velocity changes resulting from the closure of a valve at the upstream end of the horizontal pipe, based on the method of characteristics is described. A comparison of the measurements with these calculated results showed a number of discrepancies. This comparison together with the photographic study of water column separation fromed the basis for proposing a new mathematical model to describe flow conditions for a one dimensional non steady flow with the resulting pressures near to the vapour pressure. The role of the cavitation bubbles occurring during the transients along the pipe length in the momentum loss and in the celerity decrease is emphasised. The mathematical model proposed, uses a combined momentum loss coefficient to account for both the wall friction and the resistance offered by the compression and the expansion of the cavitation bubbles. Finite difference relations for the solution of the differential equations describing the flow subject to initial and boundary conditions are presented. These are particularly useful for digital computations to predict the resulting conditions numerically. Appropriate procedures for the determination of the momentum loss coefficient and the celerity decrease rate from experimentla measurements are introduced. Numerical calculations based on the new mathematical model were used to simulate pressure and velocity changes under different test conditions. Comparisons of the calculated and measured results are presented for cases of transients in a horizontal line, siphon system and a siphon with a condenser model. Good agreement of the calculated results and the measurements was achieved.

VITA

Hemmat H. Safwat

Dissertation : Transients in Cooling Water Systems of Thermal Power

Plants

Major Field : Mechanical Engineering Fluid Mechanics

Biographical

Personal Data: Born in Cairo, Egypt, December 10, 1943

Education : Graduated from Orman High School, Cairo, in 1959;
received the Bachelor of Science degree from University
of Cairo, Egypt, in July 1964 with major in Mechanical
Engineering;

received the Master of Science degree from University of Cairo, Egypt, in May 1967;

received Doctor of Philosiphy degree in Mechanical Engineering from West Virginia University, Morgantown, West Virginia, U.S.A. in December 1968.

Professional

Experience : Held positions as

Instructor in the Mechanical Engineering Department, University of Cairo, September 1964 to September 1966; Graduate Research Assistant, West Virginia University, Morgantown, September 1966 to December 1968; Post doctoral fellow, West Virginia University, Morgan-

town, January 1969 to June 1969;

Principal investigator, Delft University of Technology since September 1969.

Awards

: awarded B.sc. with Distinction and first degree honours finished Ph.D. with a straight A average Member of Sigm X.

inemper of bigin hi

Associate member of A.S.M.E.

3 Safw.1